SCIENTIFIC RESEARCH OF THE SCO COUNTRIES: SYNERGY AND INTEGRATION

上合组织国家的科学研究：协同和一体化

Proceedings of the International Conference

Date: August 27

Beijing, China 2025

上合组织国家的科学研究：协同和一体化
国际会议

参与者的英文报告

International Conference
“Scientific research of the SCO countries: synergy and integration”

Part 2

2025年8月27日，中国北京
August 27, 2025. Beijing, PRC

Proceedings of the International Conference
“Scientific research of the SCO countries: synergy and integration” - Reports in English

(August 27, 2025. Beijing, PRC)

DOI 10.34660/conf.2025.95.53.097

这些会议文集结合了会议的材料 – 研究论文和科学工作者的论文报告。 它考察了职业化人格的技术和社会学问题。一些文章涉及人格职业化研究问题的理论和方法论方法和原则。
作者对所引用的出版物，事实，数字，引用，统计数据，专有名称和其他信息的准确性负责

These Conference Proceedings combine materials of the conference – research papers and thesis reports of scientific workers. They examine technical, juridical and sociological aspects of research issues. Some articles deal with theoretical and methodological approaches and principles of research questions of personality professionalization.

Authors are responsible for the accuracy of cited publications, facts, figures, quotations, statistics, proper names and other information.

DOI 10.34660/conf.2025.95.53.097

CONTENTS

DOI 10.34660/INF.2025.10.91.039

堪察加半岛东南部海域糠虾（甲壳纲，糠虾纲）的种类组成与分布
SPECIES COMPOSITION AND DISTRIBUTION OF MYSIDS (CRUSTACEA, MYSIDACEA) IN THE SOUTHEASTERN KAMCHATKA WATERS

Zheleznyak Maria Yurevna
Senior Lecturer
Vitus Bering Kamchatka State University

摘要：2007年，在堪察加半岛东南部海域的春季样本中发现了糠虾。共发现三种糠虾：Amblyops abbreviata、Boreomysis arctica 和 Holmesiella anomala。A. abbreviata 数量最多，B. arctica 最少。所有糠虾均发现于水深约 500 米处。

关键词：糠虾，堪察加半岛东南部海域，Amblyops abbreviata，Boreomysis arctica，Holmesiella anomala，大小和性别组成，生物量。

Abstract. *Mysids were found in a spring sample from the southeastern Kamchatka waters in 2007. Three species of mysids were found: Amblyops abbreviata, Boreomysis arctica and Holmesiella anomala. A. abbreviata was the most abundant, while B. arctica was the least common. All species were found at a depth of approximately 500 m.*

Keywords: *mysids, southeastern kamchatka waters, amblyops abbreviata, boreomysis arctica, holmesiella anomala, size and sex composition, biomass.*

Members of the order mysids (Crustacea, Mysidacea) are important component in marine plankton inhabiting all regions of the oceans. There are many brackish, estuarine species and few species occur in fresh water. They form an important link in the food chain (between microbial producers and secondary consumers) and therefore play a major role in the cycling of energy within the aquatic ecosystem.

In water of the moderate climate these crustaceans form the monospecific or polyspecific swarms. These swarms consisted of a single dominant species and up to 5 “guest” species. Dominant species accounted more than 50 % of the individuals in the group (Ohtsuka et al., 1995).

At present fauna of mysids from the Pacific Ocean (southeastern Kamchatka, Russian water) is not well studied. In the middle of past century was collected and processed extensive material from deep-water region of the Bering Sea and the

Kuril-Kamchatka Trench, allowed to define the aspectual composition and vertical distribution of mysids in given region (Birshteyn, Chindonova, 1970). There are works devoted to the species composition, bathymetric distribution of mysids and their biomass in the Okhotsok Sea and northwest part of the Pacific Ocean. A description of the common and rare epipelagic mysid species of the Kamchatka waters is given. There is also separate information about fauna of mysids from Komandorskiy reserve and Koryakiya (Petryashev, 2002, 2009; Holmquist, 1973).

The Purpose of given work was a determination of the species composition of mysids in plankton and particularities of their size and sex composition, biomass.

Material and methods

The material for the study was samples taken from the waters of southeastern Kamchatka in spring 2007 year (fig.1). The sampling depth was approximately 500 m. Plankton was caught using an ichthyoplankton conical net with an entrance diameter of 80 cm.

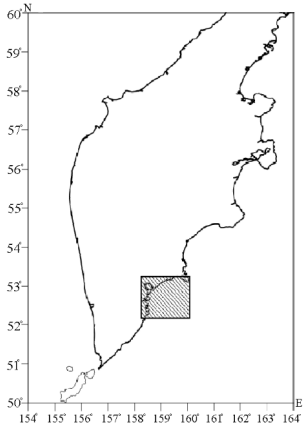

Figure 1. *Sampling area*

For identification species used keys, designed for the Bering sea (Daly, Holmquist, 1986), the Japan sea (Petryashev, 2004; Petryashov et all., 2007) and seas of the Arctic Ocean (Petryashev, 2009); Artificial key to the mysidacea of the Canadian Atlantic continental shelf (Brunel, 1960); A review of the mysidacea of the United States National museum (Tattersall, 1951). The Length measured from beginning of rostrum before the end of telson (Fig. 2).

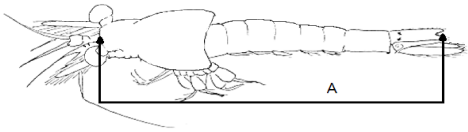

Figure 2. *Mysid measurement scheme*
A- total length.

Results and discussion

In the south-eastern Kamchatka waters 10 species were found: *Amblyops abbreviata* (Sars, 1869), *Boreomysis arctica* (Kroyer, 1861), *Pseudomma truncatum* (Smith, 1879), *Acanthomysis borealis* (Banner, 1954), *Eucopia grimaldii* (Nouvel, 1942), *Stilomysis grandis* (Goes, 1864), *Archaeomysis grebnitzkii* (Czerniavsky, 1882), *Dactylamblyops solivaga* (Birstein, Tchindonova, 1958), *Holmesiella anomala* (Ortmann, 1908), *Xenocanthomysis pseudomacropsis* (Tattersall, 1933) (Sedova et al., 2016).

In our samples we found representatives of 3 species *A. abbreviata*, *B. arctica* and *H. anomala*. All species we found belong to family Mysidae (Haworth, 1825) and are the most common and widespread species of mysids for the southeastern Kamchatka waters.

A. abbreviata. Length: length of the females 11-20 mm, male from 11 before 26 mm, juveniles — 10 mm.

Description. The main features are a small lateral-cephalic swelling of the carapace, rudimentary eyes in the form of a plate; the eye plates do not merge into one, they are quadrangular in shape, the outer edges are rounded. The outer edge of the antennal scale is naked, forming a tooth at the end, the inner edge is covered with setae. The telson is tongue-shaped, rounded at the end. Pleopods in females are rudimentary, in males they are long, biramous, well developed (fig.3). Marsupium of females consists of 2 pairs of well-developed oostegites.

Distribution: bathypelagic species (depths from 183 to 1375 m), inhabiting the northern parts of the Pacific and Atlantic oceans (Kathman et al., 1986).

A total of 29 specimens were found in the sample. Females dominated, there were 21 specimens, juveniles were 3 specimens. The ratio of males to females was 1:5. The biomass of this species was 11.7 mg/m^3.

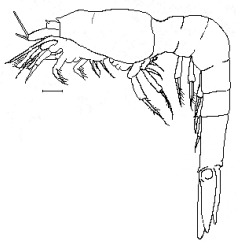

Figure 3. *Mature male of Amblyops abbreviata (Sars, 1869)*

B. arctica. Length: length of the females 25 mm, male from 12 before 22 mm, juveniles before 10 mm.

Description. The carapace has a flat rostrum. At the back, the carapace forms lateral angles. The eyes are large, the visual part is kidney-shaped and extends beyond the edges of the optic stalk. The antennal scale is less than twice the length of the antenna, the outer edge is naked, ending in a powerful tooth extending beyond the edge of the scale, the inner edge is covered with bristles. The telson is 3 times longer than the width of the abdominal segment. The telson has a median cleft, the depth of which is equal to 1/4 of the width of the telson. The telson's cleft is armed with teeth. Pleopods are absent in females, rudimentary in males. The marsupium of females consists of 7 pairs of oostegites.

Distribution: widespread, boreal species. Distribution depth: 365-1900 m (Kathman et al., 1986).

This species was present in the sample in the smallest quantity, only 8 specimens. The ratio of males to females was 3:1, there was only 1 immature specimen. The biomass of *B. arctica* was 5.3 mg/m^3.

H. anomala. Length: length of the females 15-28 mm, male 12-27 mm, juveniles were absent in the samples.

Description. The carapace forms a rostral plate. The eyes are large and spherical. The antennal scale is long, lanceolate, extending beyond the distal edge of the antennular stalk; the location and length of the distal tooth varies. The telson is elongated-triangular with a narrowly truncated apex, on which there is one pair of plumose setae and two pairs of spines, of which the inner pair is noticeably shorter than the outer; there are 11-22 spines on its lateral edges. The endopodites of the fourth pleopods of the male are longer than the exopodites and end in a long seta. Females have 3 pairs of oostegites, the first is reduced (Kathman et al., 1986). The uropods are slender, longer than the telson.

Distribution: Widespread, Pacific boreal species; from the Sea of Japan to the coast of Korea and from southern California to the Bering Sea. Sublittoral, upper bathyal species, inhabiting depths from 10-25 m to 1320 m (Kathman et al., 1986).

This species was present in the sample in almost the same quantity as the *A. abbreviata*, 28 specimens. Males dominated, there were 19 specimens, juveniles were not found. The ratio of males to females was 2:1. *H. anomala* mysids biomass was 17.4 mg/m3.

In the south-eastern Kamchatka waters there is an alternation of the most widespread species of mysids: in some years, it is *B. arctica* and *A. abbreviata*, in others, *Xenacanthomysis pseudomacropsis*. In 2007, the most widespread species for these waters, *X. pseudomacropsis*, was not found in the samples. *H. anomala*, which usually ranks third after *A. abbreviata* and *X. pseudomacropsis*, has now taken 2nd place in terms of numbers, having overtaken *B. arctica*.

References

1. Birshtein Ya.A., Chindonova Yu.G. New mysids (Crustacea, Mysidacea) from the Kuril-Kamchatka Trench region // Transactions of the Institute of Oceanology. Vol. 86. 1970. Pp. 277–291.

2. Brunel Pierre. Artificial key to the Mysidacea of the Canadian Atlantic continental shelf // Can. J. Zool. –1960. –Vol. 38. –P. 851–855.

3. Daly K.L., Holmquist C. 1986. A key to the Mysidacea of the Pacific Northwest. Can. J. Zool, V. 64 (6). P. 1201–1210.

4. Holmquist C. 1973. Taxonomy, distribution and ecology of the three species: Neomysis intermedia(Czerniavsky), N. awatschensis (Brandt) and N. holmes (Crustacea, Mysidacea) // Zool. Jb. Syst. Bd. 100. P. 197–222.

5. Ohtsuka S., Inagaki H., Onbe T., Gushima K., Yoon Y.H.1995. Direct observations of groups of mysids in shallow coastal waters of Western Japan and Southern Korea // Mar. Ecol. Pro. Ser. 123. P. 33–44.

6. Petryashev V.V. Fauna of crustaceans Leptostraca, Mysidocea, Isopoda and Decapoda (Anomura) of the Chukchi Sea and adjacent waters: conditions of existence and species composition // Biol. of the sea. Vol. 28, No. 2. 2002. Pp. 85–92.

7. Petryashev V.V. Order Mysids – Mysidacea // Biota of Russian waters of the Sea of Japan Vol. 1. Part 1. Crustaceans (cladocerans, thin-shelled crustaceans, mysids, euphausids and sea spiders). Ed. O.G. Kusakin. Vladivostok: Dalnauka. 2004. Pp. 107–128.

8. Petryashev V.V. Order Mysids – Mysidacea // Biota of Russian waters of the Sea of Japan Vol. 1. Part 1. Crustaceans (cladocerans, thin-shelled crustaceans, mysids, euphausids and sea spiders). Ed. O.G. Kusakin. Vladivostok: Dalnauka. 2004. Pp. 107–128.

9. Petryashev V.V. Mysidacea order // Illustrated keys to free-living invertebrates of the Eurasian seas and adjacent deep-water parts of the Arctic, Volume 1,

Rotifers, sea spiders and crustaceans: barnacles, thin-shelled, euphausids, incomplete tails, crabs, mysids, hyperiids, caprellids. 2009. 181 p.

10. Petryashov V.V., Turpaeva E.P., Rivyer I.K., Shkoldina A.G., Pogodin A.G., Borisov B.M. 2007. Crustacea (Cladocera, Leptostraca, Mysidacea, Euphausiacea) and Pycnogonida / Biota of the Russian Waters of Sea of Japan. V. 1, part 2. Vladivostok: Dalnauka, 161 p.

11. Sedova N.A., Murasheva M.Yu., Grigoriev S.S. Characteristics of numerous species of mysids (Crustacea, Mysidacea) from Kamchatka and adjacent waters // Bulletin of Kamchatka State Technical University. 2016a. No. 35. P. 65-73.

12. Tattersall, W. M. 1951. A review of the Mysidacea of the United States National Museum. Bulletin of the US National Museum, 201:1-292.

DOI 10.34660/INF.2025.42.41.040

人工通气对7.1岁以上儿童急性脑衰竭心肌需氧量的影响

THE EFFECT OF ARTIFICIAL VENTILATION ON MYOCARDIAL OXYGEN DEMAND IN ACUTE CEREBRAL FAILURE IN CHILDREN OVER 7.1 YEARS OLD

Muhitdinova Hura Nuritdinovna
Doctor of Medical Sciences, Full Professor
Center for the Development of Professional Competence of Medical Workers

Dadabayeva Erkinoy Isakjanovna
Resuscitator
Namangan branch of the Republican Scientific Center for Emergency Medical Care

Shamurodov Akmal Yangiboy ugli
Anesthesiologist-resuscitator
2nd Children's City Clinical Hospital of Tashkent

摘要。合并 OCN 的重症肺炎患儿的自主呼吸昼夜节律会发生变化，在机械呼吸支持 (MRS) 下，这种变化会有所减弱且不可靠。第 1 天，第 2 组患儿的 CPB CR 中值显著高于第 1 组 19%。第 1 组的 CPB SCR (118±3%) 高于第 2 组 (105±2%)。这一特点可通过对合并 OCN 的更重症肺炎进行有效的人工通气压力限制疗法来解释。第 2 组的 CPB CR 倒置持续时间最长（35 天中的 16 天）。在观察的前7天中，第2组患者每日生物钟中完全没有出现峰值期和深潮期的生理性投射，而第1组患者在7天中有3天在早晨检测到了正常的峰值期投射。急性心力衰竭（ACI）并发感染加重，导致PMC指标升高，这自然会降低心输出量，而心输出量是急性心力衰竭（AHF）的主要原因之一。在自主呼吸过程中，外周血管对PMC升高的反应更为明显。在第2组中，这种关系减弱且变得不可靠。

关键词：肺人工通气、心肌需氧量、急性脑供血不足、儿童。

Abstract. *Changes in the circadian rhythm during spontaneous breathing in children with severe pneumonia complicated by OCN occur, which somewhat weaken and become unreliable with mechanical respiratory support (MRS). On the first day, the mesor of the CR of the CPB in children of the 2nd group was significantly 19% higher than in the 1st group. In the 1st group, the SCR of the CPB was at a higher level (118±3%) than in the 2nd group (105±2%). The revealed feature can be explained by effective stress-limiting therapy with the use*

of artificial ventilation in connection with more severe pneumonia complicated by OCN. The longest inversion of the CR of the CPB was in the 2nd group (16 days out of 35). In the first 7 days of observation in group 2, the physiological projection of acrophase and bathyphase on the daily clock was completely absent, while in group 1, normal projection of acrophase in the morning hours was detected for 3 days out of 7. Aggravation of infection complicated by ACI, increasing the PMC indicator, naturally reduces cardiac output, being one of the leading causes of acute heart failure (AHF). A primary more pronounced reaction of peripheral vessels to an increase in PMC during spontaneous breathing is shown. This relationship decreases and becomes unreliable in group 2.

Keywords: *artificial ventilation of the lungs, myocardial oxygen demand, acute cerebral insufficiency, children.*

Relevance. It has been experimentally proven that severe ACI is accompanied by depression of cardiac contractility and increased myocardial dependence on oxygen and glucose supply, which may be associated with such pathogenetic factors as hypoxia, impaired bioenergetics, oxidative stress and Ca2+ imbalance. However, there is insufficient information on changes in myocardial oxygen demand, the degree of circadian rhythm disturbance of cardiac function in children with ACI caused by pneumonia, the pathogenetic and etiological significance of cardiac dysfunction in the occurrence and development of MODS have not been sufficiently studied, which significantly complicates the development of comprehensive intensive care (CIT) for this contingent of victims. Due to the lack of a complete picture of changes occurring in systemic hemodynamics in patients with ACI during mechanical ventilation, we set the goal of studying the effect of MCI on hemodynamic parameters, myocardial oxygen demand during infection in children over 7.1 years old [1-5]. Objective of the work. To study the effect of artificial lung ventilation on the circadian rhythm of myocardial oxygen demand in acute cerebral failure in school-age children.

Material and methods of the study. The results of continuous prolonged monitoring with hourly registration of body temperature, hemodynamic parameters, and respiration were studied in children admitted to the ICU of the RRCEM in a critical condition due to infection complicated by respiratory, acute cerebral failure at the age of 7.1-18 years. Intensive care was carried out according to the recommendations in the relevant clinical protocols. Group 1 included 8 children (average age was 13 ± 3 years) who had no indications for mechanical respiratory support upon admission to the clinic and throughout intensive care. All patients of group 2 (8 children) aged 12.6 ± 2.6 years were on mechanical ventilation from the moment of admission to the clinic according to indications. Factors aggravating the general condition of patients in group 1 were severe pneumonia, observed in

88% (7), acute respiratory failure grade 1-2A in 50% (4), and acute respiratory failure grade 1-2 in 75% (6) of children. While in group 2 the severity of the condition and the need for external respiration prosthetics were in children due to the severity of pneumonia in 100% (8), secondary encephalopathy in 100% (8), acute respiratory failure of 2-3 degrees in 87% (7), acute respiratory failure of 2 AB stage in 75% (6), convulsive syndrome in 37% (3). In general, the most severe pathological conditions that were complications of the underlying disease were observed in group 2. These were severe complicated pneumonia, which accounted for 50% of the studied cohort of patients, secondary encephalopathy complicated by coma of 1-2 degrees (50%), convulsive syndrome (36%), acute respiratory failure 42%, acute respiratory failure - 36%. Impairment of cerebral function upon admission to the clinic was assessed using the Glasgow scale and was 9.1±0.4 in group 1 and 6.5±1.0 points in group 2, which corresponded to a reliably significant suppression of brain function by 29% in group 2, which determined the duration of MCI and the duration of intensive care in the ICU. After awakening, restoration of adequate breathing, reflexes, and consciousness within one to two days, the children were transferred to a specialized department. The research data were processed by the variation statistics method using the Excel program by calculating the arithmetic mean values (M) and errors of the mean (m). To assess the reliability of differences in two values, the parametric Student's criterion (t) was used. The relationship between the dynamics of the studied parameters was determined by the paired correlation method. The critical significance level was taken to be 0.05. Results and discussion. A reliably significant difference in the average 7-day observation of the PMC indicator in the acrophase by 14%, bathyphase by 12%, and in the acrophase by 21% for 19 days confirmed the change in PMC in both groups in the circadian rhythm (Table 1).

Table 1.

Average values of the parameters of the phase structure of the circadian rhythm of PMC at age 7

Groups	Mesor	In acrophase	In the bathyphase	Amplitude	Daily range
1 (7 days)	103±6	118±6*	89±6*	14±4	29±6
2 (7 days)	114±6	127±9	100±5*	13±4	26±7
1 (19 days)	118±13	143±21*	99±12	25±11	45±17
2 (35 days)	105±9	125±9*	86±12	20±6	38±11

*- the difference is reliable relative to the mesor index

Table 2.
Mezor CR PMK

Days	1 group	2 group
1	110±6	131±7‴
2	107±7	117±8
3	93±6*	104±2*‴
4	107±4	107±6*
5	103±4	116±3*
6	94±9*	112±6*
7	111±7	111±7*
8	112±5	120±7
9	123±12	115±8
10	122±12	120±5
11	125±14	121±8
12	127±16	89±8*
13	129±16	123±5
14	106±11	113±8
15	119±11	94±7
16	143±18	96±8
17	148±5	107±12
18	127±7	101±8
19	138±7	102±6
20		102±8
21		101±4
22		103±9
23		100±12
24		92±10
25		98±8
26		104±11
27		98±7
28		98±10
29		102±13
30		96±9
31		91±7
32		98±11
33		98±12
34		102±11
35		88±10

Table 3.

Average circadian rhythm of the PMC

Hours	1 group 7 days	2 group 7 days	1 group 19 days	2 group 35 days
8	113±7	114±11	122±16	108±14
9	114±4	113±11	127±17	105±13
10	110±5	114±12	121±17	106±13
11	105±7	117±12	121±14	106±13
12	105±6	116±14	117±16	104±12
13	106±5	114±7	123±19	108±10
14	109±9	111±8	122±14	105±12
15	108±5	113±5	118±10	105±10
16	105±8	117±4	117±13	105±13
17	108±9	115±6	119±11	103±14
18	107±9	116±7	117±12	106±11
19	106±6	116±6	118±11	107±13
20	106±6	116±8	124±19	108±11
21	101±7	116±7	119±15	107±11
22	99±5	112±8	113±12	106±11
23	99±12	115±8	113±16	104±13
24	97±7	117±7	118±17	106±9
1	96±8	118±9	115±19	106±11
2	98±9	108±8	114±17	101±10
3	98±11	106±7	113±15	101±9
4	97±9	112±9	114±18	101±11
5	95±6	112±10	113±17	102±12
6	100±6	115±9	116±17	104±11
7	100±4	115±8	117±16	106±9

*- the difference is reliable relative to the indicator on day 1

‴ - reliable relative to the indicator in group 1

On day 1, in children of group 2, the meso of the CR of the PMC was significantly 19% ($p<0.05$) higher than in group 1. During intensive therapy, with preserved spontaneous breathing, on day 3, the meso of the CR of the PMC decreased by 15%, remaining within the normal range for up to day 8. In the following days of observation, an increase in the meso of the CR of the PMC to 148% on day 17 was observed in child K., 9 years old, with a diagnosis of progressive nervous system disease such as leukoencephalitis, acute respiratory asphyxia, stage 1 acute respiratory failure, stage 1 acute respiratory failure, pre-cerebral edema, right-sided hemiparesis, convulsive syndrome, stage 2 anemia (Fig. 1). In group 2, the initially higher 19% level of PMC decreased by 20%, 17%, 11%, 14%,

15%, 32% ($p<0.05$, respectively) in the following 3-7, 12 days, remaining slightly above the normative level in the following days of intensive care. Thus, MRP had a significant effect on tissue respiration, performing a preventive correction of cellular catabolism, reducing PMC, primarily with medication (sedatives, hypnotics, muscle relaxants), preventing energy deficiency. This is confirmed by the normal level of the PMC indicator in a child who was on mechanical ventilation for 34 days: patient R., 9 years old, brain tumor, left-sided polysegmental pneumonia, focal pneumonia on the right, complicated by acute cerebral insufficiency, grade 2 coma (Table 2).

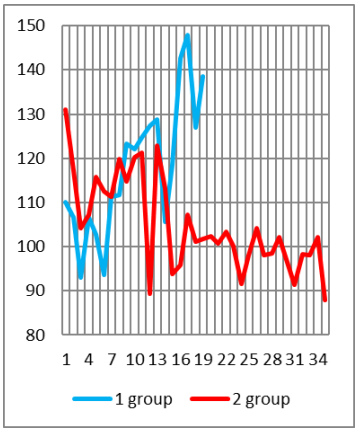

Figure 1. *Mesor of circadian rhythm of PMC in %.*

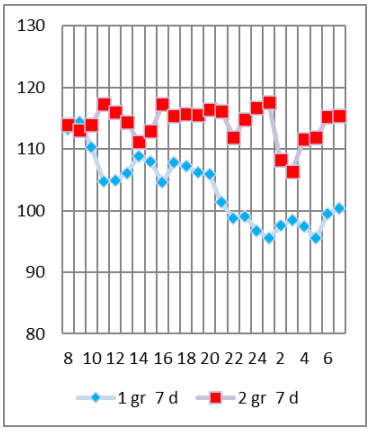

Figure 2. *CCPR of PMC in the first 7 days, %.*

Despite the absence of significant, reliable differences in CCPR of PMC by groups (Table 3), a slightly increased level of fluctuations in CCPR of PMC in group 2 in the first 7 days of acute inflammatory reaction was noteworthy (Fig. 2). Thus, CCPR of PMC in group 1 was 103±5%, in group 2 114±2%. That is, in group 2 CCPR in the first 7 days was significantly higher than in group 1 by 11%. While throughout the entire period of intensive care in group 1 CCPR of PMC was at a higher level (118±3%) than in group 2 (105±2%). The identified feature can be explained by more effective stress-limiting therapy using artificial ventilation in connection with more severe pneumonia complicated by acute cerebral insufficiency (Fig. 3).

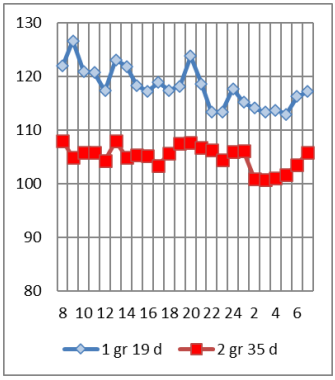

Figure 3. *SCR of PMH in the intensive care unit, %.*

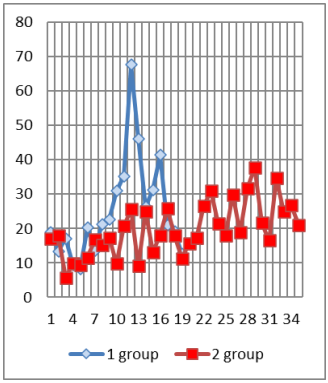

Figure 4. *Amplitude of CR of PMC, %.*

The average values of the amplitude of the CR of the PMC in group 1 were 25±11%, in group 2 - 20±6%, i.e. no significant differences were found in the groups. An increase in the amplitude of the CR of the PMC in group 1 on day 12 was observed in patient K. due to the insufficient effectiveness of pathogenetically substantiated intensive anti-inflammatory therapy, which led to an exacerbation of the stress reaction to the systemic inflammatory response (SIR) (Fig. 4). Almost synchronous fluctuations in daily fluctuations of the PMC were observed in both groups (Table 5). In group 1, the average value of daily fluctuations in the PMC was 45±17%, in group 2 38±11%.

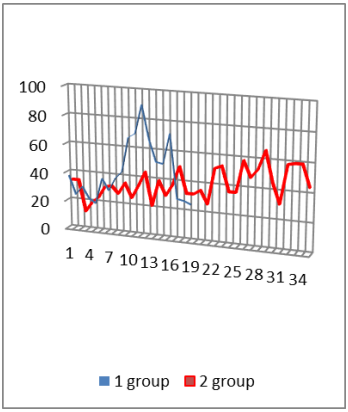

Figure 5. *Daily range of oscillations of the PMC in %.*

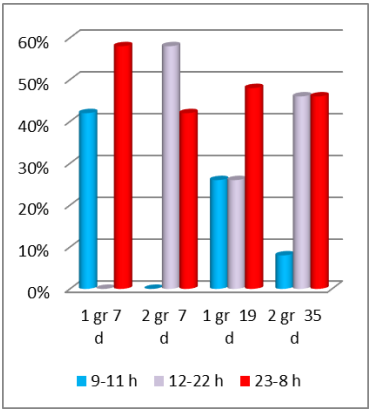

Figure 6. *Duration of inversion of the CR PMC*

The longest inversion of the CR PMC was in group 2 (16 days out of 35), which amounted to 46% (Fig. 6). The findings corresponded to the severity of pneumonia complicated by OCN. It should be noted that already in the first 7 days of observation in group 2 there was a complete absence of the physiological projection of the acrophase and bathyphase on the daily dial, while in group 1 a normal projection of the acrophase in the morning hours was observed for 3 days out of 7.

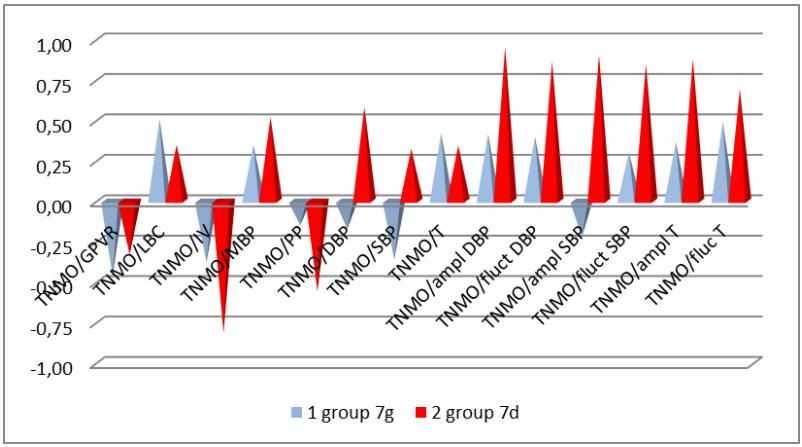

Figure 7. *Correlation relationships of the mesor of the CR, PMC and hemodynamics during the first 7 days.*

High information content of the examination results in the first week of intensive care for acute CI complicated by SIR caused by severe pneumonia was expressed in the results of differentiated assessment in the studied groups. Thus, in group 1, the insignificant slope of the inverse correlation between PMC and SV (-0.38) significantly increased to (-0.82). This means that the insignificant slope of the negative effect of an increase in PMC on the value of SV in more severe pneumonia and ACI became natural, amounting to (-0.82) (Fig. 7). Aggravation of infection complicated by ACI, increasing the PMC indicator, naturally reduces cardiac output, being one of the leading causes of acute heart failure (AHF). One of the many pathogenetic mechanisms of AHF in ACI is an increase in the PMC indicator in severe ACI requiring MCI. An increase in the meso of the circadian rhythm of the PMC under mechanical ventilation causes an increase in the amplitude of vascular tone fluctuations (0.95), daily changes in DBP (0.86), amplitude of the circadian rhythm of SBP (0.9), daily fluctuations in SBP (0.84), and amplitude of the circadian rhythm of body temperature (0.88). Thus, the development of

myocardial oxygen starvation with unsatisfied increased PMC during a systemic inflammatory response of the body with ACI already during the first 7 days of intensive care increases the negative impact at the cellular, tissue, and organ level due to the instability of protective reactions of compensatory changes in hemodynamic parameters during adaptation under mechanical ventilation, contributing to the depletion of energy resources due to cellular hypercatabolism, causing the development of MODS. The lack of understanding of this mechanism and the underestimation of the advisability of replenishing not only wasted energy resources, but also creating conditions for ensuring more active metabolic processes, the so-called "biochemical detoxification", significantly reduces the effectiveness of intensive therapy and optimization of the prognosis in this group of pediatric patients.

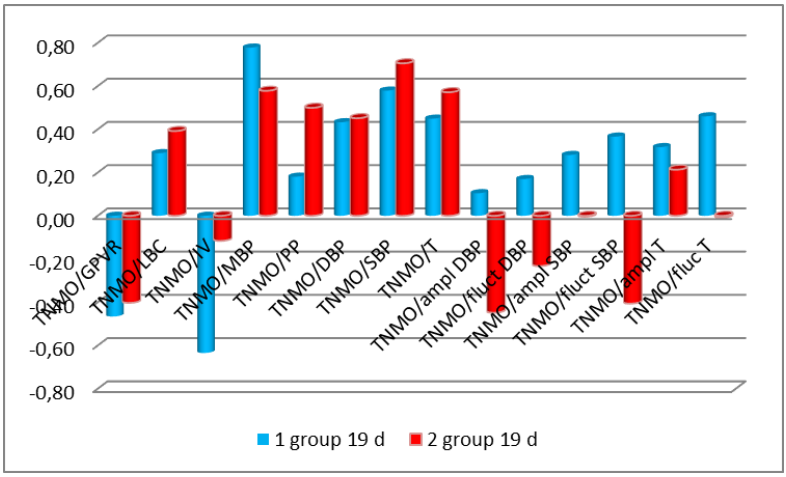

Figure 8. *Correlation links of the mesorum of the CR of the PMC in the intensive care unit.*

Longer intensive therapy with spontaneous breathing in children causes the formation of a direct correlation link between the PMC and the MAP (0.78). That is, an increase in the tone of the peripheral vessels causes an increase in cardiac output (Fig. 8). This relationship is somewhat weakened in more severe patients against the background of mechanical ventilation (0.58). In group 2, a direct correlation link between the PMC and the SBP was also found (0.71), which corresponds to a compensatory increase in the SBP in response to tissue hypoxia in children with prolonged mechanical ventilation. Direct correlation links were found between the CR of the PMC and the CR of the MAP in group 1, which

amounted to in the first 7 days (0.71) and during 19 days (0.8). Also, in the first 7 days, the correlation relationship was between the CPVR and the DBP CPVR (0.7), and over the course of 19 days (0.79). Thus, a primary more pronounced reaction of peripheral vessels to the growth of CPVR during spontaneous breathing is shown (Table 4). This relationship decreases and becomes unreliable when children are transferred to mechanical ventilation in group 2. Only in the acute period (7 days) was a strong direct dependence of the change in the CPVR of the SBP on the CPVR of the CPVR (0.73) revealed, weakening with prolonged mechanical ventilation.

Table 4.

Correlation relationships of the CPVR of the CPVR

	1 gr 7 days	**2 gr 7 days**	**1 gr 19 days**	**2 gr 35 days**
SCR PMK/SCR OPSS	0,29	-0,36	0,21	-0,20
SCR PMK/SCR IOC	0,00	0,27	-0,04	0,19
SCR PMK/SCR UOK	-0,60	0,14	-0,53	0,16
SCR PMK/SCR SrAD	0,71	0,60	0,80	0,38
SCR PMK/SCR PAD	-0,60	0,41	-0,22	0,63
SCR PMK/SCR DAD	0,70	0,45	0,79	0,28
SCR PMK/SCR SAD	0,52	0,73	0,70	0,57
SCR PMK/SCR T	0,15	0,20	0,42	-0,27

Conclusion. Changes in the CPB during spontaneous breathing in children with severe pneumonia complicated by ACI occur in a circadian rhythm, which somewhat weakens and becomes unreliable in the case of MCI. On the first day, the mesor of the CPB CR in children of group 2 was significantly 19% higher than in group 1. In group 1, the SCR of the CPB was at a higher level (118±3%) than in group 2 (105±2%). The revealed feature can be explained by effective stress-limiting therapy using mechanical ventilation due to more severe pneumonia complicated by ACI. The longest inversion of the CPB CR was in group 2 (16 days out of 35). In the first 7 days of observation in group 2 there was no physiological projection of acrophase and bathyphase on the daily clock, while in group 1 normal projection of acrophase in the morning hours was detected for 3 days out of 7. Aggravation of infection complicated by ACI, increasing the PMC indicator, naturally reduces cardiac output, being one of the leading causes of acute heart failure (AHF). A primary more pronounced reaction of peripheral vessels to an increase in PMC during spontaneous breathing is shown. This relationship decreases and becomes unreliable in group 2.

Sources

1. Belkin A.A., Zislin B.D., Leiderman I.N., Domansky D.S.; Clinical Institute of the Brain, SSC RAMS; Journal "Intensive Care" No. 3, 2006. 2. Likhterman L.B., Kravchuk A.D., Okhlopkov V.A., Mogila V.V., Likhterman B.L.; Federal State Autonomous Institution "National Medical Research Center of Academician N.N.Burdenko"; S.I. Georgievsky Medical Academy of the Federal State Autonomous Educational Institution of Higher Education "V.I.Vernadsky Kazan Federal University"; Federal State Autonomous Educational Institution of Higher Education "I.M.Sechenov First Moscow State Medical University" of the Ministry of Health of the Russian Federation (ConsiliumMedicum portal, journal "Neurology and Rheumatology" No. 1, 2018.

3. https://intensive-care.ru/index.php/acc/article/view/31/2071

4.https://mknc.ru/spravochnik-zabolevaniy/10107/ostrye-narusheniya-mozgovogo-krovoobrashcheniya/2/?kt_lang=ru

5.https://cyberleninka.ru/article/n/osobennosti-tserebralnoy-i-ekstratserebralnoy-nedostatochnosti-u-bolnyh-s-neblagopriyatnym-prognozom-hirurgicheskogo-lecheniya

DOI 10.34660/INF.2025.62.38.041

7.1岁以上儿童急性脑供血不足植物神经紧张昼夜节律特征
FEATURES OF THE CIRCADIAN RHYTHM OF VEGETATIVE TONE IN ACUTE CEREBRAL INSUFFICIENCY IN CHILDREN OVER 7.1 YEARS OLD

Muhitdinova Hura Nuritdinovna
Doctor of Medical Sciences, Full Professor
Center for the Development of Professional Competence of Medical Workers

Rahimova Suraye Ruzmetovna
Deputy Chief Physician
Republican Scientific Center for Emergency Medical Care

Mirzayeva Adiba Damirovna
Head of Department
Republican Scientific Center for Emergency Medical Care

摘要。重症监护前7天，第1组自主神经张力中观节律（CR　VT）平均值增加40%，第2组增加50%。在ICU整个住院期间，第1组平均CR　VT提示交感神经紧张反应比正常值高60%，第2组高30%。在两组患儿中，VT与PMC均观察到生理相关性（分别为0.71和0.93），表明心肌需氧量增加与交感神经紧张反应直接相关，交感神经紧张反应比正常年龄水平高40-60%。将患者转入机械通气时，注意到中枢和外周血流动力学适应性重建的高动力方向减弱。在自主呼吸背景下的适应性重建是通过血流动力学的适应性重建方法进行的，这种方法是当今众所周知的——形成高动力类型的血液循环。根据指征将患儿转入人工呼吸机，导致血流动力学生理性高动力重构趋于平缓，但对新的生存条件（炎症反应更为严重，需硬件呼吸支持）的适应并未停止，昼夜节律相位结构的其他组成部分也参与其中（峰值从峰值向倒置转变、振幅改变、每日波动，以及随后植物性调节交感神经紧张的昼夜节律中期转变）。

关键词：昼夜节律，植物性紧张，急性脑供血不足，儿童。

Abstract. *The average values of the mesocircadian rhythm of autonomic tone (CR VT) were increased in the first 7 days of intensive care in group 1 by 40%, in group 2 - by 50%. Over the entire period of stay in the ICU, the average CR VT indicated a sympathotonic reaction 60% higher than normal in group 1, and 30% in group 2. In both groups of children, a physiological correlation was observed between VT and PMC (0.71 and 0.93, respectively),*

characterizing a direct dependence of an increase in myocardial oxygen demand with a hypersympathotonic reaction 40-60% higher than the normal age level. A decrease in the hyperdynamic direction of the adaptive restructuring of the central and peripheral hemodynamics was noted when transferring patients to mechanical ventilation. Adaptation against the background of spontaneous breathing was carried out by the method of adaptive restructuring of hemodynamics, which is well known today - the formation of a hyperdynamic type of blood circulation. Transferring children to artificial ventilation according to indications led to the leveling of physiological hyperdynamic restructuring of hemodynamics, but adaptation to new conditions of existence with a more severe inflammatory reaction with hardware respiratory support did not stop, and other components of the phase structure of circadian rhythms participated in it (shift of the peak of acrophase to inversion, change in amplitude, daily fluctuation and only then shift of the meso of the circadian rhythm of the sympathetic tone of vegetative regulation).

Keywords: *circadian rhythm, vegetative tone, acute cerebral insufficiency, children.*

Relevance. The autonomic nervous system (ANS) in the acute period of acute cerebral failure (ACF) is the leading link modulating cardiac functions. Violation of the dynamic organization of the ANS, which implies the interaction and mutual modulation of the sympathetic and parasympathetic neuroeffector mechanisms of cardiac activity control, contributes to disadaptive reactions, which increases the sensitivity of the myocardium to damaging agents. Researchers have shown that the development of transient cardiac disorders is directly related to acute cerebral damage and is designated by the term “cerebrocardial syndrome” (CCS). The development of CCS in cerebral ischemia is based on structural myocardial disorders that are not associated with coronary blood flow disorder. In the pathogenesis of CCS, the leading role is played by disorders of the autonomic regulation of the cardiovascular system and changes in the function of the hypothalamic-pituitary-adrenal system, leading to the development of morphofunctional changes in cardiomyocytes. Patients with different progression of the pathological process have different variants of changes in vegetative regulation and different degrees of their expression, which allows using the assessment of changes in both parts of the ANS to predict the severity and outcome of the disease. In diseases or disorders of brain functions, damage to the structures that carry out central regulation of the cardiovascular system leads to various deviations from the norm, including hypertension, pronounced changes in the frequency and rhythm of heart contractions. It has been proven that intracranial hypertension in ACN leads to a violation of neurohumoral regulatory processes and vegetative functions, as well

as to a breakdown of compensatory mechanisms. The regulatory role responsible for the integration of vascular reactions during changes in intracranial pressure is played by the suprasegmental structures of the ANS. Heart rhythm disorders - supraventricular and ventricular extrasystoles, paroxysms of atrial fibrillation, atrioventricular conduction disorders are the most common symptoms of CCS. Heart rhythm disturbances can negatively affect the reparative processes in the cerebral ischemia zone. It has been proven that frequent supraventricular extrasystole causes a reduction in cerebral blood flow by 7%, ventricular extrasystole - by 12%, and ventricular paroxysmal tachycardia - by 40-75%. Heart rhythm disturbances, such as sick sinus syndrome, developing in ACI, are the cause of additional neurological deterioration. Due to the lack of information on the specifics of managing children aged 7.1 - 18 years with severe acute pneumonia, an attempt was made to assess the state of autonomic regulation under conditions of mechanical respiratory support in systemic inflammatory reaction SIR complicated by acute cerebral failure based on the study of circadian rhythm monitoring data of autonomic tone (VT) [1-7].

Objective. To study and evaluate the features of the circadian rhythm of autonomic tone in acute cerebral failure in children over 7.1 years old. Material and methods of the study. The results of continuous prolonged monitoring with hourly recording of body temperature, hemodynamic parameters, and respiration were studied in children admitted to the ICU of the RRCEM in a critical condition due to infection complicated by respiratory failure, acute cerebral failure at the age of 7.1-18 years. Intensive care was carried out according to the recommendations in the relevant clinical protocols. Group 1 included 8 children (average age 13±3 years) who had no indications for mechanical respiratory support upon admission to the clinic and throughout intensive care. All patients of group 2 (8 children) aged 12.6±2.6 years were on mechanical ventilation from the moment of admission to the clinic according to indications. In general, the most severe pathological conditions that were complications of the underlying disease were observed in group 2. These were severe complicated pneumonias, which accounted for 50% of the total cohort of patients studied, secondary encephalopathy complicated by grade 1-2 coma (50%), convulsive syndrome (36%), acute respiratory failure 42%, and acute heart failure 36%. Impaired cerebral function upon admission to the clinic was assessed using the Glasgow scale and amounted to 9.1±0.4 in group 1 and 6.5±1.0 points in group 2, which corresponded to a reliably significant suppression of brain function by 29% in group 2, which determined the duration of MCI and the duration of intensive care in the ICU. After awakening, restoration of adequate breathing, reflexes, and consciousness, the children were transferred to a specialized department within one to two days. The research data were processed by the variation statistics method using the Excel program by calculating the arith-

metic mean values (M) and errors of the mean (m). To assess the reliability of differences in two values, the parametric Student's criterion (t) was used. The relationship between the dynamics of the studied parameters was determined by the paired correlation method. The critical significance level was taken to be 0.05. Results and discussion. The average values of the CR VT meso were increased in the first 7 days of intensive care in group 1 by 40%, in group 2 - by 50%. For the entire period of stay in the ICU, the average CR VT indicator in group 1 indicated a sympathotonic reaction 60% above the norm, in group 2 by 30% (Table 1). A reliable increase in VT in the acrophase by 70%-80%, as well as a decrease in the indicator in the bathyphase in the first 7 days in both groups of patients by 40% and 30%, respectively, confirm that the violation of the dynamic organization of vegetative regulation, which means the interaction and mutual modulation of the sympathetic and parasympathetic neuroeffector mechanisms of cardiovascular function control, occurs in a circadian rhythm, contributes to disadaptive reactions, which increases the sensitivity of the myocardium to damaging agents. On the first day, sympathetic regulatory activity was increased by 70% in group 2 and prevailed relative to the indicator in group 1 by 30% (Table 2).

Table 1.

Average level of values of the parameters of the phase structure of the circadian rhythm of VT, units

Groups	Mesor	In acrophase	In the bathyphase	Amplitude	Daily fluctuation
1 (7 days)	1,4±0,1	1,7±0,1*	1,0±0,2*	0,3±0,1	0,6±0,1
2 (7 суток)	1,5±0,1	1,8±0,1*	1,2±0,1*	0,3±0,1	0,6±0,1
1 (19 суток)	1,6±0,2	2,1±0,3	1,1±0,3	0,5±0,2	1,0±0,4
2 (35 суток)	1,3±0,2	1,8±0,2*	1,0±0,2	0,4±0,2	0,8±0,2

*- the difference is reliable relative to the mesor index

In dynamics, a reliable significant change was revealed in group 2 on day 4 (a decrease of 30%, $p<0.05$). No significant differences in the activity of autonomic regulation were found either in the first 7 days or throughout the entire period of treatment in the intensive care unit between the studied groups (Table 3).

Table 2.

Mezor CR VT st 7 years, units

Days	1 group	2 group
1	1,4±0,3	1,7±0,1
2	1,5±0,1	1,5±0,2
3	1,3±0,1	1,5±0,1
4	1,3±0,1	1,4±0,1‴
5	1,5±0,1	1,5±0,1
6	1,1±0,1	1,5±0,1
7	1,5±0,1	1,5±0,1
8	1,5±0,2	1,7±0,1
9	1,9±0,2	1,5±0,1
10	1,6±0,3	1,7±0,1
11	1,4±0,4	1,6±0,1
12	1,4±0,3	1,2±0,2
13	1,4±0,3	1,6±0,1
14	1,7±0,2	1,4±0,2
15	1,7±0,3	1,2±0,2
16	2,0±0,3	1,1±0,2
17	2,3±0,1	1,5±0,2
18	1,8±0,1	1,4±0,2
19	1,7±0,2	1,3±0,2
20		1,3±0,2
21		1,5±0,1
22		1,3±0,2
23		1,1±0,2
24		1,1±0,2
25		1,0±0,2
26		1,0±0,2
27		1,1±0,2
28		1,3±0,2
29		1,1±0,2
30		1,2±0,2
31		1,3±0,1
32		1,3±0,2
33		1,3±0,3
34		1,1±0,2
35		1,3±0,2

Table 3.

SCR VT st 7 days, units

Hours	1 group 7 days	2 group 7 days	1 group 19 days	2 group 35 days
8	1,3±0,3	1,5±0,1	1,5±0,3	1,4±0,2
9	1,3±0,3	1,5±0,1	1,7±0,3	1,4±0,2
10	1,3±0,2	1,6±0,1	1,6±0,3	1,4±0,2
11	1,3±0,2	1,6±0,1	1,5±0,3	1,4±0,3
12	1,3±0,1	1,5±0,2	1,6±0,3	1,3±0,3
13	1,4±0,1	1,5±0,1	1,7±0,3	1,4±0,2
14	1,5±0,2	1,4±0,1	1,6±0,3	1,3±0,2
15	1,5±0,1	1,5±0,1	1,6±0,2	1,3±0,2
16	1,4±0,2	1,6±0,1	1,5±0,2	1,4±0,2
17	1,4±0,2	1,5±0,1	1,5±0,4	1,3±0,2
18	1,4±0,2	1,5±0,1	1,6±0,4	1,4±0,2
19	1,4±0,1	1,5±0,1	1,6±0,3	1,3±0,2
20	1,5±0,1	1,5±0,1	1,7±0,4	1,3±0,2
21	1,4±0,2	1,6±0,1	1,6±0,3	1,3±0,2
22	1,4±0,2	1,5±0,2	1,5±0,3	1,4±0,3
23	1,4±0,3	1,5±0,1	1,6±0,3	1,3±0,3
24	1,3±0,2	1,6±0,2	1,6±0,4	1,3±0,3
1	1,3±0,2	1,6±0,2	1,6±0,3	1,3±0,2
2	1,3±0,2	1,5±0,1	1,6±0,3	1,3±0,2
3	1,3±0,2	1,4±0,1	1,6±0,3	1,2±0,2
4	1,3±0,2	1,5±0,2	1,5±0,3	1,3±0,2
5	1,3±0,1	1,5±0,2	1,6±0,4	1,3±0,2
6	1,4±0,1	1,5±0,2	1,6±0,4	1,3±0,2
7	1,4±0,2	1,6±0,1	1,6±0,3	1,4±0,2

Noteworthy is the fluctuation in the dynamics of the mesor of the CR VT in group 1 with fluctuation periods of 7, 6.6 days, in group 2 7, 5, 5, 6, 6.5 days with a more pronounced deformation of the circa-week biorhythm in group 2 (Fig. 1).

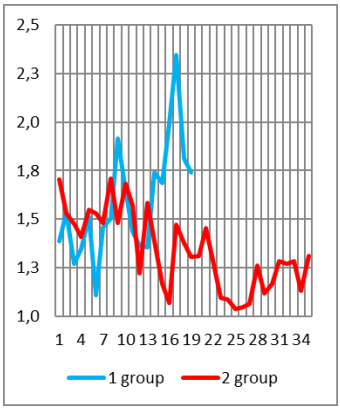

Figure 1. *Dynamics of the mesor of the CR VT, units*

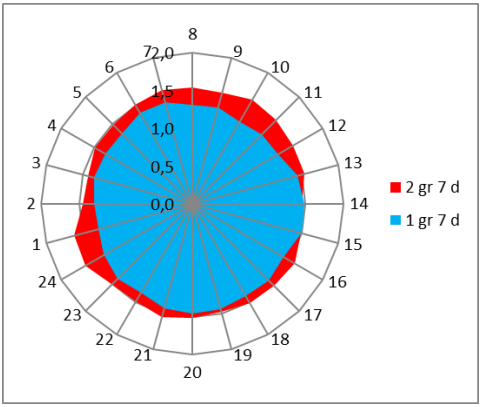

Figure 2. *SCR VT in the first 7 days*

Notable is the higher level of sympathetic regulation in the first 7 days in children of group 2, amounting to 1.5 ± 0.04 units. During the same period, in group 1, VT was 1.4 ± 0.1 units. Dysadaptive deviation of the circadian rhythm of VT in the first 7 days in group 1 was characterized by an insignificant shift in the peak of acrophase (to 2 p.m.), projection of the bathyphase at 10 a.m. While on these same days in group 2, the projection of the peak of the acrophase of the CR VT shifted to 12 a.m. (inversion), bathyphase at 3 a.m. (Fig. 2). Over the entire observation period, the average level of autonomic sympathetic regulation was 1.3±0.04 units against the background of mechanical ventilation, and 1.6±0.04 units in group 1. The difference found was most likely associated with the effectiveness of stress-protective therapy (sedatives, hypnotics) in group 2. During the treatment in the intensive care unit, with a higher average level of sympathetic regulation activity, the deformation of the circadian rhythm was expressed in the following: in group 1, the peak of the acrophase was shifted by 9 o'clock clockwise, the bathyphase by 6 o'clock counterclockwise; in group 2, a normal projection of the acrophase of the VT was noted (10 o'clock in the morning), the bathyphase at 3 o'clock in the morning (Fig. 3). Thus, the adaptation process necessarily involves the phase structures of the circadian rhythm of the VT, in some cases by increasing the amplitude, the daily range of oscillations, as well as by shifting the peak of maximum activity of the autonomic regulation from physiological daytime hours to the dark time of the day, and by shifting the mesor of the circadian rhythm of the VT. Taking into account the comparatively higher average level of sympathetic nervous system activity in group 1 by 23% ($p<0.05$) (with a favorable outcome), it can be assumed that it is advisable to maintain a comparatively higher level of

sympathetic regulation than is observed in clinical practice under conditions of drug adaptation to mechanical ventilation as part of more extensive stress-protective therapy (sedatives, hypnotics, muscle relaxants). The question arises in the case of more severe acute cerebrovascular insufficiency, acute respiratory failure in the first 7 days of the advisability of providing more massive stress-protective anti-inflammatory therapy with more effective restoration of perfusion characteristics, with more active, starting from the second week of mechanical ventilation, supporting/restoring the activity of compensatory systems, autonomic regulation, and organ function.

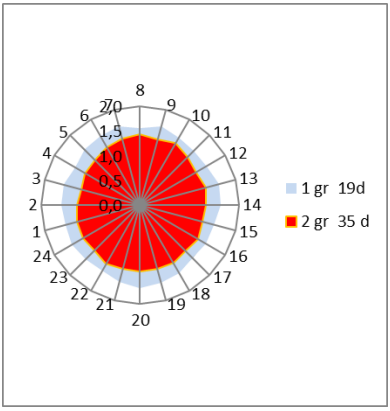

Figure 3. *Circadian rhythm of VT in the intensive care unit, units.*

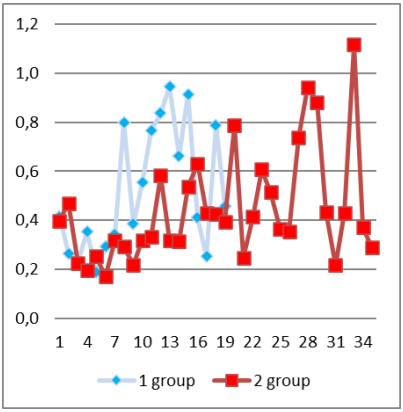

Figure 4. *Amplitude of circadian rhythm of VT, units.*

The increase in the amplitude of the circadian rhythm of VT on days 8–17, as well as in group 2 on days 13–32, reflected the active participation of the amplitude, daily fluctuations of the circadian rhythm of VT in adaptation, ensuring an adequate increase in the function of the pituitary-adrenal system in compensatory reactions, primarily of the cardiovascular system, in the process of restoring the regulatory function of the ANS centers (Fig. 4, 5).

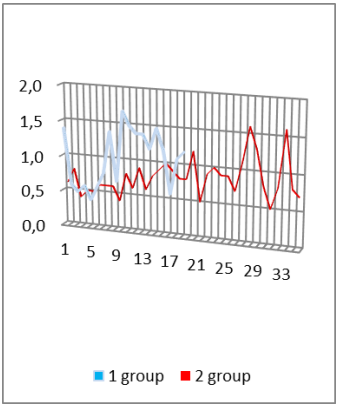

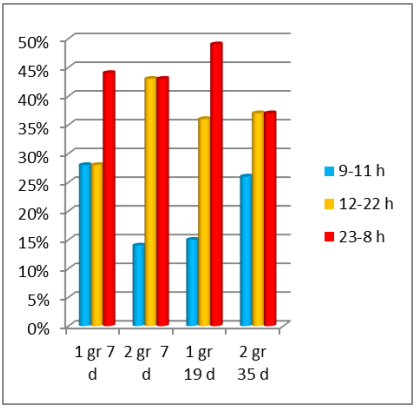

Figure 5. *Daily fluctuations of VT, units.*

Figure 6. *Duration of CR VT inversion.*

One of the objective indicators of stress reaction is the inversion (shift of the peak of acrophase) of the circadian rhythm of the studied indicator. Thus, the longest duration of CR VT inversion was found in group 2 (13 days), which amounted to 37% relative to the duration of intensive care in the ICU (Fig. 6).

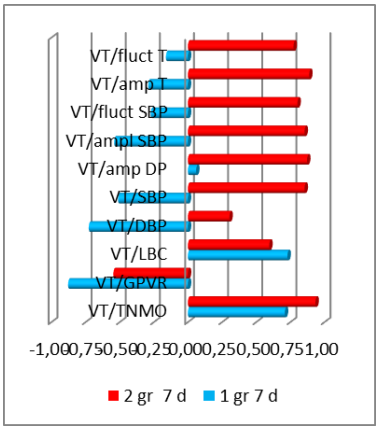

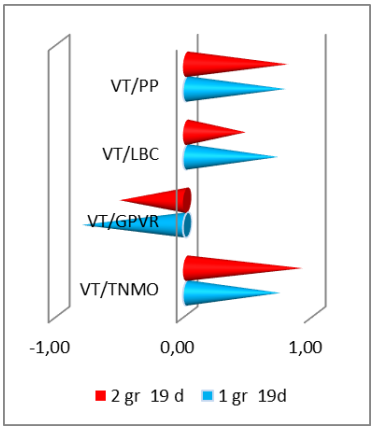

Figure 7. *Correlation of VT in the first 7 days*

Figure 8. *Correlation of VT for 19 days*

In both groups of children, a physiological correlation was observed between VT and MVC (0.71 and 0.93, respectively), characterizing a direct dependence

of an increase in myocardial oxygen demand with a hypersympathotonic reaction by 40-60% above the normative level for age. A decrease in the hyperdynamic direction of the adaptive restructuring of central and peripheral hemodynamics was noted when transferring patients to mechanical ventilation. Thus, if in group 1 in the first 7 days of treatment an inverse correlation was observed between VT and OPSS (-0.88), VT and DBP (-0.73) and a direct correlation between VT and IOC (0.73), then in group 2 these correlations became unreliable and amounted to (-0.55; 0.6, respectively). However, at the same time, the emergence of a strong inverse relationship between VT and SBP (0.85), VT and the amplitude of DBP (0.87), VT and the amplitude of SBP (0.85), VT and daily T fluctuations (0.77) was noted. The findings indicated a change in the participants of compensatory reactions in the process of adaptation to changes in homeostasis parameters due to mechanical ventilation under conditions of a pronounced systemic inflammatory reaction. That is, in group 1, adaptation against the background of spontaneous breathing was carried out by a well-studied method of adaptive restructuring of hemodynamics - the formation of a hyperdynamic type of blood circulation. When transferring children to mechanical ventilation according to indications, this led to the leveling of the physiological restructuring of hemodynamics, but adaptation to new conditions of existence with a more severe inflammatory reaction did not stop, but other components of the phase structure of circadian rhythms participated in it. This is the amplitude, daily fluctuations, shift of the peak of acrophase and bathyphase, which were also preventive mechanisms for the development of functional insufficiency of organs and systems in the 2nd group of children in the first 7 days (Fig. 7). In the following 19 days of observation, the direction and severity of correlations in both groups coincided, with some tendency to decrease in the 2nd group (Fig. 8).

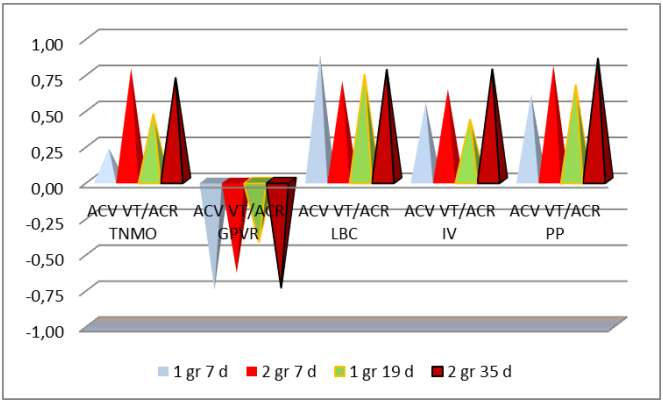

Fig.9. Correlation relationships of the CR VT

No significant differences between the groups of correlation relationships of the CR VT with the PMV, OPVR, SV, and PBP were found (Fig.9). The data obtained corresponded to the physiological increase in the PMV, IOC, SV, PBP and the inverse with the OPVR both in the first 7 days and throughout the entire stay in the ICU.

Conclusion. The average values of the CR VT mesor were increased in the first 7 days of intensive care in group 1 by 40%, in group 2 - by 50%. Over the entire period of stay in the ICU, the average CR VT indicator in group 1 indicated a sympathotonic reaction 60% higher than normal, in group 2 by 30%. In both groups of children, a physiological correlation was observed between VT and PMC (0.71 and 0.93, respectively), characterizing a direct dependence of an increase in myocardial oxygen demand with a hypersympathotonic reaction by 40-60% above the age-standard level. A decrease in the hyperdynamic direction of the adaptive restructuring of central and peripheral hemodynamics was noted when transferring patients to artificial ventilation. Adaptation against the background of spontaneous breathing was carried out by a well-studied method of adaptive restructuring of hemodynamics - the formation of a hyperdynamic type of blood circulation. When children were transferred to artificial ventilation according to indications, physiological hyperdynamic restructuring of hemodynamics was leveled, but adaptation to new conditions of existence with a more severe inflammatory reaction with apparatus respiratory support did not stop, other components of the phase structure of circadian rhythms participated in it (shift of the peak of acrophase to inversion, change in amplitude, daily fluctuation and only then shift of the mesor of the circadian rhythm of the sympathetic tone of vegetative regulation).

References

1. Gromov V.S., Belkin A.A., Levit A.L. Effect of sympathomimetics on systemic and cerebral hemodynamics in patients with acute cerebral insufficiency / // Ural Medical Journal. - 2007. №6. - P. 18-22.

2. Gadzhieva N.Sh., Gromov. Dynamic metabolic monitoring as a basis for nutritional support in acute cerebral insufficiency of vascular genesis // Anesthesiology and resuscitation. - 2008. - No. 2. - P. 16-20.

3. Belkin A. A., Zislin B. D., Leiderman I. N., Domansky D. S.; Clinical Institute of the Brain, SUNC RAMS; journal "Intensive Therapy" No. 3, 2006.

4. Likhterman L. B., Kravchuk A. D., Okhlopkov V. A., Mogila V. V., Likhterman B. L.; Federal State Autonomous Institution "National Medical Research Center of Academician N. N. Burdenko"; Medical Academy named after S. I. Georgievsky, Federal State Autonomous Educational Institution of Higher Education "KFU named after V. I. Vernadsky"; Federal State Autonomous Educational Institution

of Higher Education "First Moscow State Medical University named after I.M. Sechenov" of the Ministry of Health of the Russian Federation (ConsiliumMedicum portal, Neurology and Rheumatology journal, No. 1, 2018.

5. https://intensive-care.ru/index.php/acc/article/view/31/2071

6. https://mknc.ru/spravochnik-zabolevaniy/10107/ostrye-narusheniya-mozgovogo-krovoobrashcheniya/2/?kt_lang=ru

7. https://cyberleninka.ru/article/n/osobennosti-tserebralnoy-i-ekstratserebralnoy-nedostatochnosti-u-bolnyh-s-neblagopriyatnym-prognozom-hirurgicheskogo-lecheniya

DOI 10.34660/INF.2025.20.14.042

预测 I-III 期乳腺癌患者不良预后的列线图的开发和验证
DEVELOPMENT AND VALIDATION OF A NOMOGRAM FOR PREDICTING UNFAVORABLE OUTCOMES IN BREAST CANCER PATIENTS WITH STAGE I-III DISEASE

Nadyrov Eldar Arkadyevich
MD, PhD, Associate Professor
Gomel State Medical University, Republic of Belarus

Volchek Vladislav Stanislavovich
Assistant of Professor
Gomel State Medical University, Republic of Belarus

Zaitseva Evgeniya Vadimovna
Student
Gomel State Medical University, Republic of Belarus

Zhukova Nina Vladimirovna
Student
Gomel State Medical University, Republic of Belarus

Kavaleu Ilya Uladzimiravich
Student
Gomel State Medical University, Republic of Belarus

摘要：本研究纳入了198例I-III期浸润性乳腺癌患者。为了预测病程，将患者分为两组：随访结束时疾病未进展组（96例），以及5年内疾病进展组（102例）。研究调查了以下关键预后因素：年龄、肿瘤大小（pT）、淋巴结数量、生长方式、肿瘤象限定位、肿瘤分级、手术类型、肿瘤栓子数量、组织学肿瘤类型、ER/PR受体SCORE指数以及绝经状态。单因素和多因素logistic回归分析确定了疾病进展的独立危险因素（肿瘤大小、pT、转移性淋巴结数量、生长方式和肿瘤象限定位）。这些因素被用于构建列线图。该列线图显示出良好的预测性能，训练队列的曲线下面积（AUC）为 0.879（95% CI：0.825-0.934），验证队列的曲线下面积（AUC）为 0.874（95% CI：0.785-0.964）。

关键词：乳腺癌，临床、组织学和免疫组织化学参数，疾病进展，列线图。

Abstract. *The study included 198 patients with stage I–III invasive breast cancer. To predict disease course, two patient groups were formed: those without disease progression by the end of the follow-up period (96 patients) and those*

with progression within 5 years (102 patients). The following key prognostic factors were investigated: age, tumor size (pT), number of lymph nodes, growth pattern, tumor location by quadrant, tumor grade, type of surgery, number of tumor emboli, histological tumor type, SCORE indexes for ER/PR receptor, and menopausal status. Univariate and multivariate logistic regression analyses identified independent risk factors for progression (tumor size, (pT), number of lymph nodes with metastasis, growth pattern, and tumor location by quadrant). These factors were used to develop a nomogram. The nomogram demonstrated good predictive performance, with an area under the curve (AUC) of 0.879 (95% CI: 0.825–0.934) for the training cohort and 0.874 (95% CI: 0.785–0.964) for the validation cohort.

Keywords: *breast cancer, clinical, histological, and immunohistochemical parameters, disease progression, nomogram.*

Introduction

Breast cancer (BC) is the leading type of cancer in terms of incidence among women worldwide. According to the Global Cancer Observatory 2022 data, BC was diagnosed in 2,261,419 women, accounting for approximately 11.7% of all new cancer cases. Furthermore, over 684,000 patients die from this disease annually. The highest incidence rates are recorded in developed countries: in Europe, the age-standardized rate (ASR) is 69.2 cases per 100,000 female population, in North America - 76.8, and in Australia - 85.6. The lowest rates are observed in Western African countries (less than 30 cases per 100,000) [1–4].

Despite significant advances in BC treatment, some patients experience unfavorable outcomes, including recurrence, metastasis, and reduced survival. In this context, the development of accurate prognostic tools for treatment personalization is particularly relevant. Nomograms, which integrate clinical, pathological, and molecular data, are highly valuable for risk stratification and clinical decision-making [5,6].

Therefore, the aim of our study was to develop and validate a nomogram for predicting the risk of BC progression within 5 years from the start of treatment.

Materials and Methods

The study material was selected from the archives of the Pathology Department of the “Gomel Regional Clinical Oncology Dispensary” and the “Republican Scientific and Practical Center for Oncology and Medical Radiology”. The material was collected from 1987 to 2019. The study cohort consisted of 198 women with stage I–III invasive BC. Two groups were identified: without disease progression for 5 years and with BC progression (up to 5 years). The progression of the disease was considered to be the occurrence of relapse or death due to the underlying disease. Disease progression was defined as the occurrence of recurrence

or death from the primary disease. The first group included 96 patients, and the second group included 102 patients. We studied the following clinical, pathological, and immunohistochemical parameters: age, Grade (1-3), pT (1–4), number of tumor emboli in peritumoral vascular invasion (0–absent, 1–minimal, 2–moderate, 3–abundant), location by breast quadrant (1–upper-outer, 2–upper-inner, 3–lower-inner, 4–lower-outer), growth pattern (1–unifocal, 2–multifocal), histological type (1–ductal, 2–lobular, etc.), SCORE indices (1–8) for ER and PR, type of surgery (1–mastectomy, 2–breast-conserving surgery), and menopausal status (0–premenopausal, 1–postmenopausal).

Univariate and multivariate logistic regression analyses were performed using the IBM SPSS Statistics 27.0.1 software package. A P-value of <0.05 indicated a statistically significant difference. To build the nomogram for predicting disease progression, patients were randomly divided into two subsets: a training cohort and a validation cohort in a 7:3 ratio. The baseline characteristics of the validation cohort were generally consistent with those of the training cohort. The R programming language (version 4.4.2) was used to construct and validate the nomogram.

Results

To investigate potential predictors of disease progression, a multivariate analysis based on clinical, morphological, and immunohistochemical characteristics was performed in the training cohort (Table).

Table.

Clinical, morphological and immunohistochemical characteristics of patients in the training cohort

Characteristics	**Univariate Logistic Regression**		**Multivariate Logistic Regression**	**P**
	$\chi 2$	P	OR (95% CI)	
Age	1.058	0.304	-	>0.05
pT	11.197	0.011	*2.266 (1.15 - 5.160)*	*0.011*
Number of lymph nodes	23.634	<0.001	*1.950 (1.447 – 2.628)*	*<0.001*
Grade	0.964	0.326	-	>0.05
Number of tumor emboli	2.667	0.102	-	>0.05
Growth pattern	3.908	0.048	*0.068 (0.005 - 145.249)*	*0.935*
Quadrant	35.686	0.029	*0.094 (0.011 - 0.789)*	*0.029*
Histological type	2.109	0.550	-	>0.05
ER SCORE	5.414	0.020	-	>0.05
PR SCORE	4.101	0.043	-	>0.05
Type of surgery	3.912	0.048	-	>0.05
Menopausal status	0.163	0.686	-	>0.05

$\chi 2$: chi-squared test; OR: relative risk; CI: confidence interval

As shown in the table (Univariate Logistic Regression) tumor size pT (p=0.011), number of lymph nodes (p<0.001), growth pattern (p=0.048), tumor location by quadrant (p<0.001), ER SCORE (p=0.020), PR SCORE (p=0.043), and type of surgery (p=0.048) were statistically significantly associated with disease progression within 5 years.

These 7 variables were subsequently included in a multivariate logistic regression analysis. The results demonstrated that pT (p=0.011; OR: 3.266, 95% CI: 1.732-6.160), number of lymph nodes (p<0.001; OR: 1.950, 95% CI: 1.447-2.628), growth pattern (p=0.935; OR: 0.068, 95% CI: 0.005-145.249), and tumor location by quadrant (p=0.029; OR: 0.094, 95% CI: 0.011-0.789) were identified as independent factors of progression. Thus, these factors were considered risk factors for disease progression in the construction of the nomogram.

Nomogram construction

Based on the 4 risk factors identified by the multivariate analysis of the training cohort, the model was presented as a visual nomogram (Figure 1).

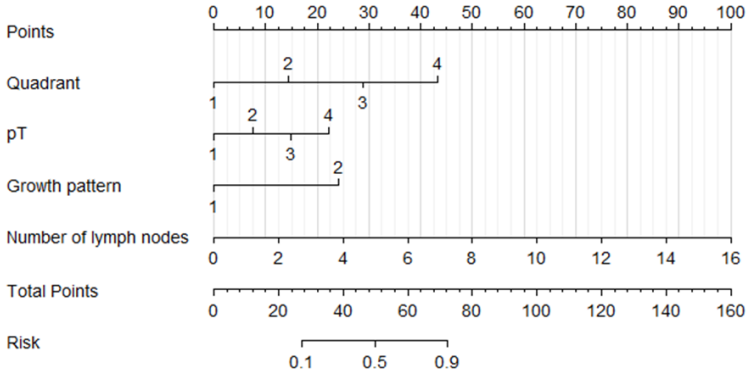

Figure 1. *Nomogram predicting the probability of disease progression*

Checking the model

To evaluate the predictive ability of the nomogram model to assess the risk of progression, we used the receiver operating characteristic curve (ROC), calibration curve, and decision analysis curve (Figure 2).

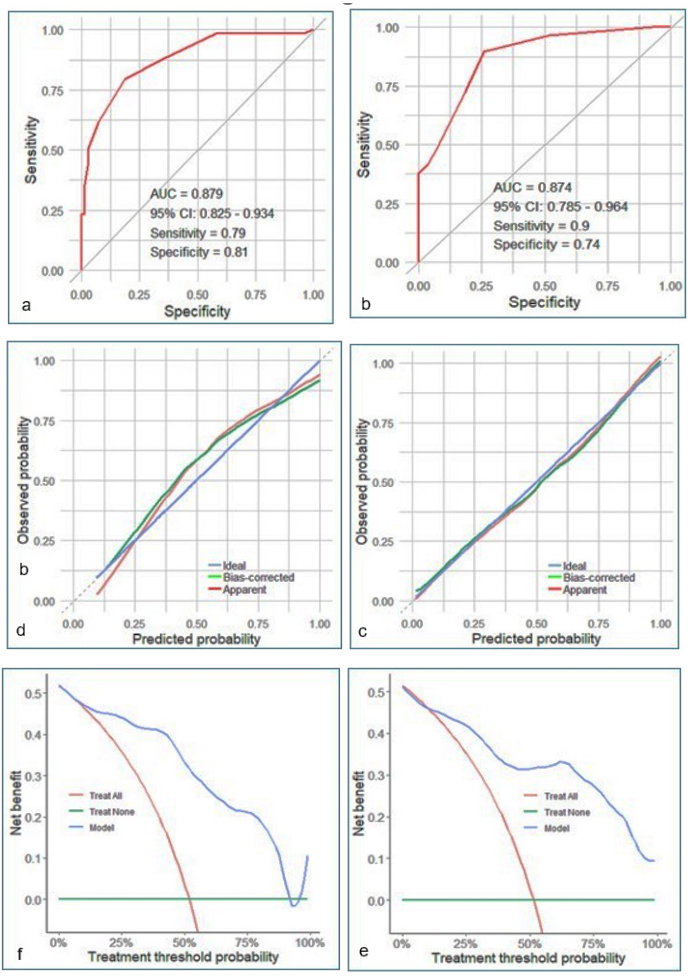

Figure 2. *Predictive ability of the nomogram model for the risk of progression.* ***a****. ROC curve for the training cohort;* ***b.*** *ROC curve for the validation cohort;* ***c****. Calibration curve for the training cohort;* ***d.*** *Calibration curve for the validation cohort;* ***e.*** *Decision curve analysis for the training cohort;* ***f.*** *Decision curve analysis for the validation cohort*

The number of lymph nodes with metastases had an equally high AUC value (0.807) in the training cohort, indicating its high predictive ability. Tumor location by quadrants (AUC 0.73) and pT (AUC 0.665) also demonstrated high predictive

ability in the training cohort. Growth pattern (AUC 0.548) had lower predictive ability. In the validation cohort, the number of lymph nodes with metastases (AUC 0.807) and pT (AUC 0.76) showed high predictive ability, while Quadrant (AUC 0.58) and Growth pattern (AUC 0.462) demonstrated lower predictive ability.

As shown in Figure 2 a, b, the area under the curve (AUC) was 0.879 (95% CI: 0.825–0.934) and 0.874 (95% CI: 0.785–0.964) in the overall training and validation cohorts, respectively. The calibration curves (Figure 2 c, d) demonstrated strong agreement between the predicted probability and observed probability in both cohorts. The Apparent and Bias-corrected lines were close to the ideal line, indicating good model calibration. The decision curve analysis (Figure 2 e, f) demonstrated greater net benefits within the 0–50% probability range in both the training and test cohorts. The probability of disease progression was most accurately predicted at a threshold of >0.5 (50%) in the training cohort and >0.75 (75%) in the test cohort. However, to increase the accuracy of determining BC cancer progression, we adopted a threshold value of 0.5 (50%). Overall, the nomogram demonstrated good discriminative and calibrating ability.

Conclusion

This study revealed that tumor quadrant location, tumor size (pT), growth pattern, and the number of lymph nodes with metastasis are independent risk factors for the progression of BC within 5 years. These factors were used to develop a nomogram. The nomogram showed good predictive performance. Despite certain limitations (being a retrospective study only) and the lack of an external validation cohort, this nomogram can be used by oncologists to identify patients at high risk of BC progression.

References

1. Global Cancer Observatory [Electronic resource] : International Agency for Research on Cancer. – URL: https://gco.iarc.fr/en. (accessed: August 17, 2025).

2. World Health Organization. Global cancer burden growing, amidst mounting need for services [Electronic resource] / World Health Organization. – Lyon, France; Geneva, Switzerland. – URL: https://www.who.int/news/item/01-02-2024-global-cancer-burden-growing--amidst-mounting-need-for-services. (accessed: August 18, 2025).

3. Kim J., [et al.] Global patterns and trends in breast cancer incidence and mortality across 185 countries // Nature Medicine. –2025. – Vol. 31. – P. 1154–1162.

4. Zhukova, L.G., Andreeva, Yu.Yu., Zavalishina, L.E. [et al.] Breast Cancer. Clinical guidelines // Sovremennaya Onkologiya [Modern Oncology]. – 2021. – Vol. 23, No. 1. – P. 5–40. (in Russian)

5. Grishina, K.A., Muzaffarova, T.A., Khaylenko, V.A. [et al.] Molecular genetic markers of breast cancer // Opukholi Zhenskoy Reproduktivnoy Sistemy [Tumors of Female Reproductive System]. – 2016. – No. 3. – P. 36–42. (in Russian)

6. Bray, F., Ferlay, J., Soerjomataram, I. [et al.] Global cancer statistics 2018: GLOBOCAN estimates of incidence and mortality worldwide for 36 cancers in 185 countries // CA: A Cancer Journal for Clinicians. – 2018. – Vol. 68, No. 6. – P. 394–424.

DOI 10.34660/INF.2025.51.44.043
UDC 616.314-089.5:615.814.1

针刺减轻利多卡因慢性毒性的实验
REDUCTION OF LIDOCAINE CHRONIC TOXICITY WITH ACUPUNCTURE IN EXPERIMENT

Pohodenko-Chudakova Irina Olegovna
Doctor of Medical Sciences, Professor, Head of Department
Belarusian State Medical University

Maksimovich Ekaterina Viktorovna
Associate Professor
Belarusian State Medical University

Kuralenya Svetlana Fyodorovna
Head of Laboratory
Minsk Clinical Consultative and Diagnostic Center

注释。本研究旨在研究在针灸实验中，颌面部局部麻醉药 2% 利多卡因盐酸盐反复注射是否有可能降低其毒性。实验在两组白色实验室小鼠上进行，用于确定化学物质的毒性和制剂的标准化，实验对象为 33 只成年雄性小鼠。所有实验动物分为两组，每 3-4 天在颌下区域注射 50 mg/kg 体重的 2% 利多卡因盐酸盐。第一组由 16 只动物组成，作为对照组。第二组由 17 只动物组成，这些动物之前已根据我们的 Su-Jok 疗法方案在动物后爪上接受过电针治疗。在实验的每个阶段，我们都收集了处死的实验动物并取出其实质器官，以进行病理形态学研究。在分析了实验结果后，我们得出结论，针刺作为预防性治疗可以显著减少利多卡因重复注射后的慢性毒性现象。

关键词：慢性毒性，局部麻醉药，利多卡因，形态测量学。

Annotation. *Aim of examination was to study the possibility of the toxicity reducing of the local anesthetic 2% lidocaine hydrochloride during its frequent repeated injections in the maxillofacial region in the experiment with acupuncture. The experiment was performed on two series of white laboratory mice used to determine the toxicity of chemicals, the standardization of preparations, on 33 adult male. All experimental animals were divided into two series which were injected every 3-4 days with 2% lidocaine hydrochloride in dose of 50 mg/kg of body weight in the submandibular region. The first series consisted of 16 animals and served as a control. The second series consisted of 17 animals who had previously received a course of electroacupuncture device on the back paw of the animals according to our scheme of Su-Jok therapy. We collected the parenchymal organs of killed and*

taken out of the experiment animals for pathomorphological study at each stage of the experiment. After having analyzed the results of experimental examinations we conclude that acupuncture as a prophylactic tretment can significantly reduce the phenomenon of chronic toxicity after repeated injection of lidocaine.

Keywords: *chronic toxicity, local anesthetics, lidocaine, morphometry.*

Introduction. The problem of drug safety now can be assigned to one of the most vital in modern medicine and pharmacy. As you know, there is no absolutely safety drugs, especially when the terms of there rational use are violated [4, 13, 14].

Local anesthesia makes an integral part of the daily work of all dentists, but the safe choice of local anesthetic remains the issue of the day.

General toxic reactions to local anesthetics are demonstrated in changes of the central nervous system (CNS) and cardiovascular system (CVS) [3, 4, 11, 13].

Due to the deterioration of the demographic situation and the current tendency towards the population aging («European statistical review for 2010» states that by 2030 the population 65 years old will consist 19% in Belarus and it was 14.1% in 2009) the number of old patients became higher who require repeated injection of local anesthetics during the oral cavity sanation for orthopedic indications. The women in the postpartum period having multiple carious sanation lesions should be included into the same group. Often, these patients want to do all the manipulations quickly and they have double local anesthetic injections, usually every 2-3 days. Old patients have a particular state of the body characterizing by reduction of compensatory and adaptive capacities. This is due to atherosclerotic changes of the coronary, cerebral, hepatic and renal vessels and functional circulation of the blood failure, decreased metabolic rate, respiratory function and the sensitivity of the respiratory center to carbon dioxide reductions appear. Renal function according to research may be reduced to 50%, the inhibition of the function of the liver is fixed which reduces the intensity of the hepatic metabolism. The excretory function of these organs is limited. Respectively, the excretion of drugs decreases, the concentrations of drugs longer circulating in the body becomes higher. Reduction of drugs distribution in the body and blood plasma binding by proteins can lead to a high concentration of drug in the blood due to the old age. It is necessary to take it into consideration when using the local anesthetics of amide type (lidocaine mepivocaine, prilocaine, bupivcaint) that are metabolizing by liver and removing by kidneys. For example, the half-value period of lidocaine is extended from 100 to 120 minutes what must be kept in mind when repeated injections of anesthetics [3, 10, 14].

Maxillofacial region being the object of stomatological treatment has a good innervation and blood supply because of its topographical and functional features,

that's why the invasive surgeries of this area cause response reactions from different parts of body systems [16].

It should be noted that population allergization which tends to rapid growth limiting the ability of the standard methods of prevention, treatment and rehabilitation of disorders is the most frequently fixed in dentistry. Therefore, actual prevention, treatment and rehabilitation methods should include not only the current level of treatment of the disease but also to consider the status of the background of the patient. The above is the basis for wider use of non-drug methods in the dental practice, in particular, acupuncture (A) [9, 15].

Acupuncture can be considered the treatment method corresponding to all requirements of modern medicine. It is effective, harmless can be combined with other methods and replace them, if necessary, such as medicaments and physical therapy treatments, used alone or in combination with preventive and treatment and rehabilitation methods. The successful use of acupuncture in clinical practice is confirmed by a significant number of papers. In 1980 the WHO recognized the acupuncture as scientifically well-grounded and recommended it for use in the world care practice [1].

The mechanism of therapeutic and prophylactic effect of acupuncture is neurohumoral factor that may have an impact on the vasculature and on the activity of reparative processes in tissues. Acupuncture, focusing on the common and local pathogenetic mechanisms of toxic reactions, contributes the recovery of the physiological and morphological homeostasis. The result is the elimination of the pathogenic effects, the normalization of the immune and emotional status of the patient, the stimulation of reparative processes of the body [1, 15].

All this points to an interest of dentists in application of acupuncture in daily practice as an independent method of treatment and in a complex of preventive and rehabilitation treatment.

One of main clinical researches is related to the study of pathological changes in the body during acute and chronic toxic effects of certain drugs and the search for ways to prevent them. Experiments provide substantial help in studying the mechanisms of morphological and functional complications of acute and chronic toxicity of drugs including dental. They allow tracking the dynamics of pathological changes in the body, to understand and describe the development of pathological processes on the system, organ, cell levels which is a main condition for the development of effective methods of prevention. The toxicity of chemicals modeling is often performed in rodents. White laboratory mice, which are home albino gray mouse is usually used to determine the toxicity of chemicals and standardization of pharmaceutical preparations. Preference is given to males in toxicology studies, since they do not show sharp and significant changes in hormone levels.

Most sources of specialized information highlights that during the experimental study of toxicity of caused pathology, special attention should be given to ways of modeling the concentrations of toxic substances, corresponding to the real conditions of clinical practice. In the study of the absolute majority of drugs, including the local anesthetics, we used the method of intraperitoneal injection in preclinical studies. However, it should be noted that all dental procedures performed in the maxillofacial region, have different intensity of vascularization and innervation, as well as proximity of the CNS. Now, 2% lidocaine hydrochloride is one of the most accessible and commonly used local anesthetics in daily dental practice in the Republic of Belarus. In the available domestic and foreign literature found no information on the results of a comparative evaluation of morphological changes in different types of 2% lidocaine hydrochloride injection in experiment [2, 7].

Lidocaine belongs to the amide anesthetics - xylidine (tertiary amines with aromatic moiety containing two methyl groups). Amide anesthetics are metabolized in the liver by two successive reactions: oxidation which leads to the formation of polar metabolites and hydroxylated metabolites conjugation with glucuronic acid or amino acids. Lidocaine is metabolized to form monoethylglicinexylidyne and glicinexylidyne. Monoethylglicinexylidyne and glicinexylidyne remain active partly and can have toxic effects. About 10% of the injecteds dose is excreted in the urine in unchanged form [3, 4, 13].

All these facts confirm the relevance of this work and determine the expediency of studies.

Aim of examination was to study the possibility of the toxicity reducing of the local anesthetic 2% lidocaine hydrochloride during its frequent repeated injections in the maxillofacial region in the experiment with acupuncture.

Objects and methods. The experiment was performed on two series of white laboratory mice used to determine the toxicity of chemicals, the standardization of preparations, on 33 adult male of white mice weighing 22-35 grams. Animals were obtained from the nursery of the Central Research Laboratory of «Belarusian State Medical University». Before the experiment the animals were two-week quarantined and kept on a standard diet. Experimental studies were carried out in accordance with the requirements governing the work with experimental animals [6] and permission of Belarusian State Medical University Committee for Bioethics. The therapeutic dose of lidocaine was calculated per unit of body weight based on the data of clinical pharmacology.

We modeled a subchronic experiment (2 weeks). All experimental animals were divided into two series which were injected every 3-4 days with 2% lidocaine hydrochloride in dose of 50 mg/kg of body weight in the submandibular region (option extraoral mandibular anesthesia access). The first series consisted of 16 animals and served as a control. The second series consisted of 17 animals who

had previously received a course of acupuncture with electroacupuncture device «Vityaz AET-01» (Republic of Belarus) on the back paw of the animals according to our scheme of Su-Jok therapy.

We studied the behavioral responses of animals during the anesthetic injection: we fixed toxic effects on the central nervous system (CNS): convulsive effects, floppiness, hemiparesis or paraparesis phenomenon, hyperactivity. We recorded the breathlessness and fixed facts of mortality.

We collected the parenchymal organs of killed and taken out of the experiment animals, including the control series, for pathomorphological study at each stage of the experiment.

Results of the study. We fixed mortality after the drug injection in the 1-series in 37.5%, in the second - 23.5%. Deaths occurred within 5 minutes after injection with pronounced symptoms of hemiparesis on the side of injection, without convulsive manifestations, sometimes during injection. All animals had shortness of breath with the auxiliary muscles participation in breath.

According to the results of pathological studies in the 1-series after five injections, the liver preparations had weak pronounced nuclear polymorphism; a few small focuses of necrosis of hepatocytes with perifocal inflammatory reaction (large number of eosinophils was fixed in the infiltrate); sparse inflammatory infiltration in some portal tracts; not sharply marked, mainly intraduct, cholestasis. In some specimens a more pronounced inflammatory response revealed in the portal tracts, determined in all portal tracts. Inflammatory infiltration was observed around the central vein. Inflammatory infiltrate was primarily represented by lymphocytes mixed with a small number of eosinophils and isolated neutrophils. We stated the more numerous small focuses of necrosis of hepatocytes (pic. 1). Eosinophilic intranuclear inclusions were revealed in some nucleuses.

Mild plethora with single diapedetic bleeding, uneven plethora glomerules, dystrophic changes in the tubular epithelium and a few small roundcells infiltrates in the interstitium were fixed in kidneys during the post mortem examination. In some preparations the number of infiltrates and their size were bigger and glomerular vascular disorders (mucoid and fibrinoid swelling) in isolated glomerules were found.

Animals of the 2nd series also had focuses of necrosis of hepatocytes with perifocal inflammatory infiltration at post mortem examination of the liver. But these changes were mostly small, single.

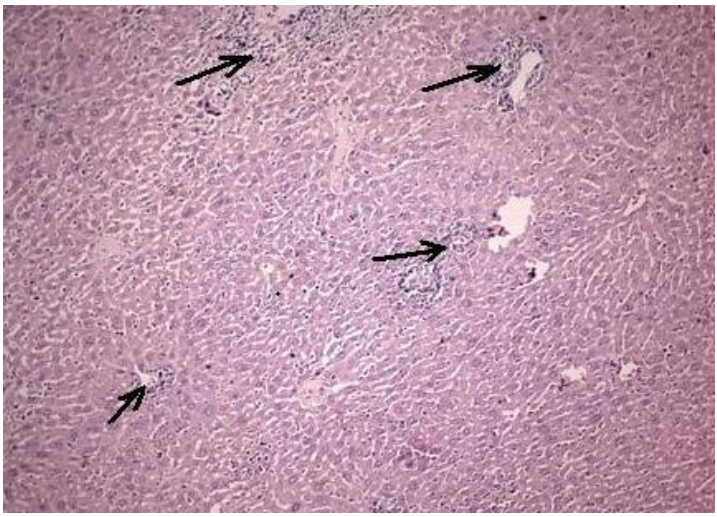

Picture 1. *Focuses of hepatitis necrosis for animals of 1st series (hematoxylin-eosin stain). Image magnification. x200*

We fixed a moderate plethora, slight inflammatory infiltration of single portal tracts. Periportal cholestasis was slightly developed. Some specimens had weakly expressed albuminous degeneration. Around the small focuses of necrosis of hepatocytes in the perifocal inflammatory infiltration we found an important number of eosinophils and neutrophils (the last were prevalent). We observed groups and short chains of cells of lymphocytes with an admixture of eosinophils and neutrophils in sinuses. Inflammatory infiltration was present in almost all portal tracts, sometimes going outside the boundary of the plate and necrosis of the surrounding tissue of the liver. The inflammatory reaction was observed also around single central veins.

During examination of kidney for the animals of the 2nd series we found focuses of petrification and packed eosinophilic masses into the collecting ducts as well as very small and single, mainly perivascular, roundcellular infiltrates in the intersticium, we fixed weak plethora.

When carrying out the morphometry examinations by method of serial sections, we discovered that the speciments of animals of the 1st series had no necrosis and had inflammatory changes in the portal tracts, cholestasis; lymphoid cells dominated among the cells of inflammatory infiltration, the number of neutrophils and eosinophils was small.

Animals of the 2nd series had less number of necrosis (pic. 2) with smaller in size (up to 1-4 cells), cholestasis was almost not expressed, a lot of eosinophils in the inflammatory infiltration, inflammation in the portal tracts was more weaker.

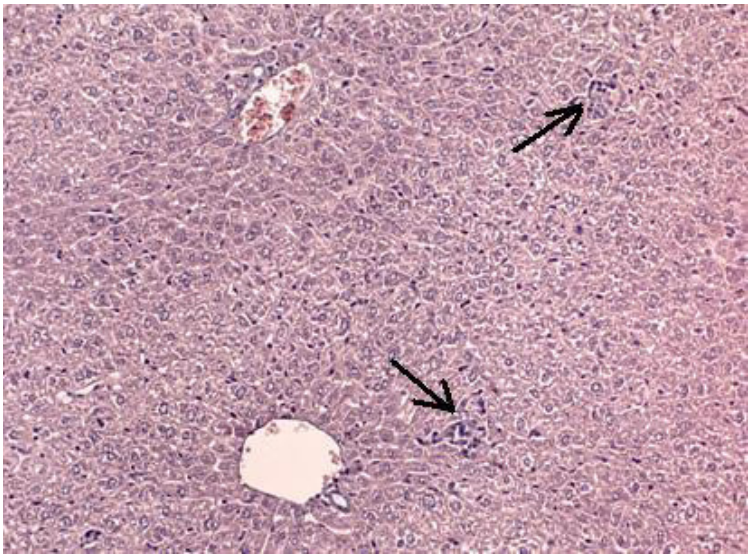

Picture 2. *Focuses of hepatitis necrosis for animals of 2nd series (hematoxylin-eosin stain). Image magnification x 200*

A quantitative comparison of the results of morphometric studies is presented in the table 1.

Table 1

Quantitative comparison of morphometric examinations results, (p<0,05).

Type of changes	1st series	2nd series
Necrosis focus of hepatocytes cells 1-2 cells	72,5%	44,3%
Necrosis focus of hepatocytes cells 3-4 cells	22,5%	17,2%
Necrosis focus of hepatocytes cells 6-8 cells	7,5%	1,43%
Periportal necrosis 2-3 cells	2,5%	1,43%
Periportal necrosis 6-8 cells	5%	1,43%
Periportal necrosis 10-14 cells	5%	-
Periportal inflammation	55%	15,7%
Periportal cholestasis	52,5%	2,86%

Hepatotoxic action of lidocaine can be explained by pharmacokinetics and pharmacodynamics of the drug. 70% of the injected drug undergoes biotransformation during the first passage through the liver. 90-95% of the lidocaine dose is metabolized in the liver by microsomal oxidases by oxidative M-dealkylation of aminogroup, hydroxylation ring, spliting of the amide bond and conjugation. The resulting metabolites (monoethylglicinexylidyne and glicinexylidyne) partly remain active and are able to have a toxic effect. Monoethylglicinexylidyne can cause convultions and glicinexylidyne – depreses the CNS. In addition, these compounds have ganglion blocking effect, influence on the blood pressure and cardiac function. During the lidocaine injection without vasoconstrictor the blood vessels dilate is rapidly absorbed what provokes the risk of side effects and shorten the drug action [5, 8, 12].

Thus, it is clear that frequent repeated injections of 2% lidocaine solution is not always safe for the body, especially during the plasma choline esterasedeficit that may occur during the involutive changes of the liver. Significant frequency of toxic effects on the central nervous system can be explained by particular features of the drug injection as well as features of innervation and vascularization of the head and neck.

At post mortem examination of the animals liver who received acupuncture treatment before injection of 2% lidocaine hydrochloride, we fixed a significant reduction of necrosis of hepatocytes focuses, reduction of eosinophilic infiltration. It demonstrated the protective effect of acupuncture.

Conclusion. After having analyzed the results of experimental examinations we conclude that acupuncture as a prophylactic tretment can significantly reduce the phenomenon of chronic toxicity after repeated injection of lidocaine.

References

1. Acupuncture / under total. ed. Hoang Bao Chau, Quang La Nyepi, transl. from Vietnam. P.I. Aleshin. M., Medicine, 1988.

2. Astakshin E.A. Guidance on laboratory animals and alternative models in biomedical technologies. M., «Standartinform», 2010.

3. Baard J.A., Brand H.S. Local anesthesia in dentistry: Transl. from English. M., «Med. Lit.», 2010.

4. Belousov Y.B., Gurevitch K.G. Clinical pharmacokinetics. The practice of drugs dosing: special issue a series «Rational Pharmacotherapy». M., «Litterra», 2005.

5. Bircher A.J. Delayed-type hypersensitivity to subcutaneous lidocaine with tolerance to articaine: confirmation by in vivo and in vitro tests. Contact Dermatitis 34 (6): 387-389, 1996.

6. Denissov S.D., Morozkina T.S. Requirements for scientific experiment with animals. Health 4: 40-42, 2001.

7. Fisenko V.P. Guidelines for experimental (preclinical) studies of new pharmacological substances. M., ZAO IIA «Remedium», 2000.

8. Harbaugh R.U. Guidelines for experimental (preclinical) studies of new pharmacological substances. M., OAO «Ed. Of» Medicine»», 2005.

9. Katikova O.U. Liver diseases in the middle age, clinical manifestations. Pathogenesis, Treatment. Clinical Gerontology 7, 2004.

10. Kutsenko S.A. Fundamentals of toxicology: manual. - St. Petersburg, Military Medical Academy named after SM Kirov, 2002.

11. Polovinkin L.V. Requirements for experimental studies for primary assessment of toxic substances and hygienic regulation: Statement 1.1.-11-12-35-2004. Minsk, 2004.

12. Stolyarenko P.Y. History of the lidocaine. Samara, Samara State Medical University, 2001.

13. Verstakova O.L., Arzamastsev E.V. High-quality pre-clinical toxicological study of drugs on the licensing stage - the basis of safety clinical trials and medical application of drugs. Bull. scientific. center ekspert. sources med. appl. 1: 28-33, 2006.

14. Verstakova O.L., Kalyanova N.A., Zhogoleva I.B., Syubaev R.D. Modern approaches to the pre-registration toxicological examination of generic medicines. Bull. scientific. center ekspert. sources med. appl. 1: 17-22, 2007.

15. Vogralik V.G., Vogralik M.V. Acupuncture (puncture reflexology). Gorkiy, Volga-Vyatka Publishers, 1978.

16. Vorobyev A.L. Clinical anatomy and operative surgery of the head and neck. St. Petersburg, Albe, 2008.

DOI 10.34660/INF.2025.32.31.044

胃内容物微量吸入对支气管肺发育不良发生发展及病程的影响
EFFECT OF MICROASPIRATION OF GASTRIC CONTENTS ON THE DEVELOPMENT AND COURSE OF BRONCHOPULMONARY DYSPLASIA

Bryksina Evgeniya Yurievna
Doctor of Medical Sciences, Professor
Rostov State Medical University

Letifov Gadzhi Mutalibovich
Doctor of Medical Sciences, Professor, Head of Department
Rostov State Medical University

Bryksin Vladislav Serafimovich
Neonatologist, anesthesiologist-resuscitator
"City Clinical Emergency Hospital" in Taganrog

Olgeiser Ekaterina Valerievna
Pediatric student
Rostov State Medical University

摘要：支气管肺发育不良 (BPD) 因其重要的临床意义，在新生儿疾病结构中占有特殊地位。鉴于支气管肺系统与胃肠道在胚胎起源上的共性，以及新生儿抗反流机制不成熟、多种因素导致胃内容物微量误吸的情况下，其结构和功能之间具有密切的联系，有必要研究该病理对 BPD 病程的影响程度。

关键词：支气管肺发育不良、微量误吸、新生儿、胃蛋白酶、反流。

Abstract. *Bronchopulmonary dysplasia (BPD) occupies a special place in the structure of neonatal morbidity due to its high clinical significance. Given the structural and functional relationship between the bronchopulmonary system and the gastrointestinal tract, due to the commonality of embryonic origin, as well as the high frequency of gastrointestinal dysfunctions in the neonatal period against the background of immaturity of antireflux mechanisms and the presence of a wide range of factors that contribute to the microaspiration of gastric contents, it is advisable to study the degree of influence of this pathology on the course of BPD.*

Keywords: *bronchopulmonary dysplasia, microaspiration, neonates, pepsin, reflux.*

One of the main morphological changes in the bronchopulmonary system in BPD is focal fibrous degeneration of the lung tissue with the development of deformation of the bronchial tree and hyperinflation of neighboring areas [1, 2]. The damaging effect of components of duodenal and gastric origin, due to microaspiration, consists in inactivation of surfactant, stimulation of local inflammatory response and prolongation of the infectious-inflammatory process, thereby contributing to fibrous remodeling of lung tissue against the background of weak reparative abilities of a premature baby [3]. Bronchopulmonary pathology combined with microaspiration in the neonatal period are aspiration pneumonia, bronchospastic conditions, possible respiratory rhythm disturbance and apnea. Microspiration is accompanied by damage to the mucous membrane of the respiratory tract throughout, as well as the epithelium of the alveoli. The endothelium of the microvasculature of the lungs is involved in the pathological process, with an increase in vascular permeability and the development of interstitial edema, accumulation of fluid in the alveolar cavity, which leads to impaired gas exchange function [4, 5]. Thus, the combined bronchopulmonary and gastrointestinal pathology interact with each other in the type of mutual burden, which makes it necessary to take an integrated approach in solving pathogenetic, clinical, diagnostic and treatment-rehabilitation issues.

The aim of the work is – determining the frequency of development and features of the course of bronchopulmonary dysplasia in children with verified mycoaspiration of gastric contents.

Materials and methods

The study included 373 children, aged 1 day to 4 months of life, who were on mechanical ventilation in the neonatal period. Depending on the gestation period, patients were divided into groups: Group 1 included 44 infants of which 22 were full-term infants (subgroup 1A) and 21 infants born at 35-37 weeks of gestation (subgroup 1B), group 2 was represented by 185 infants: 77 full-term infants (subgroup 2A) and 108 infants born at 34-32 and 31-29 weeks of gestation (subgroup 2B), group 3 included 47 infants with gestational less than 29 weeks. The comparison group, comparable in age at the beginning of the study, gender, HB, duration of mechanical ventilation after birth, concomitant diseases with the main study groups, consisted of 97 children who did not have microaspiration of gastric contents: 1 group - 25 full-term children; Group 2 - 22 children with a gestation period of 37-35 weeks; Group 3 - 31 children with a gestation period of 34-32 and 31-29 weeks; Group 4 - 19 children, with a gestation period of less than 29 weeks.

Diagnosis of microaspiration of gastric contents was carried out using the developed method of pepsin isolation in TBA (patent No. 2480753) [13]. The diagnosis of BPD was established on the basis of clinical and radiological criteria [14] . Statistical processing of the study results was carried out using the Statistica 15 for Windows program (Stat Soft).

Results and its discussion

According to the dynamic determination of pepsin activity in TBA, the maximum extinction values in group 1 were noted on days 10-14 of the study: 0.539 ± 0.024, followed by a decrease. In patients with a gestation period of 34-29 weeks and less than 29 weeks, the level of pepsin activity increased over time and in long-term ventilated children on day 21 of the study were 1.133 ± 0.012 and 1.647 ± 0.022, respectively. The greatest extinction values of 1.647 ± 0.022 occurred in children in group 3, whose gestation period was below 29 weeks.

The study revealed that in children with microaspiration, the incidence of BPD at all degrees of gestational maturity significantly exceeded the corresponding indicators in the comparison group ($p = 0.004$) and increased as the gestational age decreased ($p = 0.00026$). Thus, the number of children suffering from BPD in groups 1, 2 and 3 was 27.3%, 31.3%, 95.7%, respectively. Whereas in the comparison group in groups 1, 2, 3 and 4, these indicators were 4.0%, 27.3%, 32.3% and 63.2%, respectively.

The severity of the course of BPD increased in proportion to a decrease in the gestation period and an increase in the severity of microaspiration of the gastric contents. Thus, the maximum number of cases of severe BPD in children with microaspiration was noted in group 3. Patients in the comparison group at all gestational ages were distinguished by the absence of severe cases and statistically significant ($p < 0.0005$) prevalence of mild BPD. It should be noted that in children born at the same gestational age, but with different extinction values in TBA, a more severe course of BPD occurred with greater pepsin activity ($p = 0.0035$).

According to the results of the analysis of the structure of BPD, in the studied population of children there was a predominance of the classical form of BPD of prematurity, but the distribution of the number of children with this form of BPD, as well as with BPD of full-term and “new” BPD was statistically significantly different in children with microaspiration of gastric contents and without it. So the structure of BPD in the main groups of the study was as follows: BPD of full-term babies - 8.7%, the classic form of BPD of prematurity - 77.4%, “new” BPD - 13.9%. In the comparison group, these indicators were: 3.4%, 65.5% and 31.0%, respectively.

Pulmonary hypertension in patients with microaspiration had a brighter and more stable radiographic pattern, which, in particular, was associated with pronounced connective tissue remodeling of the interstitium, as well as structural components of the vascular wall with hypertrophy of its smooth muscle membrane.

As shown by follow-up over 3 years, in children with microaspiration of gastric contents, such outcomes of BPD as bronchial asthma, recurrent bronchitis, chronic bronchitis, local pneumofibrosis occurred in 27.8%, 31.3%, 13.9%, 48.7%

of cases, respectively, clinical recovery was noted in 0.9% of patients. In the comparison group, the distribution of BPD outcomes was reversed and the main number of patients (55.2%) had clinical recovery at the end of 3 years of life; bronchial asthma, recurrent bronchitis, local pneumofibrosis occurred in a significantly ($p < 0.005$) lower percentage of cases: 17.2%, 24.1%, 10.3%, none of the patients had chronic bronchitis.

Conclusions. Thus, the data obtained indicate an important role of microaspiration of gastric contents in the etiopathogenesis of BPD due to acid-peptic effects on the structures of the tracheobronchial tree and interstitium with the development of an inflammatory reaction and subsequent fibrous transformation of the lung parenchyma. Based on the results of the study, the following conclusions can be drawn:

1. Patients born prematurely showed an earlier increase and less pronounced regression in the number of cases of microaspiration of gastric contents compared to full-term babies.

2. Pepsin activity in tracheobronchial aspirate increased as gestational age decreased at birth with maximal rates in infants born at less than 29 weeks gestation.

3. Maximum extinction values in groups 1 and 2 of the study were observed from days 10 to 14 of the study, while in group 3 the highest pepsin activity was recorded on day 21, which indicated the progressive nature of microaspiration of gastric contents in children born at a gestational age of less than 29 weeks.

4. In children with microaspiration of gastric contents, BPD developed in a significantly greater number of cases and was characterized by a more severe course and predominance of the clissic form of BPD in prematurity.

5. At the end of 3 years of life, 55.2% of children with BPD without microaspiration of gastric contents had clinical recovery, while in patients with microaspiration this outcome occurred only in 0.9% of patients with BPD.

References

1. State of health of children of modern Russia. A.A. Baranov, V.YU. Al'bickij, L.S. Namazova-Baranova, R.N. Terleckaya. Moscow: Pediatr, 2018. - 116 p. ISBN 978-5-6042577-1-5.

2. Chahin N., Yitayew M.S., Richards A., Forsthoffer B., Xu J., Hendricks-Muñoz K.D. Ascorbic acid and the premature infant // Nutrients. - 2022. - V. 14. - No 11: 2189. doi: 10.3390/nu14112189.

3. Tauzin M., Gouyon B., Liu J., Lapillonne A., Lorrain S., Bellaiche M., Jung C. Prescriptions of anti-reflux drugs in neonatology and neonatal intensive care units: A large multicentre observational study (2014-2022) // British Journal of

Clinical Pharmacology. - 2024. - V. 90. - No 12. – pp. 3201-3211. doi: 10.1111/bcp.16198.

4. Nelson S.P., Chen E.H., Syniar G.M. et al. Prevalence of Symptoms of Gastroesophageal Reflux During Infancy A Pediatric Practice-Based Survey. Arch Pediatr Adolesc Med. 1997; 151 (6): 569-572.Anur'ev A.M., Gorbachev V.I. Hypoxic-ischemic brain lesions in preterm newborns // Journal of Neurology and Psychiatry named after S.S. Korsakov. – 2019. – V. 119. - No 8-2. – pp. 63-69. doi: 10.17116/jnevro201911908263.

5. Bryksina E.Ju Upper gastrointestinal dysfunction in neonates in relation to gastric microaspiration // Neonatology: news, opinions, training. – 2014. - No 4. – pp. 48-54.

6. Pochivalov A.V., Bryksina E.Ju., Bryksin V.S., Vasilenko D.Ju. A method for diagnosing the severity of the course of bronchopulmonary pathology against the background of gastroesophageal reflux in children on artificial ventilation. Patent for invention No. 2480753 under application No. 2012112393/15 dated 02.04.2012, priority from 02.04.2012, IPC G 01 N 33/483. – 11 p.

7. Bronchopulmonary dysplasia: Monograph / Ed. D.Yu. Ovsyannikova, N.A. Geppe, A.B. Malakhova, D.N. Degtyareva. M.: SevenPrint. - 2022. - 176 pp. ISBN: 978-5-91556-726-8.

DOI 10.34660/INF.2025.22.43.045

食管胃十二指肠镜检查提高小儿高位先天性肠梗阻综合征的诊断准确性
ADVANCING THE DIAGNOSTIC ACCURACY OF HIGH CONGENITAL INTESTINAL OBSTRUCTION SYNDROME IN PEDIATRIC PATIENTS USING ESOPHAGOGASTRODUODENOSCOPY

Marakhouski Kirill Yurjevich
Candidate of Medical Sciences, Head of Department
Republican Scientific and Practical Center for Pediatric Surgery,
Minsk, Republic of Belarus

摘要：本研究评估了食管胃十二指肠镜检查 (EGD) 在鉴别婴儿（包括新生儿）高位先天性肠梗阻 (HCIO) 类型方面的诊断潜力。“HCIO”一词用于描述一系列影响十二指肠、空肠和回肠的先天性梗阻，在英文医学术语中缺乏直接对应的术语。最接近的类似术语是“先天性十二指肠梗阻”或“不完全性十二指肠梗阻”。本研究基于内镜特征的识别和系统化，然后使用灵敏度、特异性、比值比、ROC 分析和约登指数进行统计学验证。EGD 表现出较高的诊断准确性，尤其是在十二指肠受外部结构压迫的情况下（灵敏度 100%，特异性 97%）。该方法不仅对诊断有价值，而且对手术计划也有价值，能够区分腔内和腔外的梗阻原因。研究结果支持将视觉内镜模式纳入标准化分类系统，并强调了早期胃肠道疾病 (EGD) 对疑似高位先天性肠梗阻 (HCIO) 新生儿的重要性。0.97 的约登指数证实了 EGD 作为此类诊断工具的卓越可靠性。

关键词：高位先天性肠梗阻，小儿内镜检查，十二指肠梗阻，诊断系统化，约登指数，ROC 分析。

Abstract. *This study evaluates the diagnostic potential of esophagogastroduodenoscopy (EGD) in differentiating types of high congenital intestinal obstruction (HCIO) in infants, including neonates. The term “HCIO” is used to describe a spectrum of congenital obstructions affecting the duodenum, jejunum, and ileum, and lacks a direct equivalent in English medical terminology. The closest analogs are “congenital duodenal obstruction” or “incomplete duodenal obstruction.” The research is based on the identification and systematization of endoscopic features, followed by statistical validation using sensitivity, specificity, odds ratios, ROC analysis, and Youden’s Index. EGD demonstrated high diagnostic accuracy, particularly in cases of duodenal compression from external structures (sensitivity 100%, specificity 97%). The*

method proved valuable not only for diagnosis but also for surgical planning, enabling differentiation between intraluminal and extraluminal causes of obstruction. The findings support the inclusion of visual endoscopic patterns into standardized classification systems and highlight the importance of early EGD in neonates with suspected HCIO. Youden's Index of 0.97 confirms the exceptional reliability of EGD as a diagnostic tool in this context.

Keywords: *High congenital intestinal obstruction, pediatric endoscopy, duodenal obstruction, diagnostic systematization, Youden's Index, ROC analysis.*

High congenital intestinal obstruction (HCIO) is a collective term that unites congenital obstructions of the duodenum, jejunum, and ileum. It has no direct English-language analogue; the closest terms are congenital duodenal obstruction and incomplete duodenal obstruction. HCIO syndrome is a collective term and does not have a direct coding in ICD 10. The causes of HCIO can be intraluminal (membranes, atresia, annular pancreas) or external (Ladd's syndrome, embryonic bands, volvulus). The clinical picture varies from complete obstruction with a radiographic symptom of a "double bubble" to subclinical forms.

High congenital intestinal obstruction (HCIO) is a clinically significant, but terminologically unformalized concept that unites cases of congenital obstruction of the duodenum, jejunum, and ileum. The closest English-language analogues are congenital duodenal obstruction and incomplete duodenal obstruction, but they do not cover the entire spectrum of pathologies included in CGDI. The causes of CGDI can be both intraluminal (membranes, atresia, annular pancreas) and external (Ledd's syndrome, embryonic bands, volvulus). The clinical picture varies from complete obstruction with a radiographic symptom of a "double bubble" to subclinical forms detected only by esophagogastroduodenoscopy (EGDS). Although radiography remains the main method of primary diagnosis, modern trends towards minimally invasive surgery expand the meaning of other methods, including EGDS. Its applicability is especially relevant for clarifying the anatomical cause of obstruction and planning interventions. Individual cases of diagnosing CGDI using abdominal ultrasound have been described [1]. EGDS is especially relevant when differentiating the anatomical causes of obstruction and planning interventions. Modern trends towards less invasive methods in pediatric surgery have even affected pyloric stenosis, the surgical treatment of which would seem to be maximally effective and safe. A treatment method in the form of tunnel myotomy, which is performed from the internal lumen of the stomach, has been proposed [2, 3]. In this regard, there is a need to systematize endoscopic signs obtained during EGDS in children with suspected VVKN.

Research objectives.

To improve the accuracy of diagnosis of high congenital intestinal obstruction based on the systematization (to identify common features) of the obtained en-

doscopic image (video) of changes in the duodenum in high congenital intestinal obstruction, and in high congenital partial intestinal obstruction. To assess their compliance with the anatomical forms of obstruction (intraluminal and external).

Material and methods. The study was conducted at the Republican Scientific and Practical Center for Pediatric Surgery of the Republic of Belarus (hereinafter referred to as the RSPC DS), Minsk. During the year, about 2,500 diagnostic examinations and more than 450 operations using flexible endoscopy are performed in the endoscopic room of the RSPC DS. The digital technologies used make it possible to identify pathological changes at early stages, and thoroughly monitor the course of examination or surgery, and conduct consultations during the study. Modern endoscopic equipment from Olympus and Pentax is used. The availability of small-diameter ("pediatric") endoscopes and ultra-thin endoscopes allows for safe examination and treatment of children of all age groups, including newborns. Most endoscopic interventions are performed under general anesthesia, in a hospital setting. In all cases, informed consent from parents is obtained. The study included 89 pediatric patients with suspected VCHI, of whom 81 underwent high-resolution esophagogastroduodenoscopy (EGDS).

In this study, the study group included:

- non-operated children with signs of obstruction at the level of the duodenum,
- children with a suspected level of obstruction at the level of the pylorus, while children with "classic" pyloric stenosis were not included in the study,
- children operated on for congenital duodenal obstruction who showed signs of slowing or absence of transit through the duodenum in the postoperative period,
- in all cases, the child's age should be less than 1 year.

Table 1

Main characteristics of the "High congenital intestinal obstruction syndrome" group.

Parameter	Value
Number of patients	81
Mean age	1,94 months (95% CI 1.37 – 2.51)
Median age	0,7 months
Percentage of boys	60,2%
Normal distribution	Testing denies normality of distribution (p = 0,0002)

In this group, the final diagnosis was made in most cases based on the results of surgical treatment. The total number of pediatric patients included in the group was 89 people, the mean age in days was 58.5 days 95% CI = 41.24 - 75.76 days, with a significant shift in the median at a younger age of 21.0 days. Of the 89 patients, 41 were boys (46.1%, with 95% CI from 35.4 to 57.0).

Statistical analysis revealed significant differences in age between the subgroups, reflecting the difference in pathogenesis:

Subgroup 3.1 (intraluminal obstruction): median age 6 days.

Subgroup 3.3 (pyloric stenosis): median 60 days.

Subgroup 3.4 (postoperative assessment): median 60 days. The group was divided into the following subgroups:

3.1 - with the presence of clinical signs of intraluminal obstruction at the level of the apex of the duodenal bulb and distal, verified endoscopically. The cause was an intraluminal obstruction. This group included duodenal atresia, duodenal membrane (with or without an opening), annular pancreas (33 patients or 37.1% at 95% CI = 27.1 - 48.0);

3.2 with the presence of clinical signs of intraluminal obstruction (complete or partial) at the level of the duodenum and distal, due to compression of the duodenal lumen from outside the organ, verified endoscopically. This group included: volvulus, Ledd's s-m, embryonic bands, incomplete rotation (17 patients or 19.1% at 95% CI = 11.5 - 28.8);

3.3 - children with clinical signs of VVKN (complete or partial) at the pylorus level (16 patients or 18.0% at 95% CI = 10.6 - 27.5);

3.4. - endoscopy after surgical treatment of VVKN or VVCHKN, including for the purpose of inserting an enteral tube distal to the anastomosis zone (11 patients or 12.3% at 95% CI = 11.5 - 28.8);

3.5 - - children with clinical signs of VVKN or VVCHKN, but during endoscopy the upper floor of the gastrointestinal tract was passable up to the projection of the ligament of Treitz on the duodenum (12 or 13.5% at 95% CI = 7.2 - 22.4).

Identification of common features in endoscopic images (systematization) obtained in groups 3.1 and 3.2 allowed us to distinguish the following variants: group A - presumably compression of the duodenum from outside the organ and group B - cases without compression of the duodenum (atresia). In this group of patients, it was possible to completely straighten the blind section of the duodenum and obtain a complete image of its mucous membrane. An additional analysis of 42 video recordings of EGDS was carried out to clarify the possibilities of identifying endoscopic criteria for these two variants. Additionally, 44 video recordings of endoscopies of the upper gastrointestinal tract were selected for the analysis of the systematization criteria in children from groups 3.1 and 3.2. In all cases, endoscopy was performed after an X-ray examination, which revealed signs of VVKN or VVCHKN. Video endoscopic examination was performed using a device with an external diameter of 5.4 mm and a video resolution of SD. All studies were archived and saved on the hard drive as a video file in .mkv format. One photograph was selected from each video recording that most objectively reflected the state of the mucosa when the distal end of the device was located at the most distal accessible point of the duodenum.

Results.

1. Classification and visualization: from clinical group to endoscopic pattern.

Clinical assessment.

When conducting an analysis for the presence of age differences in the group of signs of high congenital intestinal obstruction (complete or partial), the following results were obtained. The results are presented below in Table 2.

Table 2

Assessment of age differences in the selected subgroups.

Test with evaluation criteria		**Results**	
Kruskal-Wallis test			
Test statistic		25,8	
Corrected for ties		25,8	
Degrees of Freedom (DF)		4	
Significance level		P = 0,000034	
Jonckheere-Terpstra trend test			
Post-hoc analysis (Dunn)			
Test statistic		2140,5	
Standard Error		136,0	
z statistic		4,7	
P-value (two-sided)		<0,00001	
Differences in clinical signs			
Categorical factor	N	Average Rank	(P<0,05)
3.1 With the presence of clinical signs of VKD at the level of the duodenum (intraluminal obstruction)	33	28,58	(3.3)(3.4)
3.2 With the presence of clinical signs of VKD at the level of the duodenum (compression from outside the organ)	17	45,26	
3.3. 2 With the presence of clinical signs of VKD at the level of the pylorus	16	60,53	(3.1)
3.4 After surgical treatment of VKD at the level of the duodenum, for the purpose of placing a jejunal tube	11	63,77	(3.1)
3.5 In the presence of clinical signs, without endoscopic confirmation	12	51,88	

The conducted analysis shows a reliable difference in the age of EGDS, i.e. the presence of a clinic, in subgroup 3.1 (median age 6.0 days, ICR 4.0 - 16.0), in which an intraluminal obstruction was endoscopically verified (atresia of the duodenum, duodenal membrane (with or without an opening), annular pancreas) with subgroups 3.3, an obstruction at the pylorus level (median age 60.0 days, ICR 27.5 - 112.5), and 3.4, EGDS to assess the patency of the anastomosis and placement

of a nasojejunal enteral tube (median age 60.0 days, ICR 24.7 - 142.5 days). The analysis shows that this group requires further differentiation. The clinical picture of obstruction in the postpyloric zone (duodenum) develops in the first 10 days of life, and then requires EGDS to clarify the cause, and is reliably different from the slowdown in transit at the pylorus level, which develops in the period of 2 months of life and is probably associated with the so-called “late pyloric stenosis” and incomplete prepyloric membranes.

These data confirm the need for early EGDS in case of suspected intraluminal obstruction and its limited role in pyloric stenosis.

Postoperative disorders of duodenal transit are also characteristic of the age of two months, but begin to develop from the 20th day after the surgical period.

2. Identification and systematization of common elements of the endoscopic image in variants of congenital duodenal obstruction. Analysis of compliance with anatomical variants.

The systematization process consisted of two stages:

Stage I: systematization of first-order endoscopic signs.

Identification of common features in endoscopic images (systematization) obtained in groups allowed us to identify the following variants: A - presumably compression of the duodenum from the outside. The following pathological variants belong to compressions from the outside of the intestine in the group of causes of VVKN syndrome: Volvulus, embryonic cords, hyperfixation of the duodenum, Leda syndrome, incomplete rotation of the intestine. The conclusion about belonging to the group was made on the basis of the totality of the endoscopic image and the features of the “behavior” of the endoscope. In these cases, it was impossible to obtain a “tight” distension of the blind section of the duodenum / small intestine. At the same time, the video endoscope used showed the absence of movement in the distal direction (with its distal part) and the presence of signs of loop formation in the stomach. The picture from the maximum distal part of the duodenum contained a semilunar fold of the mucosa that was superimposed on the subsequent wall of the intestine. Group B – in cases assigned to this group, it was possible to obtain a complete image, due to complete distension, of the blind section of the duodenum.

Analysis of 42 EGDS video recordings allowed us to identify two types of endoscopic picture:

- Type A – signs of external compression: no tight distension, endoscope loop, semilunar fold.

- Type B – signs of intraluminal obstruction: visualization of the blind section, possibility of complete insufflation.

The analysis included 42 photographs. There were 17 boys, which amounted to 40.5%. The average age of patients at the time of EGDS (obtaining an endo-

scopic photo) was 29.5 days 95% CI 10.4110 - 48.4938, but with a median shifted to a younger age of 5.5 days. The Shapiro Wilk test denies the normality of the distribution $p < 0.0001$. In most cases, endoscopy was performed in the early neonatal period - 26 of 42 patients included in this database (61.9%), in 10 newborns (23.8%) - in the late neonatal period. In 6 cases (14.3%), the diagnosis was established later than the neonatal period. This subgroup is an example of late diagnosis of the syndrome of VVKN. The results of the systematization of signs during EGDS in comparison with the signs found after surgery are presented in Table 3.

Table 3

Systematization of signs during EGDS in comparison with the signs found after surgery.

Signs	Binomial scale (yes or no)
Signs during EGDS (Assessed value)	External cause (1-yes) internal cause (0- no) based on endoscopy results
Signs after surgery (Classification standard)	External cause (1-yes) internal cause (0- no)_ based on surgical treatment results
Area under the ROC curve (area under the ROC curve (AUC)	
Area under the ROC curve (AUC)	0,985
Standard error	=0,0147
95% Confidence interval	0,891 - 1,0
z statistics	33,0
Significance level P (Area=0.5)	<0,0001
Youden's Index)	0,97

Comment. Youden's Index is a statistical indicator used to evaluate the effectiveness of a diagnostic test. It helps determine how well the test is able to distinguish sick people from healthy people, i.e. to identify true positive and true negative cases. The range of values: 0 - The test has no diagnostic value (results are random), 1 - Ideal test (100% sensitivity and specificity), >0.5 - Good diagnostic ability, <0.5 - Limited diagnostic value.

Youden's Index was 0.9706, which means: 1 - EGDS as a diagnostic tool for IVCD has an extremely high accuracy; 2 - Almost all cases of intraluminal and external compression were correctly classified

Stage II: second-order signs.

In the group of patients classified, according to the results of surgical treatment, as "obstruction inside the organ" variants (group B). A description and systematization of common signs on endoscopic photos (videos) was carried out. The analysis of the correlation of endoscopic signs with the classification standard (the cause of intraluminal obstruction based on the surgical outcome) was performed. The intraoperatively established diagnosis was considered the classification stand-

ard. The EV group included 31 cases, the median age was 4.5 days, 95% CI 2.82–7.17, and IQR 2.0–10.0.

Since the group of first-order signs type B (compression from outside the organ) does not require and does not provide the opportunity to identify second-order signs, further analysis was focused on identifying second-order endoscopic signs in the group with an intraluminal obstruction. Six main signs and one auxiliary sign were identified based on intraluminal signs obtained using video endoscopy of the upper gastrointestinal tract in children in their first year of life.

Standardization of the sizes of the structure visualized on the mucous membrane had the following features. Since there is no device for accurately measuring the size during endoscopy, it was decided to classify the size of the structure relative to the biopsy forceps. Small size - less than or comparable to the diameter of closed biopsy forceps with a diameter of 1.8 mm. Medium size - less than or comparable to the span of the jaws of open biopsy forceps with a diameter of 1.8 mm. Large size - greater than the span of the jaws of open biopsy forceps with a diameter of 1.8 mm.

Table 4

Summary table of systematized endoscopic signs revealed during EGDS in cases of congenital duodenal obstruction.

	Sign		**Description**
1	Absence of any elements (1B) Longitudinal fold on the mucosa (2B) Small punctate or round structure (3B)	2	1 - Perforated membrane
			1 Annular pancreas
			0 - Membrane/atresia
2	Medium-sized round structure lined with heterogeneous elements (4B) Large round structure lined with heterogeneous elements (5B)	2	1 - Perforated membrane
			1 Annular pancreas
			0 - Membrane/atresia
3	Sign Absence of any elements (1B) Longitudinal fold on the mucosa (2B)	8	5 - Perforated membrane
			1- Annular pancreas
			2- Membrane/atresia
4	Small punctate or round structure (3B) Medium-sized round structure lined with heterogeneous elements (4B) Large round structure lined with heterogeneous elements (5B)	8	2 - Perforated membrane
			4- Annular pancreas
			2- Membrane/atresia
5	funnel-shaped depression (6B) Sign Absence of any elements (1B)	9	8 - Perforated membrane
			1- Annular pancreas
			0- Membrane
6	Longitudinal fold on the mucosa (2B)	2	2 - Perforated membrane
			0 - Annular pancreas
			0 - Membrane/atresia

In total, three anatomical variants of congenital duodenal obstruction were identified based on the results of the operation: perforated membrane (the predominant group) 19 cases – 61.3%, complete membrane or atresia – 5 cases (16.1%) and annular pancreas – 7 cases (22.6%)

The predominant endoscopic signs were: the presence of round structures of different sizes in almost equal proportions.

Due to the small number of cases in groups 1B, 2B and 6B (2 cases each), these groups were excluded from the analysis. To calculate the odds ratio of finding a perforated membrane in the round structure variants, atresia/complete membrane were combined with annular pancreas.

Table 5

Calculation of the odds ratio of detecting a congenital perforated membrane of the duodenum based on endoscopic signs.

	Odds ratio	
3B : 4B		P = 0,14
3B : 5B		P = 0,22
5B : 4B	24,0 (95%CI=1,7 - 330,8)	P = 0,02

Thus, the second-order features had the following characteristics. In group B (intraluminal obstruction), six endoscopic patterns were identified, including small, medium, and large round structures, funnel-shaped depressions, and longitudinal folds. The most specific feature of a perforated membrane was a large round structure with a heterogeneous lining (OR = 24.0; P = 0.0176).

It is proposed to systematize the features in the form of the scheme presented below in Table 6.

Table 6

Scheme: Systematized features of the first and second order.

Code	
Type A: External compression	Type B: Intraluminal obstruction
└ Endoscope loop	└ Dot structure (3B)
└ No bloat	└ Medium round (4B)
└ Semilunar fold	└ Large round (5B) ← most specific
	└ Funnel (6B)

Discussion.

High congenital obstruction both in the case of atresia and in the case of compression from outside the organ can be complete or incomplete. It should be remembered that the intensity of transit of food masses through the narrowed section

of the small (duodenum) intestine will determine the degree of severity of the clinical picture. This is associated with cases of late diagnosis of congenital perforated membrane of the duodenum, the larger the hole, the less pronounced the clinical picture of obstruction, up to its complete absence.

Important information for classical pediatric surgeons is the differentiation between atresia of the small intestine, variants of congenital malrotation of the small intestine, as well as variants of compression of the intestinal tube by embryonic cords, hyperfixation of the duodenum. All this suggests that the data obtained during EGDS become relevant, and in some clinical cases necessary. In addition, the systematization of endoscopic signs of VVCN or VVCN makes EGDS highly relevant for these clinical forms [4].

The presented results of EGDS assessment demonstrate high accuracy in differentiating the causes of VVCN. First-order signs allow us to determine the type of obstruction, and second-order signs - to clarify the anatomical form of the intraluminal obstruction. Visualization is especially important in the early neonatal period, when the clinical picture develops rapidly and requires immediate intervention.

Conducting ROC analysis with the calculation of the Youden index convincingly demonstrates that esophagogastroduodenoscopy can be used as a diagnostic tool in differentiating the types of high congenital intestinal obstruction (obstruction within the lumen or compression from outside the duodenum) with a sensitivity of 100% and a specificity of 97.06% relative to the classification standard (nosological form based on the results of surgical treatment). ROC analysis showed high diagnostic accuracy of EGDS: sensitivity 100%, specificity 97.06%, Youden index - 0.9706. Youden index above 0.9 is a rare indicator indicating that the test is not only sensitive, but also practically does not give false positive results.

Conclusion

EGDS has high accuracy in diagnosing the variant of EVKN obstruction (sensitivity 100%, specificity 97.06%). EGDS allows differentiating anatomical causes of obstruction at the level of external compression/intraluminal obstruction. The identified visual patterns can be included in endoscopic classifications. Of course, further studies are needed to validate the described signs in multicenter studies.

Sources Used

1. Yang B, Huang D, Zhou L, Zhong W, He Q, Wang Z, Fang Q, Wang H. The value of saline-aided ultrasound in diagnosing congenital duodenal obstruction. Pediatr Surg Int. 2020 Oct;36(10):1197-1203. doi: 10.1007/s00383-020-04723-y. Epub 2020 Jul 26. PMID: 32715324

2. Kozlov Y, Kovalkov K, Smirnov A. Gastric Peroral Endoscopic Myotomy for Treatment of Congenital Pyloric Stenosis-First Clinical Experience. J Laparoendosc Adv Surg Tech A. 2019 Jun;29(6):860-864. doi: 10.1089/lap.2018.0803. Epub 2019 Apr 23. PMID: 31017541;

3. Zhang H, Liu Z, Ma L, Li Q, Huang Y, Dong K, Ye H, Liu J, Liu H, Ren X, Yang H, Hou C, Ge K, Wang H, Zhou P, Fang Y. Gastric Peroral Endoscopic Pyloromyotomy for Infants With Congenital Hypertrophic Pyloric Stenosis. Am J Gastroenterol. 2023 Mar 1;118(3):465-474. doi: 10.14309/ajg.0000000000001973. Epub 2022 Aug 23. PMID: 36002919

4. Gfroerer S, Theilen TM, Fiegel HC, Esmaeili A, Rolle U. Comparison of outcomes between complete and incomplete congenital duodenal obstruction. World J Gastroenterol. 2019 Jul 28;25(28):3787-3797. doi: 10.3748/wjg.v25.i28.3787. PMID: 31391773; PMCID: PMC6676550

5. Kaminskaya Y, Sautin A, Marakhouski K. eP457 Endoscopic diagnostic of congenital partial high obstruction in newborns: mistakes analysis. Endoscopy 2021; 53: S247

DOI 10.34660/INF.2025.39.19.046

家庭营养状况评估是中风后患者二级预防和康复的关键要素
ASSESSMENT OF NUTRITIONAL STATUS AT HOME AS A KEY ELEMENT OF SECONDARY PREVENTION AND REHABILITATION IN POST-STROKE PATIENTS

Feofanova Tatyana Borisovna
PhD in Medical Sciences, Researcher, Cardiologist, Therapist
Federal Research Centre of Nutrition, Biotechnology and Food Safety, Moscow, Russia

Zainudinov Zainudin Musaevich
MD, chief of medicine
Federal Research Centre of Nutrition, Biotechnology and Food Safety, Moscow, Russia

摘要：中风每年影响数百万人，是第二大死亡原因，也是死亡和残疾的第三大原因。近50%的中风后患者会出现肌肉减少症。综合治疗方案已被证明具有很高的疗效，包括评估营养状况，对营养不良的患者提供高热量和高蛋白膳食，对肥胖患者提供高蛋白食品并控制每日热量摄入。通过个性化营养调整，可以减少肌肉质量损失，提高肌肉力量（握力）和运动功能，并提高生活质量。研究表明，中风后患者蛋白质摄入不足（低于0.8克/公斤体重），胆固醇和钠摄入增加，维生素D、维生素B9、钙、锌、铬和镁摄入减少。低蛋白质摄入会加重中风后患者的病情，导致各种并发症的发生，从而加重病情并影响康复前景。维生素和矿物质摄入减少会扰乱神经组织恢复、免疫功能和整体康复所需的关键生化过程。因此，评估中风后患者的营养状况是诊断蛋白质缺乏症和后续康复的关键阶段，会影响该患者群体的预后和生活质量。

关键词：中风、肌肉减少症、营养评估、家庭营养。

Abstract. *Stroke affects millions of people every year, being the second leading cause of death and the third leading cause of combined death and disability. Sarcopenia is detected in almost 50% of post-stroke patients. A comprehensive approach has shown high efficacy, including assessment of nutritional status, with the inclusion of high-calorie and high-protein meals in case of malnutrition, and high-protein products with controlled daily caloric intake in case of obesity. With individual correction of nutritional status, less muscle mass loss, increased muscle strength (grip strength) and motor function, and a higher quality of life were noted. The study revealed that post-stroke patients were found to have insufficient protein*

intake (less than 0.8 g/kg of body weight), increased consumption of cholesterol and sodium, and decreased intake of vitamin D, vitamin B9, calcium, zinc, chromium, and magnesium. Low protein intake can exacerbate the condition of post-stroke patients, lead to the development of various complications, which worsens their condition and impairs rehabilitation prospects. Reduced intake of vitamins and minerals disrupts key biochemical processes necessary for the recovery of nervous tissue, immune function, and overall recovery. Thus, assessment of the nutritional status in post-stroke patients is a crucial stage in diagnosing protein deficiency and subsequent rehabilitation, impacting the prognosis and quality of life in this patient group.

Keywords: *stroke, sarcopenia, nutritional assessment, home-based nutrition.*

Introduction.

Stroke affects millions of people annually, ranking as the second most common cause of death and the third leading cause of combined death and disability globally. The estimated global cost of stroke exceeds 721 billion US dollars (0.66% of the global GDP). In absolute numbers, over the past three decades, the global incidence of stroke has increased by 70%, prevalence by 85%, mortality by 43%, and disability by 32%, with this trend being more pronounced in low- and middle-income countries. Throughout their lives, post-stroke patients suffer from cognitive and motor impairments that affect their independence and quality of life. The spectrum of impairments - dysphagia, cognitive disorders (speech problems, impaired learning and memory, gait disturbances) - depends on the area of ischemic brain damage, the size and location of the lesion, as well as on the patient's pre-stroke health status [1,2].

Nutritional impairment is identified in 6-62% of patients at the beginning of inpatient treatment and in up to 25% of patients in the first weeks after a stroke. Sarcopenia is detected in almost 50% of post-stroke patients. Published data from cohort studies have shown an association between malnutrition and mortality within the 6-month period after a stroke, as well as a link to lower levels of functional recovery. Therefore, nutritional screening and assessment are indicated at various stages of stroke patient management. The AHA/ASA (American Heart Association/American Stroke Association), ESPEN (European Society for Clinical Nutrition and Metabolism), and Australian Clinical Guidelines for Stroke Management recommend the possible use of dietary supplements for post-stroke patients with malnutrition or at risk of developing nutritional deficiency. However, it has been established that the regular oral intake of dietary supplements by post-stroke patients in the hospital does not correlate with improved functional outcomes at 6 months after stroke. A comprehensive approach has demonstrated high efficacy; this includes nutritional status assessment, incorporating high-cal-

orie and high-protein meals in cases of undernutrition, and high-protein products with controlled daily caloric intake in cases of obesity. Individualized correction of nutritional status has been associated with less muscle mass loss, increased muscle strength (grip strength), improved motor function, and a higher quality of life [3,4]. Thus, while dietary supplements may be used for patients with nutritional impairment, there is no need for their indiscriminate use without a prior nutritional status assessment. Individualized nutritional support is crucial in post-stroke rehabilitation.

The aim of the study is to diagnose dietary patterns and assess micronutrient status disorders in overweight and obese patients who have suffered a stroke.

Materials and Methods.

A prospective comparative study was conducted in the Department of Personalized Therapy, 16 patients (9 women and 7 men) with overweight or obesity and a history of stroke into the main group (group 1).

Inclusion criteria for the study:

- age up to 73 years;
- overweight or obesity;
- stroke experienced no more than 1 year ago;
- informed consent for participation.

Exclusion criteria for the study:

- type 1 or type 2 diabetes mellitus;
- chronic heart failure (CHF III-IV FC);
- oncological diseases;
- use of any antidepressant medication.

In group 1 age of the patients was 63.3±1.6 years, ranging from 53 to 73 years (M±m). The comparison group (group 2) consisted of patients without a history of vascular events, matched for age and body weight. Analysis of the group 1 revealed class III obesity in 30% of patients, class II obesity in 9%, and class I obesity or overweight in 61% of patients. In the group 2, class III obesity was identified in 31%, class II in 15%, and class I obesity or overweight in 54% of patients. For the primary diagnosis of nutritional disorders, a computer-based assessment was conducted at home.

Statistical analysis was performed using the StatTech 4.8.11 statistics program. Results are presented as median and interquartile range (Me [Q1-Q3]) for quantitative variables. Additionally, 95% confidence intervals were calculated to assess the precision of the results.

Results

Analysis of the obtained data showed that there were no differences between the groups in terms of daily caloric intake and consumption of macronutrients - fats and carbohydrates. However, a statistically significant difference in protein

intake was noted, indicating its insufficient consumption in the group 1, amounting to less than 0.8 g/kg of body weight.

Table 1.

Assessment of total dietary caloric intake and fat consumption

Parameter	Group	M ± SD	95% confidence interval (CI)	p
Total dietary caloric, kcal	Group 2	2256.40 ± 517.12	1970.03 – 2542.77	0.795
	Group 1	2208.73 ± 455.66	1945.64 – 2471,82	
Fat, grams	Group 2	92.30 ± 29.91	75.73 – 108.86	0.185
	Group 1	106.24 ± 24.79	91.92 – 120.55	

* - p<0.05 compared to the control group

Table 2.

Assessment of protein and carbohydrate intake

Parameter	Group	Me	Q1 – Q3	p
Protein, grams	Group 2	97.67	87.41 – 103.78	0.007*
	Group 1	84.80	71.86 – 89.87	
Carbohydrate, grams	Group 2	246.16	229.05 – 299.08	0.116
	Group 1	211.61	205.50 – 235.06	

* - p<0.05 compared to the control group

Analysis of the consumption of other nutrients revealed that patients in both groups had a 68% increased intake of cholesterol, a 249% increased intake of sodium in the group 2, and a 222% increased intake in the group 1. Intake of vitamin D was reduced in both groups by 93%, vitamin B9 by 11% in the group 2 and 33.5% in the group 1; calcium by 12.3% in the group 2 and 17% in the group 1, zinc by 17% in the group 2 and 25% in the group 1, chromium by 50% in the group 2 and 72.5% in the group 1, and magnesium by 23% in the group 1.

Low protein intake can exacerbate the condition of patients who have suffered a stroke, lead to the development of various complications, which worsens their state and impairs rehabilitation prospects. A chronic deficiency of amino acids leads to a further reduction in muscle mass (which is characteristic of stroke), decreased muscle strength, slower recovery of motor functions, an increased risk of falls, and a weakened immune system. In turn, impaired nutritional status after a stroke leads to disruptions in metabolic processes, manifesting as altered oxidation rates of essential nutrients - proteins, fats, and carbohydrates - which can contribute to the development or more severe manifestation of sarcopenia. Reduced intake of vitamins and minerals disrupts key biochemical processes necessary for the recovery of nervous tissue, immune function, and overall recovery.

Thus, the assessment of nutritional status in post-stroke patients is a crucial stage in diagnosing protein deficiency and subsequent rehabilitation, impacting the prognosis and quality of life for this patient group.

References

1. Feigin, V.L., Brainin M., Norrving B., Martins S., Sacco R.L. et al. World stroke organization (WSO): global stroke fact sheet 2022. International Journal of Stroke;17(1);18-29. https://doi.org/10.1177/17474930211065917.

2. Naik N., Jenkins P., Grace P. Yang L., Prajapat S. Advances in Computational Intelligence Systems Contributions Presented at the 22nd UK Workshop on Computational Intelligence (UKCI 2023), September 6-8, 2023. Birmingham, UK. Advances in Intelligent Systems and Computing. ISBN 978-3-031-47507-8 ISBN 978-3-031-47508-5 (eBook). https://doi.org/10.1007/978-3-031-47508-5.

3. Shimazu S., Yoshimura Y., Kudo M., Nagano F., Takahiro Bise T. et al. Frequent and personalized nutritional support leads to improved nutritional status, activities of daily living, and dysphagia after stroke. Nutrition. 2021;Mar:83:111091. doi: 10.1016/j.nut.2020.111091.

4. Ko S-H., Shin Y-I. Nutritional Supplementation in Stroke Rehabilitation: A Narrative Review. Brain Neurorehabil. 2022 Mar;15(1):e3. https://doi.org/10.12786/bn.2022.15.e3.

DOI 10.34660/INF.2025.15.65.047

中风后患者身体成分评估：对功能结果和营养状况校正的预后价值
ASSESSMENT OF BODY COMPOSITION IN POST-STROKE PATIENTS: PROGNOSTIC VALUE FOR FUNCTIONAL OUTCOMES AND NUTRITIONAL STATUS CORRECTION

Feofanova Tatyana Borisovna
PhD in Medical Sciences, Researcher, Cardiologist, Therapist
Federal Research Centre of Nutrition, Biotechnology and Food Safety, Moscow, Russia

Zaletova Tatiana Sergeevna
Researcher, Cardiologist, Therapist
Federal Research Centre of Nutrition, Biotechnology and Food Safety, Moscow, Russia

摘要：中风是导致成年人残疾的最常见疾病。在三分之二的中风患者中，受损功能无法完全恢复。生物电阻抗分析 （BIA） 基于电流感应的阻抗，可以对身体成分进行全面的非侵入性评估，包括肌肉质量、脂肪质量和全身水分。在进行的研究中，超重或肥胖的中风后患者表现出肌肉质量减少（27.54 ± 4.61 千克 vs. 33.55 ± 5.98 千克），脂肪质量过剩，皮下脂肪组织百分比较高（40.47 ± 12.60 千克；43.67 ± 8.18%）。监测和纠正肌肉质量可能对中风后肌肉萎缩患者的功能恢复产生积极影响。这些结果强调需要进一步研究和开发针对此类患者的专门康复计划。

关键词：中风，肌肉减少症，身体成分，肌肉质量。

Abstract. *Stroke is a disease that most often leads to disability in the adult population. In 2/3 of patients who have suffered a stroke, incomplete recovery of impaired functions is observed. Bioelectrical impedance analysis (BIA), based on the impedance induced by electrical currents, allows for a comprehensive non-invasive assessment of body composition, including muscle mass, fat mass, and total body water. In the conducted study, post-stroke patients with overweight or obesity showed reduced muscle mass (27.54 ± 4.61 kg vs. 33.55 ± 5.98 kg), excess fat mass, and a high percentage of subcutaneous adipose tissue (40.47 ± 12.60 kg; 43.67 ± 8.18%). Monitoring and correcting muscle mass may positively impact the functional recovery of patients with muscle atrophy after a stroke. These results highlight the need for further study and development of specialized rehabilitation programs for this category of patients.*

Keywords: *stroke, sarcopenia, body composition, muscle mass.*

Introduction.

Stroke is a disease that most often leads to disability in the adult population, with approximately two-thirds of patients experiencing incomplete recovery of impaired functions. The primary system affected by stroke is skeletal muscle. Traditionally, this process has been associated with brain damage, with less attention paid to the structure, metabolism, and function of muscle tissue. Studies have shown that adaptive changes in muscle tissue structure begin as early as 4 hours after the onset of the disease, which may be linked to impaired signaling from α-motor neurons in the spinal cord. The reduction in muscle volume observed in post-stroke patients is accompanied by an increase in adipose tissue. After a vascular event, sarcopenia was detected in 53.5% of patients, and sarcopenic obesity in 28% of patients. Moreover, even comprehensive in-hospital treatment did not prevent muscle loss, which increased by approximately 30% three months after discharge but did not return to baseline levels [1-3]. Published data indicate that muscle loss occurs not only in paralyzed limbs but also in healthy ones; thus, muscle mass in post-stroke patients is significantly lower than in healthy adults. In the literature, systemic muscle loss and functional decline after stroke are referred to as "stroke-induced sarcopenia" or "stroke-related sarcopenia" [4;5]. Muscle atrophy is associated with worse clinical outcomes (mortality and physical dysfunction). Therefore, timely diagnosis of reduced muscle mass and its dynamic monitoring in the comprehensive treatment and rehabilitation of post-stroke patients is highly relevant. Bioelectrical impedance analysis (BIA), based on impedance induced by electrical currents, allows for a comprehensive non-invasive assessment of body composition, including muscle mass, fat mass, and total body fluid. According to a number of authors, the accuracy of muscle mass assessment measured using this method correlated with computed tomography results [1].

Materials and Methods.

A prospective comparative study was conducted in the Department of Personalized Therapy, 14 patients (8 women and 6 men) with overweight or obesity and a history of stroke into the main group (group 1).

Inclusion criteria for the study:

- age 40-73 years;
- overweight or obesity;
- stroke experienced no more than 1 year ago;
- informed consent for participation.

Exclusion criteria for the study:

- type 1 or type 2 diabetes mellitus;
- chronic heart failure (CHF III-IV FC);
- oncological diseases;
- use of any antidepressant medication.

The mean age of the patients main group (in group) 1 was 62.9 ± 1.5 years, ranging from 55 to 73 years (M ± m). The control group (group 2) included 13 patients without cerebrovascular disorders, with a mean age of 63.5 ± 1.2 years.

Analysis of the group 1 revealed class III obesity in 29% of patients, class II obesity in 7%, and class I obesity or overweight in 64% of patients. In the group 2, class III obesity was identified in 31%, class II obesity in 15%, and class I obesity or overweight in 54% of patients.

The groups were comparable in terms of body weight and BMI, see Tables 1-2.

Table 1.

Body weight in the study groups

Parameter	Categories	Me	Q1 – Q3	p
Body weight, kg	Group 1	90.55	83.10 – 94.65	0.356
	Group 2	92.00	88.00 – 113.30	

* - p<0.05 compared to the control group

Table 2.

Body mass index in the study groups

Parameter	Categories	M ± SD	95% confidence interval (CI)	p
Body mass index, kg/m²	Group 1	34.78 ± 6.96	30.76 – 38.80	0.486
	Group 2	36.59 ± 6.30	32.78 – 40.40	

* - p<0.05 compared to the control group

Statistical analysis was performed using the StatTech 4.8.11 statistics program. Results are presented as median and interquartile range (Me [Q1-Q3]) for quantitative variables. Additionally, 95% confidence intervals (CI) were calculated to assess the precision of the results. All patients initially underwent body composition analysis using bioelectrical impedance analysis (BIA). During the procedure, active and reactive resistance were measured. Active resistance was measured between the limbs, representing the sum of the electrical resistances of all fluids along the path of the measurement current. Reactive resistance represents the total capacitive resistance of all cell membranes along the path of the measurement current. As a result, calculated values of body composition parameters and metabolic rates were obtained, along with individually calculated normal value intervals for each parameter.

Results

Bioelectrical impedance analysis of body composition revealed a statistically significant difference between the groups in terms of muscle mass content ($p < 0.05$).

Table 3.

Assessment of muscle mass in the study groups

Parameter	Categories	M ± SD	95% confidence interval (CI)	p
Muscle mass, kg	Group 1	27.54 ± 4.61	24.88 – 30.20	0.007*
	Group 2	33.55 ± 5.98	29.93 – 37.16	

* - p<0.05 compared to the control group

Furthermore, a comparison of muscle and fat mass, as well as the percentage of subcutaneous adipose tissue (an indicator of obesity), was conducted. It was found that, despite reduced muscle mass, patients who had suffered a stroke were characterized by excess fat mass and a high percentage of subcutaneous adipose tissue, with no statistically significant differences between the groups.

Table 4.

Assessment of fat mass in the study groups

Parameter	Categories	M ± SD	95% confidence interval (CI)	p
Fat mass, kg	Group 1	40,47 ± 12,60	32,85 – 48,09	0,971
	Group 2	40.28 ± 10.62	32.11 – 48.44	
Subcutaneous adipose tissue, %	Group 1	43.67 ± 8.18	38.95 – 48.40	0.277
	Group 2	39.98 ± 9.04	34.52 – 45.45	

* - p<0.05 compared to the control group

Conclusions.

Monitoring and correcting muscle mass may positively impact the functional recovery of patients with muscle atrophy after a stroke. Comprehensive treatment for this patient group should include necessary medications, physical exercise, and nutritional status correction to increase skeletal muscle mass.

References

1. Nakanishi N., Okura K., Okamura M., Nawata K., Shinohara A. et al. Measuring and Monitoring Skeletal Muscle Mass after Stroke: A Review of Current Methods and Clinical Applications. J Stroke Cerebrovasc Dis. 2021 Jun;30(6):105736. doi: 10.1016/j.jstrokecerebrovasdis.2021.105736.

2. Yoshimura Y., Wakabayashi H., Momosaki R., Nagano F., Bise T. et al. Stored Energy Increases Body Weight and Skeletal Muscle Mass in Older, Underweight Patients after Stroke. Nutrients. 2021 Sep 19;13(9):3274. doi: 10.3390/nu13093274.

3. Li S., Gonzalez-Buonomo J., Ghuman J., Huang X., Malik A. et al. Aging after stroke: how to define post-stroke sarcopenia and what are its risk factors? Eur J Phys Rehabil Med. 2022 Oct;58(5):683-692. doi: 10.23736/S1973-9087.22.07514-1.

4. Li W., Yue T., Liu Y. New understanding of the pathogenesis and treatment of stroke-related sarcopenia. Biomedicine & Pharmacotherapy.2020;131:110721.

5. Souza J.T., Minicucci M.F., Ferreira N.C., Polegato B.F., Okoshi M.P. et al. Influence of CReatine supplementation on mUScle mass and strength after stroke (ICaRUS Stroke Trial): A Randomized Controlled Trial. Nutrients. 2024 Nov 29;16(23):4148. doi: 10.3390/nu16234148.

DOI 10.34660/INF.2025.99.54.048

银屑病合并症的患病率
PREVALENCE OF COMORBID CONDITIONS IN PSORIASIS

Guliev Magomed Okhabovich
Candidate of Medical Sciences, Head of course
Kabardino-Balkarian State University named after Kh.M. Berbekov Medical Academy

Karimova Daniia Yusufovna
Doctor of Medical Sciences, Professor
Russian Medical Academy of Continuing Professional Education of the Ministry of Health of the Russian Federation

注释：目前，银屑病被认为是一种全身性免疫炎症过程，具有显著的合并症风险。银屑病患者合并症会显著加重主要病程，降低生活质量，增加治疗费用，并增加致残风险。根据我们的数据，银屑病最常见的合并症是银屑病关节炎、甲营养不良和银屑病红皮病。所得数据突出表明，关节综合征和甲板营养不良性改变是银屑病的重要全身表现，患病率很高。这需要采用全面的跨学科方法来管理此类患者。

关键词：银屑病，合并症，跨学科方法。

Annotation. *Currently, psoriasis is recognized as a systemic immunoinflammatory process with a pronounced comorbid potential. The presence of concomitant diseases in patients with psoriasis significantly aggravates the course of the main process, worsens the quality of life, increases the cost of treatment, and increases the risk of disability. According to our data, the most common comorbid conditions in psoriasis are psoriatic arthritis, onychodystrophy, and psoriatic erythroderma. The data obtained highlight the high prevalence of joint syndrome and dystrophic changes in the nail plates as significant systemic manifestations of psoriasis. This requires a comprehensive interdisciplinary approach to the management of such patients.*

Keywords: *psoriasis, comorbid conditions, interdisciplinary approach.*

Introduction. Psoriasis has long ceased to be considered exclusively as a skin disease. Currently, it is recognized as a systemic immune-inflammatory process with a pronounced comorbid potential [4, 130]. The presence of comorbidities in patients with psoriasis significantly complicates the course of the underlying

process, worsens the quality of life, increases treatment costs and increases the risk of disability [77]. The most common are psoriatic arthritis (PsA), metabolic syndrome and cardiovascular system (CVS), which requires a comprehensive interdisciplinary approach to the management of such patients [241, 28]. Hence the need for further dynamic observations of the features of the course of psoriasis.

Objective of the study. To study the prevalence of comorbid conditions in psoriasis to justify a comprehensive interdisciplinary approach to the management of patients of this profile.

Material and methods. Data on the structure of psoriasis complications and the presence of comorbid conditions in adult patients were obtained based on the analysis of outpatient visits to the Andromeda clinic (Nalchik) for the period 2014–2023. A total of 1,687 visits from adult patients with psoriasis were registered during the specified period. The obtained data were processed using classical variation statistics methods. Results and discussion. The analysis showed that one of the most frequent and significant comorbid conditions in psoriasis is psoriatic arthritis (PsA). Our data coincide with the data of many researchers, according to which the frequency of PsA among patients with psoriasis ranges from 10 to 30%, reaching 40% in patients with a long history of the disease [207, 70, 197]. The clinical course of PsA is accompanied by pain, stiffness, joint deformation and can lead to significant disability. Often its symptoms remain undiagnosed in the early stages, which leads to a delay in the start of therapy and increases the risk of disability. Metabolic syndrome is also common among patients with psoriasis. It includes abdominal obesity, hypertension, insulin resistance, and dyslipidemia. It has been established that patients with psoriasis are 1.5–2 times more likely to suffer from obesity and type 2 diabetes mellitus compared to the general population. Psoriasis, especially in moderate and severe forms, is accompanied by chronic systemic inflammation, which contributes to the development of insulin resistance and atherogenic changes in the vascular wall. Cardiovascular diseases (CVD), including coronary heart disease, hypertension, and strokes, are also significantly more common in patients with psoriasis. Chronic inflammation, characteristic of psoriasis, is believed to accelerate the development of atherosclerosis, increase the level of C-reactive protein and other markers of vascular risk. The situation is especially unfavorable for patients with a combination of psoriasis, PsA and metabolic syndrome - the so-called “inflammatory phenotype”, in which mortality from CVD increases sharply. The presence of comorbid conditions in psoriasis significantly increases the medical and social burden. Such patients more often need observation not only by dermatologists, but also by rheumatologists, cardiologists, endocrinologists. The frequency of hospitalizations increases, the duration of stay on sick leave increases, the costs of drug treatment, including biological therapy, grow. From a social point of view, comorbidities in psoriasis

reduce the level of employment, limit professional activity and increase the risk of early loss of working capacity. Psychoemotional disorders (depression, anxiety) accompanying severe psoriasis and PsA increase patient isolation, lead to a decrease in the quality of life, and in some cases, to suicidal behavior. Additional data on the structure of psoriasis complications in adult patients were obtained based on the analysis of outpatient visits to the Andromeda clinic (Nalchik) for the period 2014–2023. A total of 1,687 visits from adult patients with psoriasis were registered during the specified period, of which 147 people (8.7%) were diagnosed with psoriatic arthritis, 187 (11.1%) with onychodystrophy, and 12 cases (0.7%) with psoriatic erythroderma. These data emphasize the high prevalence of joint syndrome and dystrophic changes in the nail plates as significant systemic manifestations of psoriasis.

The distribution of complications by age categories is especially indicative - the highest frequency of psoriatic arthritis is observed in patients aged 36-40 years (23 cases), 46-50 years (15 cases), 56-60 years (23 cases), which indicates an increased risk of articular forms of the disease starting from the third decade of life. Comparison of these results with federal data indicates a typical age-related dynamics of comorbid forms of psoriasis and emphasizes the need for early referral of patients for rheumatological examination in the presence of joint complaints.

Conclusions. The obtained data from regional clinical practice reflect the systemic nature of psoriasis, as well as the significance of onychodystrophy and arthropathy as markers of a severe and potentially disabling course of the disease. Their early diagnosis and interdisciplinary management are of fundamental importance for the prevention of disability and improving the prognosis. Detection and correction of comorbid conditions should become an integral part of modern clinical tactics for psoriasis. It is necessary to introduce multidisciplinary patient management programs and develop registries that allow taking into account not only skin manifestations, but also the systemic consequences of the disease.

References

1. Armstrong AW, Read C. Pathophysiology, Clinical Presentation, and Treatment of Psoriasis: A Review. JAMA. 2020 May 19;323(19):1945-1960. doi: 10.1001/jama.2020.4006. PMID: 32427307.

2. Rendon A, Schäkel K. Psoriasis Pathogenesis and Treatment. Int J Mol Sci. 2019 Mar 23;20(6):1475. doi: 10.3390/ijms20061475. PMID: 30909615; PMCID: PMC6471628.

3. Kubanov, A.A., Bakulev, A.L., Fitileva, T.V. et al. Disease Burden and Treatment Patterns of Psoriasis in Russia: A Real-World Patient and Dermatologist Survey. Dermatol Ther (Heidelb) 8, 581–592 (2018).

4. Arthropathic psoriasis. Psoriatic arthritis. Clinical guidelines of the Russian Society of Dermatovenerologists and Cosmetologists and the Association of Rheumatologists of Russia. 2021.

5. Duvetorp A, Østergaard M, Skov L, Seifert O, Tveit KS, Danielsen K, Iversen L. Quality of life and contact with healthcare systems among patients with psoriasis and psoriatic arthritis: results from the NORdic PAtient survey of Psoriasis and Psoriatic arthritis (NORPAPP). Archives for Dermatological Research. 2019;311(5):351-360.

6. Clinical guidelines "Psoriasis". All-Russian public organization "Russian Society of Dermatovenerologists and Cosmetologists". Approved by the Scientific and Practical Council of the Ministry of Health of the Russian Federation in 2023.

7. Kang Z, Zhang X, Du Y, Dai SM. Global and regional epidemiology of psoriatic arthritis in patients with psoriasis: A comprehensive systematic analysis and modelling study. J Autoimmun. 2024 May;145:103202. doi: 10.1016/j. jaut.2024.103202. Epub 2024 Mar 16. PMID: 38493674.

8. Bogdanova E.V., Kubanov A.A. Prediction of the timing of psoriatic arthritis development in patients with psoriasis. Medical technologies. Assessment and choice. 2023; (3): 10 17.

DOI 10.34660/INF.2025.68.15.049

呼吸道病毒性疾病合并肥胖患者生活质量研究
STUDY OF QUALITY OF LIFE IN PATIENTS WITH OBESITY AFTER RESPIRATORY VIRAL DISEASES

Zaletova Tatiana Sergeevna
Researcher, Cardiologist, Therapist
Federal Research Centre of Nutrition, Biotechnology and Food Safety, Moscow, Russia

Feofanova Tatyana Borisovna
PhD in Medical Sciences, Researcher, Cardiologist, Therapist
Federal Research Centre of Nutrition, Biotechnology and Food Safety, Moscow, Russia

Katsuba Andrey Alexandrovich
Therapist, Cardiologist
Federal Research Centre of Nutrition, Biotechnology and Food Safety, Moscow, Russia

Zainudinov Zainudin Musaevich
MD, chief of medicine
Federal Research Centre of Nutrition, Biotechnology and Food Safety, Moscow, Russia

Monisov Philip Mikhailovich
Therapist
Federal Research Centre of Nutrition, Biotechnology and Food Safety, Moscow, Russia

摘要。本研究比较了感染COVID-19（n=20）或流感（n=20）的肥胖患者（BMI≥30 kg/m²）的生活质量（QoL）和抑郁症状严重程度，并设对照组（无近期感染的肥胖个体和健康个体，每组20人）。感染后3-6个月，使用SF-36问卷和贝克抑郁量表（BDI-II）进行评估。COVID-19后组患者表现出最显著的损害：中度抑郁（24.3±5.1分 vs. 流感患者18.7±4.2分，p=0.003），SF-36的生理健康成分（52.4±11.3分）和心理健康成分（48.7±7.5分）均显著下降，CRP水平升高（7.8±2.4 mg/L）。 BMI与抑郁症（r=0.62）、BMI与身体机能（r=-0.58）以及CRP与抑郁症（r=0.51）之间存在强相关性。结果证实，与持续性炎症相关的流感相比，-COVID-19会给肥胖患者带来更严重、更持久的社会心理后果。这些发现强调了为这

类患者制定专门康复计划的必要性，其中包括心理支持和生活质量指标监测。

关键词：生活质量、COVID-19、流感、肥胖、抑郁症。

Abstract. *This study compared the quality of life (QoL) and severity of depressive symptoms in patients with obesity (BMI ≥30 kg/m²) who had contracted COVID-19 (n=20) or influenza (n=20), alongside control groups (individuals with obesity without recent infections and healthy individuals, 20 persons each). At 3-6 months post-infection, assessments were conducted using the SF-36 questionnaire and the Beck Depression Inventory (BDI-II). Patients in the post-COVID-19 group exhibited the most significant impairments: moderate depression (24.3±5.1 points vs. 18.7±4.2 for influenza, p=0.003), a marked reduction in both the physical (52.4±11.3) and mental (48.7±7.5) health components of the SF-36, and elevated CRP levels (7.8±2.4 mg/L). Strong correlations were identified between BMI and depression (r=0.62), BMI and physical functioning (r=-0.58), and CRP and depression (r=0.51). The results confirm that COVID-19 leads to more severe and prolonged psychosocial consequences in patients with obesity compared to influenza, associated with persistent inflammation. These findings underscore the necessity for specialized rehabilitation programs for this patient category, incorporating psychological support and monitoring of quality of life indicators.*

Keywords: *quality of life, COVID-19, influenza, obesity, depression.*

Introduction. Obesity is recognized as an independent risk factor for severe outcomes of both COVID-19 and seasonal influenza. However, its impact on long-term psychological consequences and quality of life (QoL) following these infections remains insufficiently studied [1]. Contemporary research indicates that patients with obesity (BMI ≥30 kg/m²) face a 2-3 times higher risk of developing post-infection depressive disorders compared to individuals with normal body weight [2, 3]. A comparative assessment of the psychosocial consequences of different respiratory infections in this vulnerable population group is thus highly relevant.

A 2023 meta-analysis revealed that symptoms of depression (Beck score ≥14 points) persist significantly more often at 6 months post-infection in obese patients after COVID-19 (34.5% vs. 18.7% in the general population) [4]. Conversely, data on the long-term impact of influenza on mental health in this patient category remain contradictory [5]. Quality of life, as assessed by the SF-36 questionnaire, in individuals with obesity following respiratory infections is characterized by a pronounced decline in both physical (PCS) and mental (MCS) health components, warranting specific investigation [6].

The **aim** of this study was to conduct a comparative analysis of quality of life and the severity of depressive symptoms in patients with obesity who had contracted COVID-19 or influenza, using standardized tools (SF-36 and Beck Depression Inventory) in the long-term period (6 months post-infection).

Materials and Methods.

A prospective comparative study was conducted in the Department of Personalized Therapy, involving 80 patients divided into 4 groups:

1. Group 1 (n=20): Patients with obesity (BMI ≥30 kg/m²) who had laboratory-confirmed COVID-19 (PCR test).
2. Group 2 (n=20): Patients with obesity (BMI ≥30 kg/m²) who had laboratory-confirmed influenza (PCR-confirmed influenza A/B).
3. Group 3 (n=20): Patients with obesity (BMI ≥30 kg/m²) without a history of respiratory infections in the last 6 months.
4. Group 4 (n=20): Control group — patients without obesity (BMI 18.5–24.9 kg/m²) and without respiratory infections.

Inclusion criteria:

- Age 18–65 years.
- For groups 1 and 2 — confirmed infection (COVID-19/influenza) within the last 3–6 months.
- Absence of severe mental disorders (based on medical records).
- Informed consent for participation.

Exclusion criteria:

- Type 1 or type 2 diabetes mellitus.
- Chronic heart failure (CHF III–IV FC).
- Oncological diseases.
- Use of any antidepressant medication.

Study limitations:

- The SARS-CoV-2 variant was not accounted for.
- Lack of long-term follow-up (assessment only at 6 months post-infection).

Group characteristics are presented in Table 1.

Table 1.

Baseline characteristics of the groups

Parameter	Group 1 (COVID + obesity)	Group 2 (Influenza + obesity)	Group 3 (Obesity only)	Group 4 (Control)	p-value
Age (years)	45.2 ± 8.1	43.7 ± 7.5	47.1 ± 6.9	44.9 ± 5.8	0.12
BMI (kg/m²)	34.5 ± 3.2	33.8 ± 2.9	32.7 ± 3.1	22.4 ± 1.7	<0.001

Quality of life (QoL) was assessed using the SF-36 questionnaire (Medical Outcomes Study Short Form-36), which includes 8 scales: Physical Functioning (PF), Role-Physical (RP), Bodily Pain (BP), General Health (GH), Vitality (VT), Social Functioning (SF), Role-Emotional (RE), Mental Health (MH). Normalized scores (0–100 points) were calculated using standard algorithms [7].

Assessment of depressive symptoms was performed using the Beck Depression Inventory (BDI-II):

A standardized 21-item questionnaire (0–63 points). Interpretation:

- 0–13 — minimal depression;
- 14–19 — mild depression;
- 20–28 — moderate depression;
- ≥29 — severe depression [8].

Anthropometric measurements were taken in the morning under standard conditions. Height was measured using a stadiometer with an accuracy of 0.1 cm, with the patient standing barefoot, heels together, back straight, and head in the Frankfurt horizontal plane. Body weight was measured on electronic scales with an accuracy of 0.1 kg in the morning on an empty stomach, with patients wearing light underwear. Body mass index was calculated using the standard formula: BMI = body weight (kg) / [height (m)]².

Venous blood sampling for C-reactive protein (CRP) determination was performed in the morning (8:00-10:00) after a 12-hour overnight fast. Blood was drawn from the cubital vein using vacuum tubes. CRP concentration was determined by immunoturbidimetric method on a biochemical analyzer. The analytical measurement range was 0.1-350 mg/L.

Statistical analysis was performed using IBM SPSS Statistics 26. The Shapiro-Wilk test was used to assess the normality of distribution of quantitative variables. As most parameters did not meet normality assumptions, nonparametric methods were employed for group comparisons. The Mann-Whitney U test was used for pairwise comparisons of independent samples. Kruskal-Wallis analysis of variance with Dunn's post-hoc test was used to assess differences between three or more groups. Correlation analyses were performed using Spearman's rank correlation coefficient. The Wilcoxon test was used for related samples. The significance level was set at $p<0.05$ for all analyses. Bonferroni correction was applied for multiple comparisons to control the type I error rate. Results are presented as median and interquartile range (Me [Q1-Q3]) for quantitative variables. Boxplots and scatter plots were used for data visualization. Additionally, 95% confidence intervals were calculated to assess the precision of the results.

Main Results.

The study revealed significant differences in quality of life indicators and the severity of depressive symptoms between the patient groups. Patients with obesity post-COVID-19 showed the most pronounced impairments: the mean Beck Depression Inventory score was 24.3±5.1, corresponding to moderate depression, which was significantly higher than in the post-influenza group (18.7±4.2, $p=0.003$), indicating a more pronounced neurotropic effect of the coronavirus infection.

Analysis of quality of life via the SF-36 questionnaire revealed a systemic deterioration across all health components in the post-COVID-19 group compared to the others. The most substantial differences were observed on the scales of: Physical Functioning: reduced to 52.4±11.3 points vs. 68.7±9.5 in the influenza group ($p<0.001$). This significant difference of 16.3 points indicates a serious and prolonged impairment in patients' daily activities. A similar pattern was observed for Vitality (45.2±8.9 vs. 57.6±7.3, $p=0.002$) and Mental Health (48.7±7.5 vs. 59.3±6.8, $p=0.001$), confirming the comprehensive negative impact of COVID-19 on all aspects of quality of life (see Table 2).

Table 2.

Comparison of depression and quality of life indicators between groups

Parameter	COVID-19 + Obesity (n=20)	Influenza + Obesity (n=20)	Obesity Only (n=20)	Control (n=20)	p-value
Beck Depression Scale	24.3 ± 5.1*†	18.7 ± 4.2*	15.2 ± 3.8	7.4 ± 2.1	<0.001
SF-36 (Physical Func.)	52.4 ± 11.3*†	68.7 ± 9.5*	72.3 ± 8.6	89.2 ± 5.4	<0.001
SF-36 (Vitality)	45.2 ± 8.9*†	57.6 ± 7.3*	63.4 ± 6.2	78.5 ± 4.8	<0.001
SF-36 (Mental Health)	48.7 ± 7.5*†	59.3 ± 6.8*	65.1 ± 5.9	82.7 ± 4.3	<0.001
CRP (mg/L)	7.8 ± 2.4*†	4.3 ± 1.7	3.9 ± 1.2	1.5 ± 0.8	0.008

* - $p<0.05$ compared to the control group

† - $p<0.05$ compared to the "influenza+obesity" group

The identified correlations are of particular interest. A strong positive correlation between BMI and the severity of depressive symptoms ($r=0.62$, $p<0.001$) supports the hypothesis of metabolically mediated mechanisms of depression development in obese patients. A concurrent inverse correlation was found between BMI and physical health component scores ($r=-0.58$, $p<0.001$), indicating a comprehensive negative impact of excess body weight on patients' functional status.

Notably, the level of systemic inflammation (CRP) in post-COVID-19 patients was significantly higher (7.8±2.4 mg/L) than in the influenza group (4.3±1.7 mg/L, $p=0.008$) and positively correlated with Beck depression scores ($r=0.51$, $p=0.003$). These data suggest that persistent chronic low-grade inflammation following COVID-19 may be an important factor contributing to the development and maintenance of depressive symptoms (Table 3).

Table 3.

Comparative characteristics of CRP and depression (BDI) correlation in the study groups

Parameter	COVID-19 + Obesity (n=20)	Influenza + Obesity (n=20)	Obesity Only (n=20)	Control (n=20)	p-value*
Correlation coefficient (r)	0.63	0.41	0.28	0.15	0.008
Mean CRP, mg/L	7.8±2.4	4.3±1.7	3.9±1.2	1.5±0.8	<0.001
Clinically significant correl.	Yes (p<0.001)	Yes (p=0.02)	No (p=0.12)	No (p=0.35)	-
Proportion of explained var. (R^2)	39.7%	16.8%	7.8%	2.3%	<0.001

*p-value for intergroup differences (ANOVA with Bonferroni correction)

The group of patients with obesity without prior respiratory infections occupied an intermediate position across all studied parameters. Although their indicators were significantly better ($p<0.05$) than those of patients post-infection, they remained significantly lower than the control group without obesity. This highlights the independent negative impact of obesity on mental health and quality of life, which is exacerbated by prior respiratory infections, particularly COVID-19.

Conclusions.

Patients with obesity following COVID-19 demonstrated clinically significant levels of depression (mean Beck score 24.3), substantially exceeding the scores of the group that had influenza (18.7 points). These findings confirm the particular neurotropic effect of SARS-CoV-2 and its long-term impact on the mental health of patients with comorbid obesity. A marked reduction was observed in all quality of life components (SF-36) in the COVID-19 group compared to other groups. A strong correlation ($r=0.62$) was identified between CRP levels and the severity of depressive symptoms, supporting the hypothesis regarding the contribution of chronic inflammation to the pathogenesis of post-infection mental disorders in obese patients. Quality of life indicators remained significantly reduced even 5-6 months after COVID-19.

This study provides compelling evidence that COVID-19 exerts a more pronounced negative impact on the mental state and quality of life of patients with obesity compared to seasonal influenza. The identified impairments are persistent and last for at least 6 months after the acute phase of the disease.

The obtained data confirm the necessity for long-term monitoring of mental health in patients with obesity after COVID-19 and the inclusion of quality of life assessment in follow-up care programs.

The study results should be considered when developing comprehensive medical and psychological rehabilitation programs for patients with obesity who have recovered from COVID-19 and other respiratory infections.

References

1. Popkin BM, et al. Individuals with obesity and COVID-19: A global perspective on the epidemiology and biological relationships. Obes Rev. 2020;21(11):e13128.

2. Stefan N, et al. Obesity and impaired metabolic health in patients with COVID-19. Nat Rev Endocrinol. 2020;16(7):341-342.

3. Anderson MR, et al. Post-COVID-19 mental health symptoms in patients with obesity: A meta-analysis. J Psychosom Res. 2023;164:111089.

4. Xue Q, et al. Persistent depression symptoms in obese COVID-19 survivors: A prospective cohort study. Lancet Psychiatry. 2022;9(10):821-832.

5. Macias AE, et al. The burden of influenza in obese patients: A systematic review and meta-analysis. Influenza Other Respir Viruses. 2021;15(6):742-751.

6. Kolotkin RL, et al. Effects of COVID-19 on quality of life in obese individuals: SF-36 results from the ACTION-IO study. Obes Sci Pract. 2023;9(1):36-45.

7. Ware JE Jr, Sherbourne CD. The MOS 36-item short-form health survey (SF-36). Med Care. 1992;30(6):473-483.

8. Beck AT, et al. An inventory for measuring depression. Arch Gen Psychiatry. 1961;4:561-571.

DOI 10.34660/INF.2025.29.93.050

治疗妊娠期妇女无症状菌尿的替代方法
ALTERNATIVE APPROACH TO THE TREATMENT OF ASYMPTOMATIC BACTERIURIA OF PREGNANT WOMEN

Kuzmina Gayane Valerievna
Lecturer
Volgograd State Medical University
Idrisova Liliya Sultanovna
Candidate of Medical Sciences, Head of Department
Volgograd State Medical University

摘要。本研究旨在比较评估草药制剂 Fitofron 单药治疗妊娠早期妇女无症状菌尿和预防妊娠期肾盂肾炎的疗效。研究对象为 40 名有习惯性流产史且确诊为无症状菌尿的孕妇（平均年龄 31.3±5.9 岁）。第 1 组 20 名孕妇服用草药制剂 Fitofron，第 2 组 20 名孕妇服用磷霉素氨丁三醇。对分离出的泌尿道病原体进行微生物学分析，并确定分离出的病原体对主要抗生素的敏感性/耐药性。疗程结束后，在对照检查中，所有患者的尿液常规分析均未发现白细胞尿和菌尿，也未发现微生物生长。推荐使用联合草药尿道感染剂作为治疗孕妇无症状菌尿的替代方法，这种方法合理且有前景。

关键词：尿路感染、无症状菌尿、妊娠、草药。

Summary. *The aim of the study was to conduct a comparative assessment of the efficacy of monotherapy with the herbal preparation Fitofron for the treatment of asymptomatic bacteriuria and prevention of gestational pyelonephritis in pregnant women in the first trimester. Forty pregnant women (mean age 31.3±5.9 years) with a history of habitual miscarriage and diagnosed asymptomatic bacteriuria were examined. 20 pregnant women in group 1 were prescribed the herbal preparation Fitofron, 20 pregnant women in group 2 - Fosfomycin trometamol. A microbiological analysis of the structure of the isolated uropathogens was performed, and the sensitivity/resistance of the isolated pathogens to the main antibiotics was determined. After the course of therapy, during a control examination, all patients showed no leukocyturia and bacteriuria in the general urine analysis, as well as no growth of microorganisms. The use of an alternative approach to the treatment of asymptomatic bacteriuria in pregnant women using combined herbal uroseptics can be recommended as reasonable and promising.*

Keywords: *urinary tract infections, asymptomatic bacteriuria, pregnancy, herbal medicine.*

One of the most common bacterial infections during pregnancy is urinary tract infection (UTI), which affects 2% - 15% of pregnant women.

The female urinary tract with a short urethra is already initially predisposed to bacterial colonization and proximal spread of infection. During pregnancy, its anatomy undergoes significant changes, hormonal and mechanical factors contribute to the expansion of the ureters, renal calyces and stagnation of urine, which further contributes to the spread of infection [1, 2].

In addition, risk factors for the development of UTI during pregnancy are considered to be young maternal age, first birth, diabetes, UTI in history, anatomical abnormalities, malnutrition and low socioeconomic status [3]. Diagnosis of asymptomatic bacteriuria, which is mandatory as part of screening in the first trimester of pregnancy, is based on the detection of bacteria in a diagnostically significant titer in two consecutive microbiological (cultural) studies of the middle portion of urine (with a difference of no more than 14 days) obtained during urination, in the absence of clinical symptoms.

UTIs during pregnancy usually follow a predictable pattern, starting with asymptomatic bacteriuria, which, if left untreated, can develop into a symptomatic infection: cystitis or pyelonephritis. Most randomized trials and meta-analyses have shown that UTIs are associated with a high risk of adverse pregnancy outcomes (pyelonephritis, chorioamnionitis, premature rupture of membranes, premature birth, low birth weight babies, postpartum endometritis, etc.) [4].

The main treatment method is antibacterial therapy aimed at eliminating asymptomatic infection [5]. However, not all antibacterial drugs can be used in pregnant women. Therefore, studies devoted to alternative methods of prevention and treatment of asymptomatic bacteriuria in pregnant women with the possibility of eliminating or reducing the duration of antibacterial therapy are of particular relevance. The aim of the study is to conduct a comparative assessment of the effectiveness of monotherapy with the herbal preparation Fitofron for the treatment of asymptomatic bacteriuria and the prevention of gestational pyelonephritis in pregnant women in the first trimester.

The study included 40 pregnant women with a history of habitual miscarriage and diagnosed asymptomatic bacteriuria at 10–12 weeks of gestation. The average age of the women was 31.3±5.9 years.

The inclusion criteria for the study were: age from 18 to 45 years; singleton pregnancy; the presence of identical bacteria in the urine at a concentration of ≥10^5 CFU/ml in two consecutive urine samples in the absence of clinical symptoms of infection; the absence of clinical symptoms of urinary tract infection (acute cystitis, exacerbation of recurrent cystitis, acute pyelonephritis, exacerbation of chronic pyelonephritis); the presence of informed consent from the patient to participate in the study.

During the examination of all patients, anamnestic data were analyzed, clinical, laboratory (microbiological), as well as ultrasound and statistical research methods were used. The sample for microbiological examination was a midstream urine sample of 50-100 ml collected in a sterile, tightly sealed container.

In order to detect bacteriuria, a urine culture study was performed for microflora to determine the qualitative and quantitative composition of the microbial component. Determination of susceptibility to antibacterial drugs was performed using the disk diffusion method in accordance with the requirements of the European Committee on Antimicrobial Susceptibility Testing.

Patients of group 1 (20 pregnant women) were prescribed the herbal preparation Fitofron as monotherapy, 2 film-coated tablets, three times a day for 1 month.

Patients of group 2 (20 pregnant women), according to clinical guidelines for the treatment of asymptomatic bacteriuria in pregnant women, took Fosfomycin trometamol 3 g once at night.

At the first stage of the study, a microbiological analysis of the structure of the isolated uropathogens was carried out.

Table 1

Frequency of detection of pathogens causing asymptomatic bacteriuria in examined women (%)

Microorganisms	Group 1 (n=20)	Group 2 (n=20)
E.coli	48,3	47,5
Enterococcus spp.	15,7	15,1
Enterobacter spp.	14,9	14,5
Klebsiella spp.	8,1	7,3
Proteus mirabilis	5,7	4,7
Staphylococcus aureus	4,6	5,1
Staphylococcus epidermidis	3,2	3,5
Streptococcus agalactiae	2,8	2,3

The leading pathogens of asymptomatic bacteriuria were predominantly gram-negative microorganisms, such as Escherichia coli, Enterococcus spp., Enterobacter spp. and Klebsiella spp., as well as gram-positive bacteria, including Staphylococcus aureus and Staphylococcus epidermidis.

At the next stage, due to the dominance of enterobacteria in the etiological structure of UTI, the sensitivity/resistance of the isolated pathogens of the order Enterobacterales was determined (Figure 1).

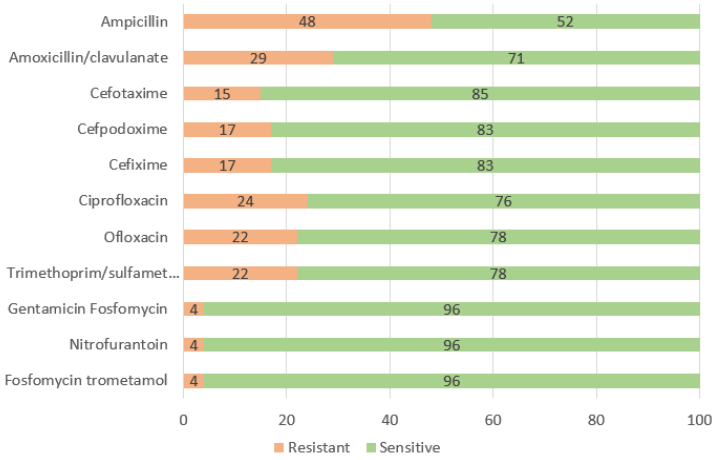

Figure 1. *Sensitivity of Enterobacteriaceae family representatives to major antibiotics*

It was found that uropathogens showed high resistance to beta-lactams (48%), third-generation cephalosporins - 15-17% and fluoroquinolones - 22-24%. In this case, the entire Enterobacteriaceae family had the highest sensitivity only to Gentamicin Fosfomycin (96%), Nitrofurantoin (96%) and Fosfomycin trometamol (96%).

Pregnant women in group 1 used the official herbal preparation Fitofron based on an extract of medicinal raw materials: centaury herb, lovage roots and rosemary leaves. Pregnant women in group 2 used Fosfomycin trometamol.

30 days after therapy, during a control laboratory examination in both groups, all patients showed no leukocyturia and bacteriuria in a general urine analysis, as well as no growth of microorganisms or growth <10^2 in a microbiological study.

During the entire observation period of the pregnant women who made up groups 1 and 2, not a single episode of adverse events from taking the drugs was detected. Throughout the entire stage of outpatient treatment of asymptomatic bacteriuria, no patients sought emergency urological care. The obtained results convincingly indicate that the use of an alternative approach to the treatment of asymptomatic bacteriuria in pregnant women using combined herbal uroseptics of complex action is justified and promising. Herbal preparations with proven effectiveness can be recommended for both the treatment and prevention of recurrent urinary tract infections during pregnancy, and, if necessary, as an addition to the main antibacterial therapy.

References

1. Habak PJ, Carlson K, Griggs, Jr RP. Urinary Tract Infection in Pregnancy. 2024 Apr 20. In: StatPearls [Internet]. Treasure Island (FL): StatPearls Publishing; 2025. PMID: 30725732.

2. Sabih A, Leslie SW. Complicated Urinary Tract Infections. 2024 Dec 7. In: StatPearls [Internet]. Treasure Island (FL): StatPearls Publishing; 2025 Jan–. PMID: 28613784.

3. Ansaldi Y, Martinez de Tejada Weber B. Urinary tract infections in pregnancy. Clin Microbiol Infect. 2023;29(10):1249-1253. doi: 10.1016/j.cmi.2022.08.015. PMID: 36031053.

4. Eshwarappa M, Rao MY, Kc G, Ms G, Swaroop A, Suryadevara S. Clinico-microbiological Profile and Outcomes of Asymptomatic Bacteriuria in Pregnancy. Indian J Nephrol. 2024;34(2):134-138. doi: 10.4103/ijn.ijn_305_21. PMID: 38681000; PMCID: PMC11044665.

5. Grant A, Bai K, Badalato GM, Rutman MP. Advances in the Treatment of Urinary Tract Infection and Bacteriuria in Pregnancy. Urol Clin North Am. 2024;51(4):571-583. doi: 10.1016/j.ucl.2024.07.001.. PMID: 39349024.

DOI 10.34660/INF.2025.68.50.051

全髋关节和膝关节置换术后患者的康复
REHABILITATION OF PATIENTS AFTER TOTAL HIP AND KNEE ARTHROPLASTY

Pletner Olga Igorevna
Head of Department
Russian Scientific Center of Surgery named after Academician B.V. Petrovsky

Karimova Daniia Yusufovna
Doctor of Medical Sciences, Full Professor
A.I. Burnazyan Federal Medical Biophysical Center" of the Federal Medical and Biological Agency of Russia

摘要：本康复方案适用于因晚期骨关节炎而接受全髋关节置换术的下肢大关节患者。该方案包括采用现代数字技术和评估工具的循序渐进、个性化康复。主要目标是恢复患者的身体活动能力，降低并发症风险，并提高患者的功能独立性和生活质量。该方案已被证明比传统康复方法更有效，值得推荐。

关键词：全髋关节置换术，康复，髋关节，膝关节。

Abstract. *The developed rehabilitation protocol is intended for patients who have undergone total endoprosthetics of large joints of the lower extremities for terminal osteoarthritis. The program includes step-by-step, individualized rehabilitation using modern digital technologies and assessment tools. The main goal is to restore physical activity, reduce the risk of complications, and increase the patient's functional independence and quality of life. The protocol has been shown to be highly effective compared to traditional rehabilitation methods and can be recommended*

Keywords: *Endoprosthetics, rehabilitation, hip joints, knee joints.*

Relevance. The increase in the incidence of deforming arthrosis and the growth of injuries are a pronounced medical and social problem, accompanied by a pronounced impairment of functionality, long-term loss of ability to work, difficulties in social adaptation of a significant proportion of the population of developed countries [1, 2, 3]. Total endoprosthetics of large joints is the most effective way to solve this problem. At the same time, for the full recovery of patients after surgery, a full-fledged system of rehabilitation measures is required [4,5].

Thus, modern rehabilitation is an important branch of health care, without which full physical and social recovery of patients after extensive surgical interventions is impossible.

Prosthetics of large joints allows the patient to return to an active lifestyle, but the success of the surgical intervention depends not only on the quality of the artificial prosthesis used and the professionalism of the operating team. Much of the responsibility for the fate of a particular patient lies with the specialists responsible for the postoperative rehabilitation of patients with an artificial joint. The task of the rehabilitation physician in the process of patient recovery after surgery is to minimize the possibility of complications and restore the patient's ability to work and social activity.

The aim of the study was to develop an optimal protocol for the rehabilitation of patients after total hip and knee arthroplasty.

Material and methods. The study included 120 patients undergoing inpatient treatment and rehabilitation after hip arthroplasty. All patients were divided into two clinical groups: the main group (n = 60), where the developed rehabilitation protocol was used, and the control group (n = 60), where the standard program was used.

The study contingent was represented mainly by older people. The distribution by age categories was as follows - 35-50 years old - 20 patients (16.7%); 51-70 years old - 64 patients (53.3%); 71 and older - 36 patients (30%).

By gender. Women - 72 patients (60%). Men — 48 patients (40%). The obtained figures correspond to the data on the epidemiology of coxarthrosis and the frequency of prosthetics in older people, especially among women.

The average body mass index in the main and control groups varied within 28.8–29.5 kg/m², which corresponds to excess body weight. A number of patients (especially in the age category 65+) had obesity of III–IV degree, which requires consideration when planning rehabilitation measures and assessing the risk of complications. The most common comorbidities were: arterial hypertension — more than 50% of cases, obesity — about 25%, diabetes mellitus type I and II (compensated forms) — 12%, fatty hepatosis, chronic pyelonephritis, hypothyroidism — singly or in combination

The presence of comorbid pathology required an individual selection of a rehabilitation program with the participation of related specialists (cardiologist, endocrinologist, etc.).

All patients were hospitalized on a planned basis by referral from a traumatologist/orthopedist after establishing indications for surgical treatment. Inclusion in the study was carried out in compliance with the principles of randomization, inclusion and exclusion criteria. For 60 patients in the control group, a retrospective analysis of the medical history was carried out, and for 60 patients in the main group, prospective observation was carried out.

Hospitalization occurred mainly in specialized traumatology and orthopedic departments. In some cases, patients were admitted after treatment in other institutions, requiring subsequent routing to the second and third stages of rehabilitation. It is noted that about 70% of patients began rehabilitation within 1-2 days after surgery; 30% of patients - with a delay of more than 3 days (usually for organizational reasons - lack of places, unpreparedness of the patient, shortage of specialists). In the main group, rehabilitation began within the framework of a personalized protocol, including early activation, functional diagnostics and the formation of target tasks.

In the control group, general schemes were used, without preliminary functional analysis and without digital monitoring of progress.

In general, the socio-demographic profile of patients corresponds to the trend of increasing number of elderly patients with degenerative-dystrophic diseases of the musculoskeletal system, which dictates the need to develop a specialized system of rehabilitation care.

Results. The developed rehabilitation protocol is intended for patients who have undergone total endoprosthetics of large joints of the lower extremities for terminal osteoarthritis. The program includes a step-by-step, individualized rehabilitation using modern digital technologies and assessment tools. The main goal is to restore physical activity, reduce the risk of complications, improve functional independence and quality of life of the patient.

The rehabilitation process is divided into three stages.

Stage I (0-3 days after surgery)

Conducted in the intensive care unit or surgery. The main objectives are the prevention of postoperative complications (thromboembolism, pneumonia, wound infection) and minimization of pain.

Measures used.

Bedside exercise therapy (breathing exercises, activation of the distal extremities);

Magnetotherapy or UHF;

Psychological support and motivation to participate in rehabilitation;

Massage that does not affect the surgical intervention area;

Initial verticalization in the absence of contraindications.

Stage II (4-10 days after surgery)

Conducted in a surgical hospital. The main focus is the formation of motor stereotypes, restoration of independent movement and self-care skills.

Measures used.

Progressive exercise therapy with a transition to exercises in a sitting and standing position;

Mechanotherapy using exercise machines;

Electro-stimulation of individual muscle groups;

Coordination and balance exercises;

Teaching the rules of safe walking and the use of assistive devices (crutches, canes).

Stage III (from 10 days to 6 months)

Is carried out in outpatient, health resort conditions or in specialized rehabilitation centers. The main goals are to restore the full range of motion, strength and endurance, develop a confident gait, and psychosocial adaptation.

Measures used.

Individual and group exercise therapy sessions;

Work with robotic systems and exoskeletons;

Use of biofeedback (BFB) to control balance and correct movements;

Telemedicine support and remote monitoring;

Training in housekeeping skills and returning to social activity.

Protocol features. Preoperative preparation (Prehab): begins before the operation and includes physical activation, psychological adjustment and teaching the patient behavior algorithms in the postoperative period. Individualization, each patient is given a detailed rehabilitation diagnosis taking into account the functions of the body, structure, activity and environmental factors.

Efficiency assessment is carried out using the Barthel, FIM, Harris Hip Score, Rivermead, VAS, EQ-5D, Leken scales, etc.

Control in the form of examinations and tests is carried out after 1, 3, 6 months and annually, more often if necessary.

The technologies used are exoskeletons with AI, digital platforms, mechanotherapeutic devices, questionnaires on the quality of life and functional independence.

Comparative characteristics of the protocols are shown in Table 3.1.

Table 3.1

Comparative characteristics of the developed and traditional rehabilitation protocols.

Rehabilitation stage	Developed protocol	Traditional protocol
Stage I (0–3 days)	Bed exercise therapy, magnetic therapy/UHF, massage, psychological support, early verticalization	General exercise therapy without early activation, minimum physiotherapy, limited verticalization

Stage II (4–10 days)	Progressive exercise therapy, mechanotherapy, electrical stimulation, coordination and balance training, safe walking training	Limited exercise therapy without individualization, no mechanotherapy, basic mobility exercises
Stage III (10 days – 6 months)	Individual and group exercise therapy sessions, exoskeletons, biofeedback, telemedicine, self-care and social activity training	Limited exercise therapy, no biofeedback and exoskeletons, rare support, no digital monitoring

Conclusions. The protocol has been clinically tested on a sample of over 100 patients and has shown high efficiency compared to traditional rehabilitation methods. It can be recommended for implementation in the practice of specialized medical institutions.

List of information sources

1. Leifer VP, Katz JN, Losina E. The burden of OA-health services and economics. Osteoarthritis Cartilage. 2022 Jan;30(1):10-16. doi: 10.1016/j.joca.2021.05.007. Epub 2021 May 20. PMID: 34023527; PMCID: PMC8605034.

2.Hunter DJ, Bierma-Zeinstra S. Osteoarthritis. Lancet. 2019 Apr 27;393(10182):1745-1759. doi: 10.1016/S0140-6736(19)30417-9. PMID: 31034380.

3. Global Burden of Disease Collaborative Network. Global burden of disease study 2019 (GBD 2019) results //Seattle. – 2020.

4. Ackerman IN, Kemp JL, Crossley KM, Culvenor AG, Hinman RS. Hip and Knee Osteoarthritis Affects Younger People, Too. J Orthop Sports Phys Ther. 2017 Feb;47(2):67-79. doi: 10.2519/jospt.2017.7286. PMID: 28142365.

5. Cieza A., Causey K., Kamenov K., Hanson S. W., Chatterji S., Vos T. (2020). Global estimates of the need for rehabilitation based on the global burden of disease study 2019: a systematic analysis for the global burden of disease study 2019. Lancet 396, 2006–2017. 10.1016/s0140-6736(20)32340-

DOI 10.34660/INF.2025.42.15.052

解痉药的分类
CLASSIFICATION OF ANTISPASMODICS

Afanasyeva Tatyana Gavrilovna
Doctor of Pharmaceutical Sciences, Associate Professor, Professor
Voronezh State Medical University named after N.N. Burdenko

Morkovin Vadim Andreevich
Postgraduate
Voronezh State Medical University named after N.N. Burdenko

注释：解痉药用于缓解器质性和功能性腹痛，帮助恢复肠道内容物的排出，并改善器官壁的血液供应[1]。腹痛在普通人群中的发病率为10%至46% [2]，这决定了研究这类药物的相关性，并考虑了解痉药的药理学（PG）、药物治疗学（PTG）和解剖治疗化学（ATC）分类的比较。

关键词：解痉药，药理学分类，药物治疗学分类，解剖治疗化学分类系统。

Annotation. *Antispasmodic drugs are used to relieve abdominal pain of organic and functional origin, help restore passage of intestinal contents and improve blood supply to the organ wall [1]. The incidence of abdominal pain ranges from 10 to 46% in the general population [2], which determines the relevance of the study of this group of drugs, taking into account the comparison of pharmacological (PG), pharmacotherapeutic (PTG) and Anatomical Therapeutic Chemical (ATC) classifications of antispasmodic drugs.*

Keywords: *antispasmodic drugs, pharmacological classification, pharmacotherapeutic classification, Anatomical Therapeutic Chemical Classification System.*

To conduct the study, we used international nonproprietary names (INN) of medicinal products (MP) related to various PG (taken from the reference books of the Register of Medicines of Russia [3] and PTG (taken from the state register of medicines, taking into account valid registration certificates at the time of 06/01/2025 [4]), the name of which combines the root is derived from the word “spasm”. All drugs related to these classifications (**n** drugs) are highlighted, of which the non-repeating INN and ATC are highlighted (Fig. 1).

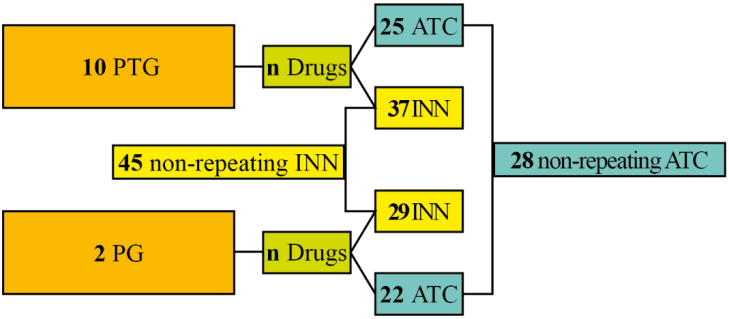

Figure 1. *Research scheme*

It has been established that the leader in the number of INN is PTG, which includes 37 INN, within the classification the leading positions are occupied by the groups antispasmodic agent of plant origin (18 INN) and antispasmodic agent (11 INN). The number of innes in the pharmaceutical group is 29, and within the classification, the leading group is 0050 myotropic antispasmodics (20 innes) (Table 1). When comparing these groups, it was found that the total number of non-repeating INN is 45.

Table 1

The number of INN in various classifications

Classification groups	Number INN
Pharmacological groups (FG)	29
0050 Myotropic antispasmodics	20
0010 Myotropic antispasmodics in combinations (subgroup)	9
Pharmacotherapeutic groups (FTG)	**37**
Analgesic non-narcotic agent + antispasmodic agent	1
Combined analgesic agent (non-narcotic analgesic agent + antispasmodic agents + barbiturate)	1
Combined analgesic agent (non-narcotic analgesic agent+ antispasmodic agent)	3
Combined analgesic agent (opioid analgesic agent+non-narcotic analgesic agent+ antispasmodic agent)	1
Analgesic antispasmodic agent combined	1
Drugs for the treatment of functional disorders of the gastrointestinal tract. Antispasmodics in combination with analgesics. Belladonna and its derivatives in combination with analgesics	1

Drugs for the treatment of functional disorders of the gastrointestinal tract; antispasmodics and holinoblockers in combination with other drugs; antispasmodics in combination with other drugs	1
Antispasmodic agent	11
Antispasmodic agent of herbal origin	18
Drugs for the treatment of functional disorders of the gastrointestinal tract; antispasmodics in combination with psycholeptics	1

Depending on the manufacturer, INN Metamizole sodium + Pitophenone + Fenpiverinium bromide refers to two PTG:

1) analgesic non-narcotic agent + antispasmodic agent;

2) combined analgesic agent (non-narcotic analgesic agent + antispasmodic agent).

INN benzocaine + belladonna leaf extract belong to two PTG:

1) drugs for the treatment of functional disorders of the gastrointestinal tract; antispasmodics and holinoblockers in combination with other drugs; antispasmodics in combination with other drugs and

2) antispasmodic agent.

There are 21 INN classifications common to PG and PTG:

1) Avisan extract dry;

2) Drotaverine;

3) Madder dye extract dry + Belladonna sum of alkaloids;

4) Mebeverine;

5) Metamizole sodium + Phenobarbital + Papaverine + Bendazole;

6) Peppermint leaf oil;

7) Peppermint leaves + Peppermint leaf oil;

8) Oxybutynin;

9) Otilonium Bromide;

10) Papaverine;

11) Papaverine + bendazole;

12) Paracetamol + Drotaverine;

13) Paracetamol + Drotaverine hydrochloride + Codeine Phosphate;

14) Pinaverium bromide;

15) Siberian fir needles oil + Peppermint leaf oil + Common hops + Wild carrot seed extract + Oregano grass extract;

16) Salicylamide + Madder dye extract dry + Canadian Goldenrod extract dry + Horsetail extract dry + Kellin + Lily of the Valley leaf glycoside;

17) Trimebutin;

18) Hop extract liquid + Carrot wild fruit extract liquid + Oregano extract liquid + Castor oil + Fir oil + Peppermint oil;

19) Madder rhizomes and roots extract;

20) Peppermint leaves;

21) common fennel fruits, which makes them the main representatives of antispasmodic medicines.

As a result, it was revealed that the total number of innes in all ATC groups (53 drugs) is more numerous than the number of INNES represented in the study (45). This is due to the registration of new drugs with the same INN by different manufacturers under different ATC. The leaders among the groups in terms of the number of INN are A03ED (6 INN) A03AX (4 INN) (Table 2).

Table 2

The number of INN in the anatomical-therapeutic-chemical classification

№	Anatomical Therapeutic Chemical (ATC)	Number INN
1	A03 - Drugs For Functional Gastrointestinal Disorders	2
2	A03A - Drugs For Functional Gastrointestinal Disorders	1
3	A03AA04 - Mebeverine	1
4	A03AA05 - Trimebutine	1
5	A03AA07 - Dicycloverine	1
6	A03AB06 - Otilonium Bromide	1
7	A03AD - Papaverine And Derivatives	2
8	A03AD01 - Papaverine	1
9	A03AD02 - Drotaverine	1
10	A03AX - Other Drugs For Functional Gastrointestinal Disorders	4
11	A03AX04 - Pinaverium	1
12	A03BA04 - Belladonna Total Alkaloids	1
13	A03C - Antispasmodics In Combination With Psycholeptics	1
14	A03DB - Belladonna And Derivatives In Combination With Analgesics	1
15	A03ED - Antispasmodics In Combination With Other Drugs	6
16	A05A - Bile Therapy	1
17	C04AX - Other Peripheral Vasodilators	2
18	C04AX11 - Bencyclane	1
19	G04B - Urologicals	1
20	G04BC - Urinary Concrement Solvents	4
21	G04BD04 - Oxybutynin	1
22	G04BX - Other Urologicals	1
23	M01AE51 - Ibuprofen, Combinations	2
24	N02BB52 - Metamizole Sodium, Combinations Excl. Psycholeptics	1
25	N02BB72 -Metamizole Sodium, Combinations With Psycholeptics	1
26	N02BE51 - Paracetamol, Combinations Excl. Psycholeptics	2
27	N02BE71 - Paracetamol, Combinations With Psycholeptics	1

28	N02CA52 - Ergotamine, Combinations Excl. Psycholeptics	1
29	There is no ATC classification	9
Total		53

Conclusion. A comparative analysis of antispasmodic drugs according to PG, PTG, and ATC classifications was performed. It was revealed that the largest number of INN is included in the composition of PTG (37 INN), within which the group of antispasmodic agents of plant origin is the leader (18 INN). The number of innes found in both PTG and PG classifications is 21. The largest group of ATC is A03ED (6 INN).

References

1. "Pharmaceutical counseling and the basics of rational pharmacotherapy for patients with gastrointestinal tract pathology : a textbook / N. V. Izmozherova, L.I. Kadnikov, E.A. Safyanik [et al.]; [under the general editorship of N.V. Izmozherova] ; Ministry of Health of the Russian Federation ; Ural State Medical University. un-T.— Title page. the screen. Yekaterinburg : UGMU, 2023. 206 p."

2. Gaus O.V., Livzan M.A., Turchaninov D.V. [et al.] Abdominal pain in young people // Russian Journal of Gastroenterology, Hepatology, and Coloproctology. - 2021. - No.

3. - pp. 26-35. 3. Register of medicines of Russia RADAR [Website]. - URL: https://www.rlsnet.ru / (Date of access: 06/01/2025). -Text: electronic.

4. The State Register of Medicines [Website].- URL: https://www.grls.minzdrav.gov.ru (Date of request: 06/01/2025). -Text: electronic.

DOI 10.34660/INF.2025.78.74.053

医疗中心在推进细胞疗法生产中的作用
THE ROLE OF MEDICAL CENTERS IN ADVANCING CELL THERAPY MANUFACTURING

Badrin Evgeny Alexandrovich
Head of Production Pharmacy
Dmitry Rogachev National Medical Research Center of Pediatric Hematology, Oncology and Immunology,
Moscow, Russian Federation

Pyatigorskaya Natalia Valeryevna
PhD of Pharmaceutical Sciences, Professor,
Corresponding Member of the RAS
I.M. Sechenov First Moscow State Medical University (Sechenov University),
Moscow, Russian Federation

摘要：细胞疗法，包括CAR-T细胞疗法和其他先进疗法药物，代表着一个快速发展的医学领域，具有巨大的治疗潜力。在医疗中心生产这些产品，为提高治疗的可及性、加速科研成果向临床实践的转化以及刺激行业增长提供了独特的机会。本文探讨了医院制造的概念，介绍了国际上的方法，分析了俄罗斯的经验，并探讨了在医疗中心开发细胞疗法生产所面临的机遇和挑战。

关键词：CAR-T细胞疗法、嵌合抗原受体、政府监管、医院豁免。

Abstract. *Cell therapies, including CAR-T and other advanced therapy medicinal products, represent a rapidly evolving field of medicine with high therapeutic potential. Manufacturing these products within medical centers provides unique opportunities to increase therapy accessibility, accelerate the translation of scientific research into clinical practice, and stimulate industry growth. This article examines the concept of hospital-based manufacturing, presents international approaches, analyzes the Russian experience, and discusses the opportunities and challenges associated with developing cell therapy production in medical centers.*

Keywords*: CAR T-Cell therapy, chimeric antigen receptor, government regulation and oversight, hospital exemption.*

Introduction

Innovative cell therapies, particularly CAR-T (chimeric antigen receptor T cells), have fundamentally transformed clinical protocols for treating hematologic malignancies, including acute lymphoblastic leukemia and lymphomas, providing high efficacy and a personalized approach. They offer individualized treatment, especially in cases of relapse and refractory disease [1].

Despite their significant therapeutic potential, the implementation of cell therapies faces several limitations, including high cost, complex logistics, and the need to adhere to strict manufacturing standards and personnel qualifications. Hospital-based manufacturing of cell therapies represents a promising strategy to overcome these barriers and accelerate the integration of innovative treatments into clinical practice.

Historical Context and Global Trends

The concept of integrating drug manufacturing within clinical centers has a long history, dating back to bone marrow transplantation in the 1960s and 1970s. At that time, hospitals prepared transplant material in-house, which allowed rapid implementation of new treatment methods [2].

With the advancement of genetic modification technologies and cell platforms, particularly CAR-T, the role of medical centers has significantly expanded. Today, leading centers in the United States, Europe, and China not only conduct clinical research but also manufacture therapies for their own patients, ensuring a personalized approach and minimizing the time between cell collection and infusion.

Hospital-Based Manufacturing as a Driver of Development

Hospital-based manufacturing of cell therapies represents a strategically important approach that fosters the development of the cell therapy field. One of the key advantages of this approach is proximity to the patient, which minimizes the time between cell collection and infusion, while also reducing the risk of losing cellular functionality during transportation. This is particularly critical for personalized therapies such as CAR-T, where each dose is derived from the patient's own cells.

Therapy personalization constitutes a second crucial factor driving the effectiveness of hospital-based manufacturing. The ability to adapt the production process to the specific biological characteristics of the patient ensures high therapeutic efficacy and reduces the risk of adverse effects. This approach also supports the concept of personalized medicine, in which treatment is tailored according to the genetic and immunological profile of each patient.

Another important aspect is integration with clinical research. Hospital-based manufacturing establishes a direct connection between laboratory development, production processes, and clinical protocols. This accelerates the translation of scientific discoveries into practice, enables rapid implementation of new technologies, and allows their adaptation to specific clinical needs.

Finally, economic efficiency represents a significant benefit. Hospital-based manufacturing reduces costs associated with logistics and large-scale industrial production, as well as expenses related to storage and transportation of cell therapies. Together, these factors position hospital-based manufacturing as a key driver of industry growth, enhancing the accessibility of innovative therapies and stimulating further development of cell medicine.

International Experience and Regulatory Aspects

Global experience in hospital-based manufacturing of cell therapies demonstrates significant diversity in approaches to organization and regulation, reflecting a balance between patient safety and the promotion of innovation. In the United States, leading academic centers manufacture CAR-T therapies directly within their institutions under strict supervision by the Food and Drug Administration (FDA) [3]. Production is conducted under the Investigational New Drug (IND) framework and in compliance with current Good Manufacturing Practice (cGMP) standards, ensuring high reliability and product quality. Moreover, integrating manufacturing processes with clinical trials enables rapid implementation of innovative therapies and adaptation to the individual needs of patients.

In Europe, hospital-based manufacturing is regulated through the hospital exemption mechanism established by European Union Regulation No. 1394/2007. This framework allows medical institutions to produce cell therapies for specific patients without obtaining marketing authorization, provided that strict GMP standards and quality control are maintained [4]. This model expands access to cell therapies in academic and specialized clinical centers while ensuring both safety and effectiveness of individualized treatments.

China demonstrates rapid development of clinical research on CAR-T and other cell therapies. Leading medical centers in the country develop hospital-based manufacturing, integrating clinical practice with research activities, which accelerates the translation of scientific findings into therapeutic applications [5]. Although the regulatory framework is less stringent compared to the United States and Europe, regulatory authorities actively promote rapid growth in production and clinical trials, creating a dynamic environment for innovation.

Russian Experience

In the Russian Federation, hospital-based manufacturing of cell therapies has emerged relatively recently, yet it has already shown significant progress. The leading center in this field is the National Medical Research Center for Pediatric Oncology, Hematology, and Immunology named after Dmitry Rogachev, which became a pioneer in implementing CAR-T therapy for children [6].

Unlike the European hospital exemption mechanism, Russia allows the production of individual biomedical cell products (iBMCP) based on a specific authorization from the Ministry of Health of the Russian Federation. This approach

enables medical institutions to manufacture therapies for their own patients while ensuring compliance with quality and safety requirements.

The Russian model of hospital-based manufacturing combines elements of academic and clinical practice with regulation aimed at minimizing patient risk. Medical centers that receive individual authorizations are required to strictly adhere to good practice standards for handling biomedical cell products and implement robust quality control and assurance systems.

Thus, the Russian experience demonstrates the gradual development of infrastructure and regulatory frameworks comparable to international practices, providing a foundation for expanding cell therapy production and integrating innovative treatment approaches into clinical practice.

Technological and Clinical Aspects

CAR-T cell manufacturing represents a complex, multi-step process that includes the collection of autologous T lymphocytes from the patient, their genetic modification using chimeric antigen receptors (CAR), cultivation under controlled conditions, quality control, and subsequent infusion into the patient. Each step is critically important: the initial quality of the cells directly affects therapeutic efficacy, while strict quality control ensures patient safety and predictable outcomes.

Hospital-based manufacturing enables all these steps to be performed within a single medical center, minimizing logistical risks, reducing the time between cell collection and infusion, and providing a personalized approach for each patient. This integration of science, production, and clinical practice is a key factor in the successful implementation of innovative cell therapies in medical care.

Economic and Social Impact

Hospital-based manufacturing of cell therapies has a significant impact not only on clinical practice but also on the economic and social development of the field. One of the key advantages is the reduction of therapy waiting times. Since production occurs in close proximity to the patient, logistical delays and risks associated with cell transportation are minimized, which is particularly critical for patients with severe and aggressive forms of disease.

Increasing the accessibility of cell therapies represents another important effect. Hospital-based manufacturing allows medical centers to produce individual biomedical products directly for specific patients, reducing dependence on centralized industrial manufacturers and making therapies more widely available.

Building human capital is also an important social aspect. The development of hospital-based manufacturing requires the training of highly qualified specialists, including biotechnologists, pharmacists, and quality control professionals. Establishing such competent teams strengthens the scientific and professional capacity of medical institutions and ensures long-term development of the field.

Finally, hospital-based manufacturing promotes the growth of local biotechnology clusters. Medical centers engaged in cell therapy production become hubs

for scientific research, startups, and industrial partnerships. This creates an innovation ecosystem that facilitates the rapid implementation of new technologies and supports the development of the biotechnology sector at regional and national levels.

Thus, hospital-based manufacturing of cell therapies exerts a comprehensive impact on the economy, social infrastructure, and scientific development, contributing to the sustainable growth of the cell medicine industry and enhancing the quality of medical care for patients.

Prospects and Challenges

The development of hospital-based manufacturing of cell therapies is accompanied by a number of structural and organizational challenges. One of the key limitations is a shortage of qualified personnel: establishing and maintaining production requires highly skilled specialists, including biotechnologists, pharmacists, quality control experts, and regulatory professionals. In most medical centers, such personnel are insufficient, which constrains the scale-up of production and the implementation of new technologies.

Infrastructure limitations also pose a significant challenge. Effective CAR-T cell manufacturing requires specialized clean rooms, bioreactors, and quality control systems, which may not be available in many medical institutions. A lack of infrastructure restricts the potential for expanding hospital-based manufacturing and integrating new technologies into clinical practice.

Another challenge is the need to harmonize international standards. Different countries apply varying approaches to regulating hospital-based manufacturing, creating difficulties in knowledge exchange, international collaboration, and conducting multicenter clinical trials. Aligning GMP standards, quality control requirements, and cell therapy safety regulations is crucial for the global development of the field.

Despite these challenges, hospital-based manufacturing of cell therapies offers broad opportunities for advancing medicine and the biotechnology sector. An important direction is the development of educational programs aimed at training qualified specialists capable of working with advanced cell therapy products.

The creation of interdisciplinary centers that integrate research, clinical practice, and cell therapy production accelerates the translation of innovations, improves therapy quality, and ensures the integration of scientific and practical expertise.

Moreover, expanding collaboration between medical centers and industrial companies fosters the growth of local biotechnology clusters, attracts investment, and accelerates the implementation of innovative cell products in clinical practice.

Thus, overcoming existing challenges and implementing these prospective strategies can ensure the sustainable development of hospital-based cell therapy

manufacturing, enhance the accessibility of innovative therapies, and stimulate growth in the industry at both national and international levels.

Conclusion

Hospital-based manufacturing of cell therapies represents a promising direction in the development of modern medicine, enabling the integration of scientific research, manufacturing technologies, and clinical practice. This approach not only accelerates the implementation of innovative therapies, such as CAR-T, but also increases their accessibility for patients by minimizing logistical delays and providing a personalized treatment approach.

International experience, including practices in the United States, Europe, and China, demonstrates the effectiveness of hospital-based manufacturing when combined with strict quality standards and integration with clinical research. The Russian experience, particularly at the National Medical Research Center for Pediatric Oncology, Hematology, and Immunology named after Dmitry Rogachev, confirms the practical feasibility of this approach and its potential to expand access to cell therapies within the country.

Successful development of hospital-based manufacturing requires systemic support, including investments in infrastructure, development of educational programs and training of qualified personnel, as well as improvement of regulatory mechanisms that ensure compliance with GMP standards and patient safety.

Overall, hospital-based manufacturing of cell therapies serves as a strategic tool for translating scientific achievements into clinical practice, stimulates the growth of the biotechnology sector, and creates conditions for sustainable expansion and increased accessibility of innovative therapies at both national and international levels.

References

1. June C. H., Sadelain M. Chimeric antigen receptor therapy //New England Journal of Medicine. – 2018. – Т. 379. – №. 1. – С. 64-73. doi: 10.1056/NEJMra1706169.

2. Simpson E., Dazzi F. Bone Marrow Transplantation 1957-2019//Front Immunol. 2019 Jun 5. 10: 1246. doi: 10.3389/fimmu.2019.01246.

3. Food and Drug Administration (FDA). Investigational New Drug (IND) Application. https://www.fda.gov/drugs/types-applications/investigational-new-drug-ind-application.

4. European Medicines Agency. Regulation (EC) No 1394/2007 on advanced therapy medicinal products. https://www.ema.europa.eu/en/human-regulatory/overview/advanced-therapy-medicinal-products.

5. Yin C. et al. Gene and cell therapies in China: booming landscape under dual-track regulation //Journal of Hematology & Oncology. – 2022. – T. 15. – №. 1. – C. 139. doi: 10.1186/s13045-022-01354-9.

6. Badrin E. A. et al. Analysis of global practices in CAR-T cell production organization and an example of implementation at the Dmitry Rogachev National Medical Research Center for Pediatric Hematology, Oncology, and Immunology //Annals of the Russian academy of medical sciences. – 2024. – T. 79. – №. 6. – C. 507-514. doi: 10.15690/vramn18005.

DOI 10.34660/INF.2025.42.82.054

用于大型结构应力应变状态监测系统的抗辐射光纤温度传感器

FIBER-OPTIC TEMPERATURE SENSOR WITH INCREASED RADIATION RESISTANCE FOR MONITORING SYSTEMS OF STRESS-STRAIN STATE OF LARGE STRUCTURES

Badeeva Elena Alexandrovna
Doctor of Technical Sciences, Associate Professor, Professor

Badeev Vladislav Alexandrovich
Laboratory assistant researcher
Scientific Research Center for Nanotechnology of Fiber-optic Systems, Penza State University

注释：研制了一种耐辐射温度的光纤微传感器，用于测量大型建筑结构材料的温度，同时监测其应力-应变状态。基于光纤传感器的信息测量系统基于将来自测量区的调制光流经光纤传输至辐射接收器，并在信息转换单元进行进一步处理的原理。

关键词：应力-应变状态、微传感器、温度、测量传感器、计量特性、微光机系统、火花-爆炸-防火安全、耐辐射。

Annotation. *A fiber-optic micro-sensor of radiation-resistant temperature has been developed, designed to measure the temperature in the material of the building structure of large structures while monitoring the stress-strain state. The information and measurement system based on fiber-optic sensors is based on the conversion of parameters of a modulated stream coming from the measuring zone via an optical fiber to a radiation receiver and subject to further processing in the information conversion unit.*

Keywords: *stress-strain state, micro sensor, temperature, measuring transducer, metrological characteristic, micro-optical-mechanical system, spark-explosion-fire safety, radiation resistance.*

Introduction. The temperature effect on the structures of buildings and structures affects the mechanical properties of building materials, leading to microstructural changes, loss of strength properties, increased plasticity and increased deformation of bearing elements [1-3]. Various control and measuring devices are used to monitor the temperature parameters of large structures. The use of temperature sensors makes it possible to study the condition of the soil, monitor the

quality of concrete mixtures, determine the thermal resistance of structures, and identify places where defects and cracks form in the stress-strain state of construction facilities. Temperature measuring instruments at important strategic facilities should timely detect overheating of structural elements, monitor over long distances, have accuracy, safety, and should not create additional electromagnetic interference, so it is important to make a choice in favor of fiber-optic measuring transducers.

Fiber-optic measuring systems are a set of fiber-optic devices for detecting various physical quantities (temperature, deformation, pressure, displacement, tilt angle, etc.). Fiber-optic sensors serve as primary transducers in fiber-optic measuring systems. A characteristic feature of sensors based on fiber technologies is the low body weight, fire safety, small overall dimensions of the sensitive part of the sensor, measuring instruments, insensitivity to electromagnetic interference, low power consumption, and radiation resistance [4-6]. The combination of these qualities makes it possible to use fiber-optic sensors in systems for long-term monitoring of the stress-strain state of engineering structures, allowing them to avoid overloading, prevent emergencies, and remotely, efficiently, and economically manage these systems.

Materials and methods. A fiber-optic temperature micro sensor is justified for use, which refers to measuring instruments with an open optical channel (fig. 1) [7, 8]. This sensor can be used during the operation of a structure, and be part of a system for monitoring the stress-strain state of large structures. According to the Patent for invention RU 2795841 C1: «the sensor housing is made of a material with good thermal conductivity (for example, a copper alloy). The sensor element (cylinder) is made of a material with a high coefficient of thermal expansion αc, for example, aluminum. The shank is made of a material with low coefficients of thermal expansion αsh. The sleeve is made of a material with small coefficients of thermal expansion, for example, made of 36NXTY steel. The coefficients of linear expansion of the materials of the ab body, the α_{sh} shank, the as sleeve and the a_c cylinder are determined by the ratio: $a_c > a_b > (a_{sh} \approx as)$ » [7]. The radiation resistance of the micro sensor will be ensured by the use of modern radio-resistant optical fiber.

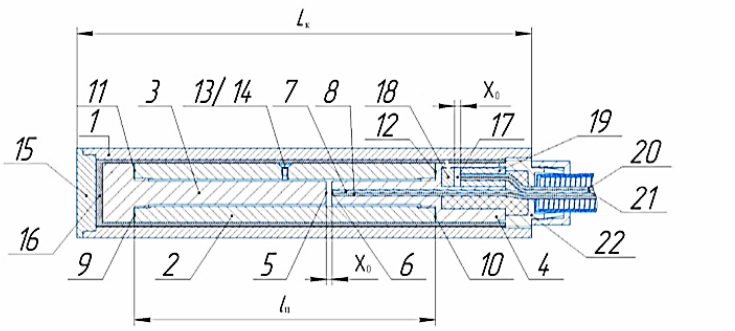

1 - Housing; 2 - Sensing element (cylinder); 3 – Shank; 4 – Sleeve; 5 - Reflective surface of the shank; 6 – End face; 7 - Incoming optical fiber; 8 - Outgoing optical fiber; 9 and 10 - Inner ends of the wide part of the shank; 11 and 12 – Welding or soldering points; 13 - through hole for filling the free space between the shank; 14 - sealing part, such as a pin; 15 - lid; 16 - heat-conducting compound; 17 - side blind hole; 18 is a fixed mirror; 19 - sleeve; 20 and 21 are Additional inlet and outlet optical fibers; 22 - shank; L_k - length of the body; L - length of the cylinder; X_0 - initial distance between the reflecting surface and the end of the optical fibers

Figure 1. *Fiber-optic temperature sensor*

During the measurement process, the luminous flux from the IR LED radiation source is fed through the working supply optical fibers into the measuring area, falls on the mirror surface of the shank, is reflected from it and enters the input of the working discharge optical fiber. Through it, the luminous flux is directed to a working radiation receiver (for example, a photodiode), where it is converted into an electrical signal.

The luminous flux from the radiation source is fed through an additional incoming optical fiber into the area of the stationary mirror, falls on its mirror surface, is reflected from it and enters the input of the outgoing optical fiber. Through the optical fiber outlet, the luminous flux is directed to the radiation receiver (photodiode), where it is converted into an electrical signal, the value of which is proportional to the distance X_0. Since the additional mirror is installed in the short part of the sleeve with a low coefficient of thermal expansion (36NXTY), the distance X0 remains unchanged during the measurement process.

Optical streams $F_1(X) \sim F_1(T)$ and $F_2(X_0)$, carrying measuring information about the measured temperature, are supplied to radiation receivers 24 and 25 of the working and additional channels. To transfer the ambient temperature due to the heat transfer process (thermal conductivity), the housing 1 and the cylindrical tube 2 are made of a material with good thermal conductivity, a heat-conducting

compound 16 having good thermal conductivity is placed between them (for example, KPT-8 or 52022 thermal paste) and providing a decrease in temperature resistance along the path of heat flow propagation.

The initial length is selected in such a way that its change in the measuring range provides a greater depth of modulation of the optical signal (up to 30%) and a linear function of the conversion F(X) of the luminous flux from the change in the distance X between surfaces 5 and 6. The initial distance X0 should be in the middle of the range 0.25 dc...0.75dc (for example, for DC = 200 microns the range of the distance X will be 50...150 microns), that is 0.5 dc (for example, for DC with dc =200 microns - X_0= 100 microns).

At the same time, if the sensor is designed to measure either negative or positive temperatures, then the initial distance X_0 may shift either towards lower values of micro-displacements, or towards higher values. The introduction of the hole 17, in which the mirror 18 and additional optical fibers 20 and 21 are fixed, is necessary to realize the compensatory conversion of sensor signals. The introduction of a compensation channel makes it possible to implement, for example, logometric signal conversion, which reduces additional errors caused by: bends of optical fibers during assembly and operation; - the influence of external influencing factors; changing the parameters of the power source, radiation sources and receivers, etc.

Conclusion. A fiber-optic temperature micro sensor can be used to create a system for remote monitoring of the stress-strain state of various objects, ranging from residential buildings to bridges, pipelines and nuclear power plants. The sensor system must be placed in critical locations to measure and collect data on the current temperature in the structural elements. The effect of temperature on a measuring instrument with an open optical channel changes the intensity of the luminous flux in the micro-optical-mechanical system of the sensor design, which leads to a change in the characteristics of the back reflection signal. The data is transmitted via optical fiber to the information conversion unit, where the optoelectronic conversion takes place, and then the signal is transmitted via a wired or wireless channel directly to the user or to cloud storage for access to monitoring results.

Acknowledgment

The research was carried out at the expense of a grant from the Russian Science Foundation № 24-29-00595, https://rscf.ru/project/24-29-00595/.

References

1. Li. Y., Luo, Y., Du, H., Liu W., Tang L., Xing F. Evolution microstructural characteristics carbonated cement pastes subjected to high temperatures evaluated MIP and SEM. Materials 2022, 15, 6037. doi: https://doi.org/10.3390/ma15176037.

2. Chaboki-Khiabani A., Bastami M., Baghbadrani M., Kordi M. (2011). Optimization of the Concrete Mix Proportions Centered on Performance after Exposure to High Temperature. In Advanced Materials Research. Vols. 268-270, pp. 372-376. doi: https://doi.org/10.4028/www.scientific.net/amr.268-270.372.

3. M. Nabiyev, O. Salimov, A. Khotamov, T. Akhmedov, K. Nasriddinov, Ul. Abdurakhmanov, R. Raximov, A. Khalimov, A. Abobakirov. Effect of external air temperature on buildings and structures and monuments. E3S Web of Conferences 474, 03011. 2024. https://doi.org/10.1051/e3sconf/202447403011

4. Egorova D.A., Kulikov A.V., Mukhtubaev A.B., Plotnikov M.Yu. Fiber-optic measuring system for determining the position and bends of extended objects in space // Scientific and Technical Bulletin of Information Technologies, Mechanics and Optics. 2020. № 3. pp. 346-352.

5. Murashkina T.I., Badeeva E.A., Kuznetsova M.V., Kukushkin A.N., Badeev V.A. Fiber-optic system for measuring large tilt angles of large-sized test benches of rocket, space and aviation equipment // Izvestiya vysshikh uchebnykh zavedeniy. The Volga region. Technical sciences. 2023. № 4(68). pp. 94-105. doi 10.21685/2072-3059-2023-4-9.

6. Murashkina T.I., Badeeva E.A., Serebryakov K.D., Udalov A.Yu., Fedotova A. Prospects for the creation of VOIIS for determining the motion parameters of large stands // Modern Electronics. 2015. № 6. pp. 70-72.

7. Murashkina T.I., Badeeva E.A., Serebryakov D.I., Dudorov E.A., Khasanshina N.A., Badeev V.A. Patent for invention RU 2795841 C1. Fiber-optic temperature sensor. Date of registration: 12.05.2023. Byul. № 14.

8. Murashkina T.I., Badeeva E.A., Bazykin S.N., Dudorov E.A., Badeev V.A. Fiber-optic system for measuring the temperature of rigid deformable media // Izvestiya vysshikh uchebnykh zavedeniy. The Volga region. Technical sciences. 2024. № 2. pp. 112-126.

DOI 10.34660/INF.2025.44.84.055

用于航空航天生命支持系统的光纤压力传感器
FIBER-OPTIC PRESSURE SENSORS FOR AEROSPACE LIFE SUPPORT SYSTEMS

Murashkina Tatiana Ivanovna
Doctor of Technical Sciences, Professor

Vladislav Alexandrovich Badeev
Laboratory assistant researcher
Scientific Research Center for Nanotechnology of Fiber-optic Systems, Penza State University

摘要：在航空航天物体生命保障系统中，对于狭窄腔体和表面不平整空间内100...500 g/cm²范围内的低压测量，目前仍采用过时且不安全的电子设备，因为测量系统可能发生电气故障或测量仪器对人体产生电磁效应，对宇航员的健康构成威胁。低压光纤传感器的设计采用了一种光纤衰减器反射式方法，将光信号直接转换为线性微位移测量传感器的微光机系统，该方法结合了衰减器和反射式压力测量传感器的优点。采用衰减器反射式调制元件的低压传感器传感元件和外壳设计，可将仪器误差降低3...5倍。

关键词：光纤压力传感器，生命保障系统，航空航天设施。

Abstract. *The measurement of low pressure in the range of 100...500 g /cm² in narrow cavities and spaces with uneven surfaces of life support systems for aerospace objects is carried out using outdated and unsafe electrical devices for the health of astronauts, due to the possible occurrence of electrical breakdown of the measuring system or electromagnetic effects from the measuring instrument on the human body. Designs of low-pressure fiber-optic sensors have been developed that implement a fiber-optic attenuator-reflective method for converting optical signals directly into a micro-optical-mechanical system of a linear micro-displacement measuring transducer that combines the advantages of attenuator and reflective pressure measuring transducers. The design of the sensing element and the outer housing of the low-pressure sensor with an attenuator-reflective modulating element reduces the instrumental component of the error by 3...5 times.*

Keywords: *fiber-optic pressure sensor, life support system, aerospace facility.*

Introduction. The spacesuit's life support monitoring system provides for monitoring the pressure of the gaseous medium [1-4]. Pressure measurements occur during leak proofness checks of the spacesuit before launch, during an astronaut's spacewalk, and also during descent to Earth, when serious pressure drops are possible. These measurements are performed by pressure sensors located in the suit between the inner and outer layers of the suit, which have uneven surfaces and a limited cavity [3, 4]. There is an urgent problem of improving astronauts' life support systems in the face of increasingly harsh effects of external factors on the astronaut's body during long-term flights. The authors have highlighted the specifics of sensors for medical and space applications, which is the need for: «absolute safety for astronauts and high reliability from 0.95 to 0.99. Their mass-dimensional characteristics should be minimal. Sensor equipment developers face the difficult task of ensuring reproducibility of the metrological characteristics of sensors from sample to sample, which currently does not exceed 30% in many medical measurements» [6, 7]. Measuring the low pressure of life support systems is associated with similar problems.

In order to exclude the effects on the astronaut's body of the electromagnetic effects of the components of life support systems, as well as in order to reduce their weight on board a spacecraft, the use of fiber-optic systems for various purposes, including measurements, has recently been considered. To solve the problems of measuring low pressure in space life support systems, small-sized fiber-optic low-pressure sensors have been developed that operate in narrow cavities with uneven surfaces of life support systems for aerospace objects.

Materials and methods. Based on the analysis of fiber-optic technologies and devices for measuring low pressure, it was decided to focus further research on low-pressure fiber-optic sensors with optical modulating elements that change the intensity of optical signals under the influence of the measured pressure [8-11]. The prototype for a fiber-optic low-pressure sensor was an attenuator-type fiber-optic pressure sensor [12]. The sensor was developed for harsh operating conditions typical of rocket and space technology, where the measured pressures far exceed the pressures of astronauts' life support systems. The main disadvantage of this pressure sensor for solving this problem is the large longitudinal dimensions associated with the presence of a standard threaded fitting for mounting the sensor on the object, which is practically unacceptable due to the limited space in the sensor installation area in space-based life support systems.

A fiber-optic attenuator-reflective pressure measurement method has been proposed, according to which new low-pressure sensor designs have been developed [12]. Figure 1 shows a simplified design of one of the variants of the low-pressure attenuator-reflective type sensor being developed with a compensation channel, which eliminates the above disadvantages. The main difference of this sensor is

the replacement of the second measuring channel with a compensation channel. In the compensation channel, the intensity of the luminous flux does not change during pressure measurement. The movement of the attenuator is 2 times less than in an attenuator-type fiber-optic low-pressure sensor.

The main modulating element in the sensor is a mirror surface, relative to which and relative to the end of the optical fibers, the microattenuator moves under pressure. The sensor contains an incoming optical fiber 4, diverting working and compensating optical fibers 5, the common end of which is fixed at a calculated distance from the fixed mirror surface 8. Under the influence of the measured pressure P, an attenuator 3 moves between the working optical fibers and the mirror surface of the optical axis.

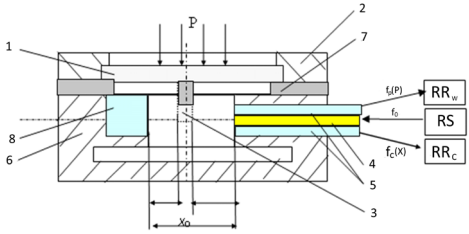

1 – sensing element (membrane); 2 – cover; 3 – attenuator;
4 – incoming optical fiber;
5 – outgoing optical fibers; 6 – housing; 7 – gasket; 8 – mirror;
RS – radiation source; RRw, RRc – radiation receivers of the working and compensation measuring channels

Figure 1. *The first variant of a simplified design of an attenuator-reflective fiber-optic low-pressure sensor*

The attenuator has such dimensions and moves to such a value that the upper half of the light cone from the incoming optical fiber 4 operates on the working measuring channel, and the lower half on the second compensation channel. The attenuator is moved to a value that provides compensatory signal conversion, since only the upper half of the light cone is covered by the attenuator. The luminous flux F0 generated by the radiation source is transmitted through the incoming optical fiber 4 to the measuring zone in the direction of the mirror surface 8. The reflected light fluxes Fp =f(P) and FC =const through the outgoing optical fiber of the working channel and the compensation channel are supplied to the working and compensation radiation receivers, respectively. The radiation receivers then convert the optical signals Fp(P) and FC into electrical signals Ip(P) and Ic(X=-const).

A second version of an attenuator-reflective low-pressure fiber-optic sensor has also been proposed, meeting the requirements of microminiaturization and increased sensitivity of optical signal conversion, the design of which makes it possible to install the sensor in a narrow space or cavity with uneven surfaces of life support systems (Figure 2) [11]. The attenuator-reflection principle of optical signal conversion used in this sensor is the same as in the sensor discussed above. The main difference from the above sensor is described in the patent and lies in the fact that: «when measuring pressure in narrow cavities, the base of the sensor rests against a point on the support surface, while the sensing element rises and pulls up the membrane, which, when the pressure is removed, returns it to its original neutral position» [11].

Improving the accuracy of pressure measurement results is achieved by reducing the error in the interaction of the measuring instrument with the measuring object due to the special design of the sensing element and the external sensor housing. In this case, the microattenuator is made as a single unit with a sensing element, on the protrusion of which there is a thin membrane.

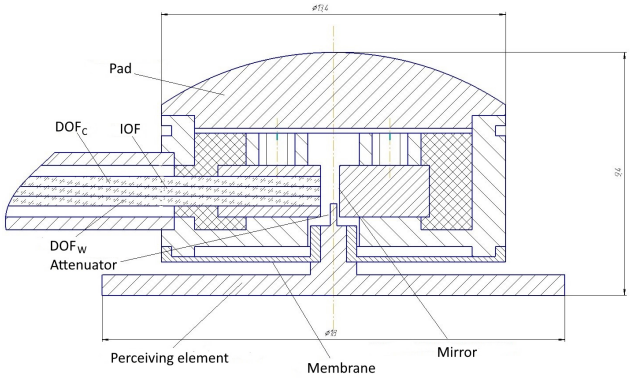

Figure 2. *The second variant of the simplified design of an attenuator-reflective fiber-optic low-pressure sensor [11]*

For accurate measurement of low pressure in narrow cavities with uneven surfaces, contact of the sensor mounting surface with one uneven surface and the surface of the sensor sensing element with another uneven surface is required, and for safety, the absence of electrical measuring elements in the measuring area. In addition, the presence of a high cylindrical protrusion in the center of the membrane reduces the measurement error caused by the displacement of the point of contact of the sensor base with the surface of the object, as it will not allow the attenuator to deviate from its vertical position.

Using the proposed fiber-optic sensor, it will be possible to: increase the accuracy of measuring the low pressure of astronauts' life support systems; reduce by 5-10 times the errors in the interaction of the measuring instrument with the measuring object by increasing the contact area of the sensing element and the measuring object and the special design of the sensor support surface in contact with the installation surface of the object; to reduce by about 2 times the additional error from the angular displacement of the optical modulating element (attenuator) relative to the reflecting surface by tightening the tolerance for manufacturing the inner diameter and lengthening the guide along which the attenuator moves; to ensure high reproducibility (up to 98%) of measurement results; to reduce by about 2 times the dynamic error caused by deflection of the membrane: compared with the prototype, the deflection of the membrane decreased from 100 microns to 50 microns for the selected optical fiber with a core diameter of 100 microns.

Conclusion. Two design variants of a fiber-optic low-pressure sensor have been developed that implement a fiber-optic attenuator-reflective method for converting optical signals, allowing for accurate pressure measurement in narrow cavities with uneven surfaces: in cosmonauts' spacesuits, in cavities of air and liquid flows in astronauts' life support systems (possibly in life support systems of medical institutions), in the mouth of an astronaut (the pressure of the tongue on the palate during pre-flight training). It is proved that the measurement accuracy increases when using the proposed measuring instrument by reducing the error in the interaction of the measuring instrument with the measuring object by increasing the area of the sensing element and executing the surface of the outer housing of the fiber-optic sensor with an attenuator-reflective modulating element opposite to the sensing element. The proposed low-pressure attenuator-reflective fiber-optic sensor combines the advantages of attenuator-type and reflective fiber-optic converters: on the one hand, high sensitivity of optical signal conversion, and on the other hand, simplicity of design and technological design and small overall dimensions.

Acknowledgements

The research was carried out at the expense of the grant of the Russian Science Foundation № 25-29-20107, https://rscf.ru/project/25-29-20107/.

References

1. Samsonov N.M., Bobe L.S., Gavrilov L.I., Kochetkov A.A., Kurmazenko E.A., Romanov S.Yu., Zheleznyakov A.G., Baranov V.M., Sinyak Yu.E. Regenerative life support systems for space station crews // Izvestiya RAS, Energetika. 2009. № 1. pp. 61-68.

2. Serebryakov V.N. Fundamentals of designing life support systems for the crew of space aircraft. Moscow: Mashinostroenie, 1983. 163 p.

3. Murashkina T.I., Badeev V.A. Low pressure measurement in space life support systems // New technologies in medicine, biology, pharmacology and ecology: proceedings of the International Conference NT + ME`25 (Gurzuf, June 1 to June 8, 2025). 2025. pp. 204-208.

4. Barer A.S., Filipenkov S.N., Vakar M.I., Golovkin L.G., Shchigolev V.V., Kovalenko E.A., Kasyan I.I., Zinchenko V.P., Osipov Yu.Y. Medical support for astronauts in outer space. In: Physiological problems of weightlessness. Moscow: Medicine. 1990. pp.179-197.

5. Katuntsev V.P., Osipov Yu.Y., Filipenkov S.N., Tarasenkov G.G., Krasnov A.N. The Russian experience of medical support for extravehicular activities of astronauts conducted from the International Space Station in 2001-2015 // Medicine of extreme situations. 2016. № 1 (55). pp. 8-18.

6. Murashkina T.I., Badeeva E.A., Kukushkin A.N., Badeev V.A., Plotnikova E.Yu., Vasiliev Yu.A., Istomina T.V. Medical fiber-optic tilt sensor // Medical Equipment, 2024. № 5(347). pp. 11-13.

7. Badeeva E.A., Murashkina T.I., Vasiliev Yu.A., Gerashchenko S.I., Brostilova T.Y. Problematic issues of the use of fiber-optic pressure sensors in medical practice // In the collection: new technologies in medicine, biology, pharmacology and ecology. Proceedings of the International Conference NT + M&Ec`2021. Spring session. Moscow, 2021. pp. 16-32.

8. Badeeva E.A., Meshcheryakov V.A., Murashkina T.I., Pivkin A.G. Fiber-optic pressure sensors of attenuator type for aircraft // Sensors and systems.2003. № 4. pp. 11-14.

9. Fiber-optic devices and systems: Scientific developments of the Scientific Research Center «Nanotechnology of fiber-optic systems» of Penza State University Part 1. T.I. Murashkina, E.A. Badeeva. St. Petersburg: Polytechnic, 2018. 187 p.

10. Badeeva E.A., Murashkina T.I., Serebryakov D.I., Badeev A.V. A method for converting a light flux and a fiber-optic pressure sensor implementing it. Patent for the invention RU2740538 G01L 13/00. Published: 15.01.2021.

11. Murashkina T.I., Badeeva E.A., Serebryakov D.I., Badeev V.A., Khasanshina N.A. Fiber-optic pressure sensor. Patent for the invention of the Russian Federation 2829195C1 G01L 13/00. Published: 25.10.2024.

12. Badeeva E.A., Murashkina T.I., Istomina T.V., Slavkin I.E., Badeev V.A. Small-sized fiber-optic pressure sensor with a compensation channel // Innovative, information and communication technologies: proceedings of the XVII International Scientific and Practical Conference, Sochi, October 01-10, 2020 / edited by S.U. Uwaisov. Moscow: Association of Graduates and Employees of the VVIA named after Professor N.E. Zhukovsky for the promotion of the preservation of the historical and scientific heritage of the VVIA named after Professor N.E. Zhukovsky, 2020. pp. 204-207.

DOI 10.34660/INF.2025.17.74.056

论现代技术对军事科学范式之一的影响
ON THE INFLUENCE OF MODERN TECHNOLOGIES ON ONE OF THE PARADIGMS OF MILITARY SCIENCE

Tikhanychev Oleg Vasilyevich
PhD in Technical Sciences, Professor
Academy Military Sciences,
Deputy Head of Department
Company group «Technoserv», Moscow, Russia

摘要：本研究以军事领域中攻防手段的对抗过程为研究对象，探讨现代高科技冲突中这一过程的特征和动态。研究旨在识别受武装对抗动态变化影响的军事科学领域，并确定这种影响的性质，从而提出改进规范性文件规定的建议，使其符合现代高科技冲突的现实。

本文认为，当前武装对抗状态的特点是积极使用包括军民两用技术在内的新技术，并将其迅速引入武装冲突过程。本文探讨了这一过程对武装冲突性质变化及其组织模式的影响。

本文运用了一般的科学分析和综合方法。基于对现代技术在武装冲突中应用的分析，本文提出了关于新技术动态引入对武装冲突作战方式变化的影响的假设，并提出了在军事指挥和控制机构的活动中考虑到这些特点的建议。研究的主要结论是：在现代条件下，武器和特种装备型号更新速度急剧加快，这不断改变着先前确定的防御和攻击手段的比例，要求指挥部改变军事行动的管理方式。上述趋势将导致军事领域的重大变化，必须考虑到这些变化，以确保做好应对现代和未来冲突的准备。

关键词：武器发展，防御和攻击手段之争，武装对抗的新因素，后工业时代战争，新武器引进动态。

Abstract. *The object of the study is the process of confrontation of means of attack and defense in military affairs, the subject of the study is the features and dynamics of this process in modern high-tech conflicts. The purpose of the study is to identify areas of military science that are affected by changes in the dynamics of armed confrontation, to determine the nature of this influence in order to formulate proposals for improving the provisions of governing documents, bringing them into line with the realities of modern high-tech conflicts.*

The article determines that the current state of armed confrontation is characterized by the active use of new technologies, including dual-use ones, their

prompt introduction into the process of armed conflict. The article considers the influence of this process on the change in the nature of armed conflict and some paradigms of its organization.

The article uses general scientific methods of analysis and synthesis. Based on the analysis of the use of modern technologies in armed conflict, assumptions are synthesized on the influence of the dynamic introduction of new technologies on changes in the methods of conducting armed conflict, proposals for taking these features into account in the activities of military command and control bodies. The main conclusions of the conducted research are that in modern conditions the dynamics of updating the model range of weapons and special equipment has increased sharply, and this continuously changes the previously established ratio of means of defense and attack, requires headquarters and command to change the approach to managing military operations. The described trend leads to significant changes in military affairs, which must be taken into account to ensure readiness for conducting modern and prospective conflicts.

Keywords: *development of weapons, struggle between means of defense and attack, new factors of armed confrontation, wars of the post-industrial era, dynamics of introduction of new weapons.*

1. Introduction

The problem of confrontation between means of attack and defense has faced military science since the advent of organized military operations. It was solved cyclically, as new weapons appeared and their effectiveness gradually decreased due to the development of means and methods of protection. New weapons, which appeared in almost every conflict, were initially imperfect, and technological capabilities did not allow them to be improved until the end of the conflict. Decades and dozens of wars passed from the first appearance of gunpowder to the spread of firearms. Several wars and a decade were needed for the active use of rapid-fire weapons. As industrialization progressed, the renewal process accelerated, but the scale remained the same: tanks and combat aircraft that appeared during the First World War did not play a decisive role in it; their development occurred before the Second World War. But during the same period, countermeasures were developing, and by the beginning of the war, the world's leading armies had a balanced set of both, although with different approaches to organizing their use. Missiles and radar that appeared during the Second World War significantly showed themselves decades later, during post-war local conflicts, etc. Let us clarify that we are not talking about improving the characteristics of weapons, which could change during one conflict, but specifically about the emergence of new types with fundamentally new properties. It was in relation to this process that the cyclicality of changes was low, being determined by decades, as a rule, in the range from

conflict to conflict. With the transition to the post-industrial era, with the advent of information technology and the development of the "digital economy", the situation under consideration, without changing in essence, has changed in dynamics: the process of the emergence of fundamentally new weapons began to occur more often and faster in time, a faster response was required [1-5]. The changed conditions require a new response to them, which makes the topic considered in the article relevant.

2. Materials and Methods

A systems approach was chosen as the methodological basis of the study. The use of a systems approach, decomposition methods and comparative analysis made it possible to consider in a complex manner the issues of changing the dynamics of the emergence of new weapons and means of combating them in the post-industrial era.

An analysis of the impact of this process on the conduct of military operations made it possible to synthesize proposals for taking into account these features in the activities of military command and control bodies.

3. Results

As an example of the dynamics of the process in the context of modern conflicts, we can cite the stages of development of technologies for the use of tactical unmanned aerial systems (UAVs) and unmanned boats (UBC) during one such conflict: the conduct of the SMO in 2023-25 [6,7,8], summarized on the basis of data from open sources (Table 1).

Table 1

Stages of change in the ratio of attack and defense during a special military operation

Stage (year)	Impact factor (attack)	Implementation of countermeasures (protection)
2023	Mass appearance of UAVs on the battlefield	Emergence of homemade passive means of protection in the form of screens and «trench electronic warfare», suppression of the GPS signal
2023	Emergence of inexpensive small-sized UAVs	Use of pine nets, installation of additional small arms on ships, use of drone aviation to destroy UAVs
2024	Use of aviation to destroy UAVs	Installation of homing anti-aircraft weapons on UAVs
2024	Activation and widespread use of electronic warfare systems to counter UAVs	Development of UAVs insensitive to electronic warfare - controlled via fiber optics, partially autonomous, oriented by a terrain map and with additional guidance at the final section

2024	Emergence of UAVs that are insensitive to electronic warfare – controlled via fiber optics and partially autonomous	Active introduction of means of physical destruction of UAVs, their distribution in small units and crews
2025	Reduction in the cost of strike systems due to the use of simple commercial UAVs and camouflage of their use	Reduction in the cost of countermeasures, abandonment of expensive SAMs in favor of inexpensive UAV interceptors and anti-aircraft artillery with improved sighting systems, specialized anti-drone SAMs and air-to-air missiles

It should be noted that the stages described in the table were implemented within the framework of one conflict, literally over two or three years. A number of stages generally fit into the duration of one year. To solve problems dynamically, various high-tech methods were used: printing the necessary UAV parts directly in front-line workshops on 3D printers, updating and replacing the software of unmanned systems developed on an initiative basis, purchasing and delivering dual-use industrial systems to the troops, and other previously unused methods. The implementation and even application of these methods is often carried out by volunteer units and volunteers. Moreover, such a situation was observed not only in the conflict under consideration (Table 1), but also in others close to it in time. For example, dual-use technologies were actively and creatively used by the Yemeni Houthis to destroy ships in the Red and Arabian Seas during the conflict with Israel in 2023-25. New technologies are being implemented and tested not only in conflicts, but also in training programs and units, an example of which is equipping unmanned units of the US Army with 3D printers for the production of UAVs and their components in the field as part of the AEWE (Army Expeditionary Warrior Experiment) program. That is, the process of supplying new weapons in modern conflicts is also changing - from fully finished “completed” systems to weapons that can be called “open”, allowing for refinement in the field. As a result of the combination of these innovations, in modern conflicts the process of changing the stages of confrontation between offensive and defensive means has become extremely dynamic, changing cyclically in a short period of time. And if earlier measures to counter new technologies during military operations were mainly organizational, with the transfer of the technical response to the post-war period, then in modern conflicts they are immediately technical, and not one cycle per conflict. This fact is facilitated by both the emergence of flexible “digital” technologies and the active use of dual technologies in military affairs, including third-party technologies purchased from other countries.

4. Discussion

Considering the dynamics of development and implementation of technologies noted in the article, in a modern conflict, the advantage is not with the side

that initially has a technical superiority, but with the one that is more creative in using new technologies and methods, including borrowed ones. Which makes the requirement for managing this process especially relevant.

The task of assessing changes in the process of armed confrontation and developing recommendations has always been assigned by governing documents to headquarters, and the final analysis - to military educational institutions of various levels and specialized research organizations (R&D) [9-12]. However, this task for headquarters, as a rule, was secondary, and the frequency of its solution by educational and research organizations was determined by the timing of preparation for the next war. Currently, the situation has changed, both due to the acceleration of the implementation of technologies in industry, and due to the emergence of "open" systems that allow the production and improvement of individual components in the field.

Within the framework of the problem addressed in the article, it should also be remembered that the task of creating a balance between the means of attack and defense is two-sided and requires management. To solve it, it is necessary not just to observe and analyze, but to actively and purposefully manage the process.

If we accept that the acceleration of the dynamics of change is a trend, and the identified pattern is very similar to a trend, it is necessary to develop an algorithm for working with the situation.

As a first approximation, such an algorithm can be as follows (Figure 1):

1) continuous targeted monitoring and analysis of the situation;

2) upon identifying a problematic situation, assess its criticality;

3) if the situation is not critical from the point of view of the emergence of new technologies of armed struggle, simply take it into account, making, if necessary, changes to the governing documents;

4) if the situation is critically different from stable, decide on a method of countering it: by involving new units and technologies, forming a task for developing measures and means of countering third-party organizations, etc.;

5) introducing new technology both in terms of counteraction and acceptance for defeat, making changes to the governing documents;

6) returning to monitoring the situation.

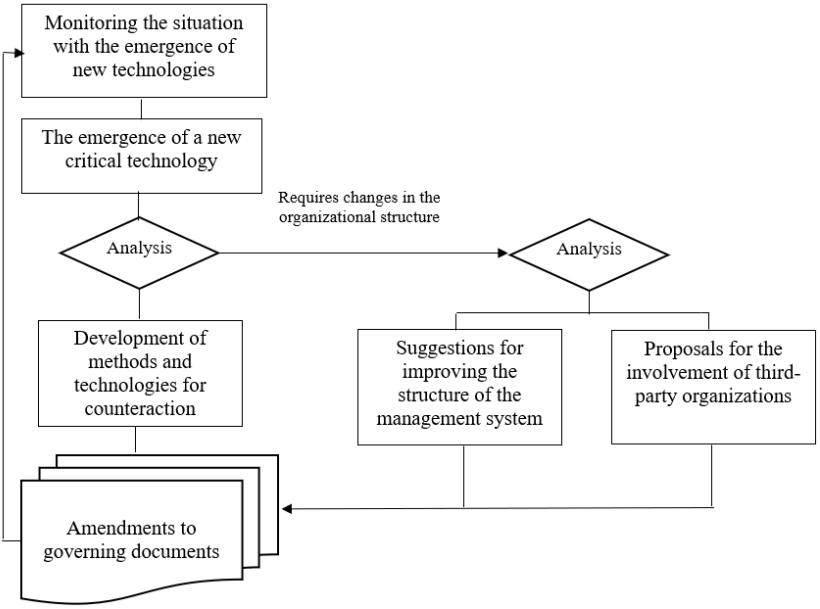

Figure 1. *Algorithm for identifying trends and countering threats*

In the context of implementing the described algorithm, headquarters, the units they control, the comprehensive support units, and the R&D departments must operate in a completely different mode from that specified in the governing documents, with expanded functionality and, possibly, with the involvement of industrial organizations developing dual technologies. The historical analogy of the latter is the initial stage of artillery development in the 14th and 15th centuries, when on the battlefield guns were not serviced by crews of military personnel, but by civilian "artels" or "outfits" producing and operating sophisticated military equipment for that time while performing tasks assigned by the military.

5. Conclusions

The analysis shows that modern warfare is a "war of algorithms" at the top level and, at the same time, a "war of technologies" at the tactical level [13]. Such a situation requires a combination of classical combat management and a scientific approach at all levels. It should be noted that the article describes the trend using unmanned systems as an example. But this is not a reason to focus on them: the problem of confrontation between attack and defense is much broader, and this trend will apply to all types of technologies and spheres of action, including information, for example, in terms of the use of artificial intelligence. Moreover, in the information sphere, the situation may become even more dynamic over time.

Based on the analysis, the following conclusions can be drawn.

Firstly, increasing the dynamism of the process of confrontation between attack and defense, its implementation on the scale of one conflict, makes military actions less predictable, the situation can change in leaps and bounds several times during the conflict.

Secondly, in modern conditions, as conflicts, for example, in the Middle East, show, a technologically backward enemy can be considered not one who does not have his own developed technologies, but one who is not able to creatively use his own and borrowed technologies.

Thirdly, the current situation requires changes in the process of organizing the conduct of military operations: both in terms of clarifying the functions of their management bodies, ensuring the dynamism of the management of the introduction of new war technologies, and in terms of requirements for military equipment and technologies, ensuring their "openness" and the possibility of improvement in field conditions.

The approach proposed in the article suggests solving the problem through continuous monitoring of new technologies, including directly during an armed conflict, in order to be able to open a "window of opportunity" at the right time, and not allow the enemy to open such a "window".

How to solve the formulated problem and reduce the distance and duration of the interaction cycle between the army and industry: emphasize the functions of headquarters by creating specialized units in them, create mobile groups of specialized R&D, involve in both options additional production capacities of repair bodies, organizations for ensuring automation of control, form new requirements for military industry enterprises? No matter how, but the problem must be solved, without this it is impossible to win in a modern war.

References

1. Hoffman F.G. (2007). Conflict in the 21-st century. The rise of hybrid wars. Arlington: Potomac Institute for policy studies Publ.

2. Chekinov S. G., Bogdanov S. A. (2017). Evolution of the essence and content of the concept of "war" in the 21st century. Military Thought. 1: 30-43.

3. Fadeev A. S., Nichipor V. I. (2019). Military conflicts of our time, prospects for the development of methods of their conduct. Direct and indirect actions in armed conflicts of the 21st century. Military Thought. 9: 33-41.

4. Tikhanychev O.V. (2024). Informatization of the battlefield: some possibilities and possible problems. National security/nota bene. 2: 1-15. DOI: 10.7256/2454-0668.2024.2.36142.

5. Litvinov E.V. (2024). Experience in the use of information technologies by NATO armed forces in military conflicts. Military Thought, 1: 131-139.

6. Bychkov V., Dorofeev I. (2024). Unmanned boats - a problem that needs to be solved. Arsenal of the Fatherland, 6 (74) URL. https://arsenal-otechestva.ru/article/1932-bezekipazhnye-katera-problema-kotoruyu-nado-reshat-chast-1.

7. Evstifeev Yu. (2024). "Smart" small calibers in the new paradigm of war. Arsenal of the Fatherland, 6(24) URL: https://arsenal-otechestva.ru/article/1935-umnye-malye-kalibry-v-novoj-paradigme-voj-ny.

8. Leonkov A. (2024). UAVs against air defense missile systems - an analysis of confrontation tactics. Arsenal of the Fatherland. 2(70) URL: https://arsenal-otechestva.ru/article/1841-bla-protiv-zrk-pvo-analiz-taktik-protivostoyaniya-chast-1

9. Kovalev A., & Kudaikin E. (2017). Information technologies in ensuring military security of the state. Administrative Consulting, 5: 20-27. https://doi.org/10.22394/1726-1139-2017-5-20-27.

10. Burenok V.M., Ivlev A.A., Korchak V.Yu. (2009). Development of military technologies of the XXI century: problems, planning, implementation. Russia, Tver: Kupol Publ.

11. Vikulov S.F. (2012). Military-economic analysis: history, methodology, problems. Armament and Economy. 4(20): 86-97.

12. Pozdnyakov A.I. (2013). The system of general patterns of development of military equipment as a basis for determining priorities in military-technical policy. Armament and Economy, 2(23): 19-36.

13. McDermott, R.N. (2023). The Technological Transformation of Russian Conventional Fires. The Journal of Slavic Military Studies, 36(3): 241–270. https://doi.org/10.1080/13518046.2023.2283962.

DOI 10.34660/INF.2025.91.50.057

气候监测数据处理系统中的信息安全挑战
INFORMATION SECURITY CHALLENGES IN CLIMATE MONITORING DATA PROCESSING SYSTEM[1][2]

Kharitonov Dmitry Ivanovich
PhD, Senior Researcher
Institute of Automation and Control Processes,
Far Eastern Branch of the Russian Academy of Sciences

Gribova Valeria Viktorovna
Doctor of Engineering Sciences, Corresponding Member of the Russian Academy of Sciences, Deputy Director for Research, Scientific Director of the Laboratory of Intelligent Systems
Institute of Automation and Control Processes,
Far Eastern Branch of the Russian Academy of Sciences

Maxur Denis Olegovich
Technician
Institute of Automation and Control Processes,
Far Eastern Branch of the Russian Academy of Sciences

摘要：日益增多的不良自然现象促使人们在自然现象分析和建模系统中引入新的数据处理方法。这些方法包括机器学习技术、大数据、启发式和统计建模，以及需要大量计算资源的现有方法的组合。本文探讨了利用分布在企业网络中、访问通道性能各异、管理策略各异的数据存储系统，在高性能计算资源上处理气候观测数据以供集体使用的技术流程。本文探讨了如何确保数据的安全访问，以及如何从数据所有者的角度保证在存储、建模和可视化过程中的完全控制。

关键词：云平台、数据安全、气候监测、自然现象建模。

Abstract. *The growing number of adverse natural phenomena stimulates the introduction of new methods of data processing in systems for analyzing and modeling natural phenomena. Such methods include machine learning technologies, BigData, heuristic and statistical modeling, as well as combinations of existing methods that require significant computing resources. The article*

[1] The work was carried out with the financial support of the Ministry of Science and Higher Education of the Russian Federation (state budget topic No. FWFW-2025-0005).

[2] The results were obtained with the use of IACP FEB RAS Shared Resource Center “Far Eastern Computing Resource” equipment (https://cc.dvo.ru).

examines the technological workflow of processing climate observation data on high-performance computing resources for collective use using data storage systems distributed in a corporate network with access channels of varying performance and various administrative policies. The article considers the problems of ensuring secure access to data, guaranteeing full control from the point of view of the data owner, both during storage and in the process of modeling and visualization.

Keywords: *cloud platform, data security, climate monitoring, natural phenomena modeling.*

1. Introduction.

In the scientific institutions of the Russian Academy of Sciences, particularly in the institutes affiliated with the Far Eastern Branch of the Russian Academy of Sciences, extensive datasets comprising observations of various climatic phenomena have been accumulated over time. The availability of such substantial volumes of observational data enables the application of diverse methods for modeling, processing, and analyzing information, thereby facilitating the extraction of new scientific insights. The Far Eastern Computing Resource Center (FECR) has traditionally played a crucial role in providing computational resources dedicated to processing these datasets, with ongoing efforts aimed at automating technological workflows to enhance efficiency.

Specifically, satellite data obtained from the Regional Satellite Monitoring of the Environment Center of the Far Eastern Branch are actively processed and analyzed. For instance, data from satellites such as TERRA, NOAA, AQUA, MODIS, and METEOR-M are utilized by specialists across multiple institutes to monitor phenomena such as harmful algal blooms [1,2]. These satellite observations are also instrumental in assessing ice thickness, structural characteristics, and dynamic behavior of ice masses; evaluating the condition of coastal waters—an essential task for navigation safety, fisheries management, and maritime safety operations in the Arctic region. Furthermore, satellite data have been employed to investigate the causes of abrupt stratospheric warming events in Antarctica [3].

Researchers at the Pacific Oceanological Institute of the Far Eastern Branch leverage satellite interferometry data to measure altitude variability along fault lines. Concurrently, cloud cover serves as a potential indicator for monitoring local faults since faults are often associated with gas emissions [4,5]. These emissions can generate condensation nuclei from aerosol particles—visible as clouds—whose shape and distribution may reflect underlying geological processes. Analyzing cloud morphology alongside gas concentration and composition provides valuable insights into crustal activity. However, distinguishing natural cloud formations from those induced by fault-related gas emissions remains a sig-

nificant challenge. One promising approach involves utilizing LiDAR technology, which can differentiate clouds based on their chemical composition [6]. Notably, variations in gas concentrations are considered more reliable indicators for predicting hazardous geological phenomena [4].

This body of evidence underscores the necessity for establishing mechanisms capable of continuous and periodic monitoring. Such systems should integrate advanced computational modeling and technological processes designed to ensure coordinated and timely responses among all involved agents when signals indicative of impending hazardous phenomena are detected. Developing these integrated monitoring frameworks is essential for improving predictive capabilities and mitigating risks associated with natural geophysical events.

2. Data Processing Scheme

The institutes of the Far Eastern Branch of the Russian Academy of Sciences are united into a distributed environment, connected by communication channels of various capacities, ranging from high-performance networks with a capacity of up to 100 Gbps inside the supercomputer center, to Internet networks with a capacity of 100 Mbps and firewalls that block unwanted traffic. Such a difference in capacity does not always allow relying on interactive interaction with data storage systems during their processing. As a result, the data processing process consists of steps that include: copying data between different nodes in the ecosystem network, converting data between different formats, and directly processing them.

The DVVR Center for Collective Use is developing a data processing environment in which the user has the ability to form a data processing scheme in the form of a simple acyclic graph in which the vertices are data processing steps, computing nodes, sources and data storage systems in the system. In the data processing scheme, each input parameter corresponds to an edge of the graph entering the processing node, and each output parameter corresponds to an outgoing edge. The amount and format of data arriving at the input of the processing function must correspond to the signature of the processing function, as well as the format of the resulting data. To execute the processing scheme, a specific location must be defined for each parameter. As the processing environment develops, the scheme can be completed algorithmically, by selecting a quasi-optimal solution, or using neural networks trained on the accumulated volume of successfully processed schemes. The execution of the processing scheme occurs by intelligent agents asynchronously on different nodes and to obtain the correct result, an agent coordinating the actions of each of the nodes is required. The task of the controlling agent is to assign specific data processing functions to intelligent agents in different network nodes, receive information from these agents about the function execution and record the state of the processing scheme execution process. In order for all processing functions to be executed, the data for the parameters must be collected in a place accessible for processing by the time it is called.

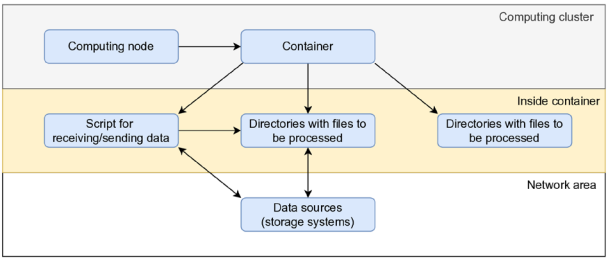

Figure 1. *The use of containerization in data processing*

Simple tasks such as data transformation, visualization, pre-processing and post-processing can be performed by intelligent agents independently. Complex tasks are processed on clusters and supercomputer resources of the DVVR CCU. For this purpose, a project concept is used in which scientists from various institutes can participate. The project provides quotas for the use of computing resources and data storage systems. To transfer computing tasks to the queue system, an agent for access to computing resources and unprivileged containers with software are used as an intermediary. The principle of using containers to organize data processing is shown in Figure 1. The main idea is that when loading, the container connects to a pre-defined network file system where files and, if necessary, scripts for data processing are located. The organization of directories in this system allows, firstly, to track the execution of the processing process, and secondly, to launch several processing processes simultaneously.

3. Data Security

The increasing sophistication of cyber threats and the growing complexity of digital ecosystems necessitate a paradigm shift in cybersecurity frameworks. Zero-Trust Architecture (ZTA) has emerged as a critical model for securing modern information systems by eliminating implicit trust and enforcing strict access controls. Traditional security models operate on perimeter-based defenses, assuming that entities within a network are inherently trustworthy. However, the rise of insider threats, advanced persistent threats (APTs), and lateral movement attacks has rendered such models obsolete. Zero-Trust Architecture (ZTA), formalized by NIST SP 800-2071 [7], adopts a “never trust, always verify” approach, ensuring continuous authentication and least-privilege access across all network segments. ZTA counters modern attack vectors such as phishing, ransomware, and supply chain compromises by enforcing dynamic access policies. In research institutions, ZTA safeguards sensitive datasets (e.g., sattelite, climate, or proprietary experimental data) from exfiltration or tampering, ensuring reproducibility and compliance with FAIR (Findable, Accessible, Interoperable, Reusable) principles [8].

The implementation of the ZTA architecture is provided at various levels. At the infrastructure level, protection of information carriers is used, ensuring

the safety of data when unauthorized users and malicious software penetrate the ecosystem. This level is provided by encryption methods for stored data on hard drives and in databases, as well as the use of container technologies that prevent the substitution of system and application software. At the level of interaction of software systems, information protection is provided by secure communication channels using SSL/HTTPS protocols and certificates confirming the validity of each of the communication nodes. using the SSL protocol to transfer significant amounts of data. Finally, at the application level, information protection is performed by authorizing each user in the system and using tokens to control access to data for all processing processes.

Let us consider information security from the point of view of storing keys for encryption and decryption of data, since the possibility of interception of the key is the main threat to data security. Figure 2 shows the part of the database scheme responsible for storing keys. The `users` table is responsible for storing the platform's user data, while user accounts are created and managed on an LDAP server. Upon account creation in LDAP, a corresponding record is generated in the `users` table. The `users.id` and `users.login` fields are derived from LDAP entries. A key pair (using an ECC algorithm) is generated randomly during this process. The private key is encrypted with a hash of the user's password—specifically, the password hash is computed using Argon2 with a salt extracted from a portion of the SHA-256 hash of the password—and then stored in `users.encrypted_private_key`. The public key is stored separately in the `public_key` field.

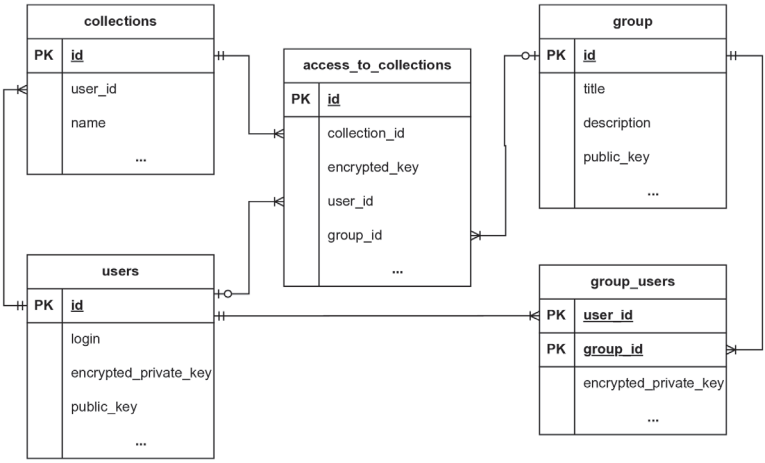

Figure 2. *Storing encryption keys in a database*

The `collections` table stores information regarding collections of climatic phenomena observations. When a data collection is created as a separate storage entity or when granting access to a collection —it is associated with the generation of a symmetric key (AES-256) selected randomly. This key is then encrypted using the public key of the data owner, retrieved from `users.public_key`, and the resulting ciphertext is stored in `collections.encrypted_private_key`. The `group_users` table records users who share identical group-based access permissions to the data. Upon the creation of a group, the group's private key is encrypted using the public key of the group members, retrieved from `users.public_key`, and this encrypted private key is stored within the table. And the `access_to_collections` table facilitates the granting of access to personal collections to other users or groups. The `access_to_collection.encrypted_key` is a modified version of `collections.encrypted_private_key`, encrypted with the public key of the designated recipient, whether an individual user or a group.

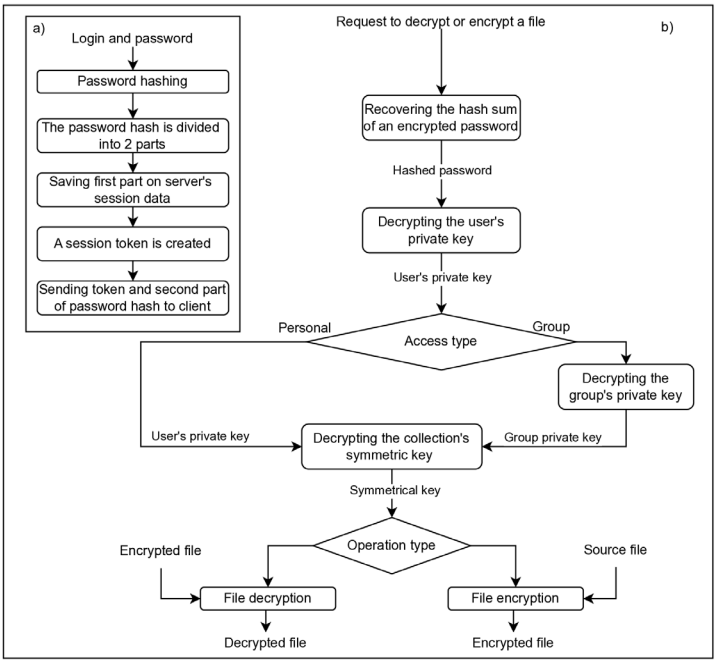

Figure 3. *Algorithms a) user authorization, b) file encryption and decryption*

The algorithm for applying keys in the process of accessing data is shown in Figure 3. User authorization, shown in Figure 3a, begins with the user providing

credentials, including a username and password. The password undergoes cryptographic transformation via the Argon2 hashing algorithm, utilizing a dynamically generated salt. This salt is derived from a partial hash produced by applying the SHA-256 function to the plaintext password. Following hash computation, the password hash is partitioned into two distinct components. To enhance security, an exclusive OR (XOR) operation is performed between these components and a cryptographically secure random string, yielding outputs designated as Part A and Part B. Subsequently, the server generates a time-bound access token uniquely associated with the user account. The client receives: the access token, part A of the processed password hash and a hashed representation of the token. The server retains the hashed token and part B for request verification purposes.

During file cryptographic operations (encryption or decryption), as depicted in Figure 3b, the client initiates a request containing the access token and password hash part A. The server authenticates the token by comparing its hashed representation against the server-stored value. Subsequently, the original password hash is reconstituted through an XOR operation between client-supplied part A and server-resident part B.

Execution diverges based on operation type (encryption/decryption) and access context (personal/group). For decryption requests, the access type (personal/group) is first determined. Personal access requires decryption of the user's private key using the reconstituted password hash, while group access necessitates decryption of the group private key contingent upon user authorization. The decrypted private key then decrypts the symmetric file encryption key, which is applied to decrypt file contents before transmission to the client. For encryption operations, an ephemeral symmetric key is generated to encrypt file contents. Depending on access context, this key is encrypted either with the user's public key (personal access) or the group public key (group access). The encrypted file and encrypted symmetric key are then persisted server-side.

4. Conclusion.

Security and sovereignty of information are the foundation for the long-term operation of any cloud platform. Accordingly, a climate monitoring platform must ensure confidentiality, integrity, and access to third-party data based on approved access policies adopted and recorded at each current moment. Zero-trust architecture is an approach to cybersecurity developed taking into account the realities of the modern computer world. By systematically eliminating trust assumptions, ZTA increases resilience to threats, ensuring the integrity and confidentiality of critical scientific and operational data. The method of separating security keys described in this paper allows maintaining control over access to data at each single processing step, while providing flexibility in separating access to data between different participants in the processes of accumulation and processing of climate observation data.

References

1. Aleksanin, A.I., Timofeev, A.N. The Influence of Observation Conditions on the Accuracy of NDVI Vegetation Index Calculation from Earth Remote Sensing Data. Cosmic Res 61 (Suppl 1), S188–S194 (2023). https://doi.org/10.1134/S0010952523700521

2. Orlova TY, Aleksanin AI, Lepskaya EV, Efimova KV, Selina MS, Morozova TV, Stonik IV, Kachur VA, Karpenko AA, Vinnikov KA, Adrianov AV, Iwataki M. A massive bloom of Karenia species (Dinophyceae) off the Kamchatka coast, Russia, in the fall of 2020. Harmful Algae. 2022 Dec;120:102337. http://dx.doi.org/10.1016/j.hal.2022.102337.

3. L. M. Mitnik, V. P. Kuleshov, M. L. Mitnik, G. M. Chernyavsky, I. V. Cherny and A. M. Streltsov, "Microwave Radiometer MTVZA-GY on New Russian Satellite Meteor-M No. 2-2 and Sudden Stratospheric Warming Over Antarctica," in IEEE Journal of Selected Topics in Applied Earth Observations and Remote Sensing, vol. 15, pp. 820-830, 2022, http://dx.doi.org/10.1109/JSTARS.2021.3133425.

4. Aiuppa, Alessandro & Bitetto, Marcello & Curcio, Luciano & Delle Donne, Dario & Lages, João & Lo Bue Trisciuzzi, Giovanni & Tamburello, Giancarlo & Vitale, Angelo & Cannavò, Flavio & Coltelli, Mauro & Coppola, D. & Innocenti, Lorenzo & Insinga, Laura & Lacanna, Giorgio & Laiolo, Marco & Massimetti, Francesco & Pistolesi, Marco & Privitera, Eugenio & Ripepe, Maurizio & Cilluffo, Giovanna. (2025). Volcanic gas changes prior to Stromboli's major explosions are statistically significant. Journal of Volcanology and Geothermal Research. 462. 108325. http://dx.doi.org/10.1016/j.jvolgeores.2025.108325.

5. Platt, U.; Bobrowski, N.; Butz, A. Ground-Based Remote Sensing and Imaging of Volcanic Gases and Quantitative Determination of Multi-Species Emission Fluxes. Geosciences 2018, 8, 44. https://doi.org/10.3390/geosciences8020044.

6. Bukin O A, Babii M Yu, Golik S S, Il'in A A, Kabanov A M, Kolesnikov A V, Kulchin Yu N, Lisitsa V V, Matvienko G G, Oshlakov V K, and Shmirko K A. Lidar sensing of the atmosphere with gigawatt laser pulses of femtosecond duration // Quantum Electronics. — 2014. — June. — Vol. 44, no. 6. — P. 563–569. http://dx.doi.org/10.1070/QE2014v044n06ABEH015431.

7. NIST. (2020). Zero Trust Architecture (Special Publication 800-207). National Institute of Standards and Technology. https://doi.org/10.6028/NIST.SP.800-207

8. Wilkinson, M. D., Dumontier, M., Aalbersberg, I. J., Appleton, G., Axton, M., Baak, A., ... & Mons, B. (2016). The FAIR Guiding Principles for scientific data management and stewardship. Scientific Data, 3, 160018. https://doi.org/10.1038/sdata.2016.18

DOI 10.34660/INF.2025.30.26.058

开发和整合信息系统以提高港口运输和技术系统的效率的构想

THE CONCEPT OF DEVELOPING AND INTEGRATING INFORMATION SYSTEMS IN ORDER TO IMPROVE THE EFFICIENCY OF PORT TRANSPORT AND TECHNOLOGICAL SYSTEMS

Chebotareva Evgeniia Andreevna
Candidate of Technical Sciences, Associate Professor,
Head of Department
Rostov State Transport University

摘要：本研究揭示了基于信息和物流原理的铁路和海运运输管理的发展演变。运输流程管理的信息化、智能化和数字化是港口运输和技术系统实现运输生产质变的最重要方面。为此，提出了信息系统开发与集成的概念，以便在以平台为中心和以网络为中心的信息平台开发框架内，提高港口运输和技术系统的效率。

关键词：铁路运输、海运、信息技术、管理、交互方式、智能化。

Abstract. *The study reveals the evolution of the development of rail and sea transportation management based on information and logistics principles. Informatization, intellectualization and digitalization of transportation process management are the most important areas of qualitative transformation of transport production in port transport and technological systems. In this regard, the concept of development and integration of information systems is proposed in order to improve the efficiency of port transport and technological systems within the framework of both platform-centric and network-centric approaches to the development of information platforms.*

Keywords: *rail transportation, sea transportation, information technology, management, forms of interaction, intellectualization.*

Problem statement. Today, the export and import potential of any country is an integral part of the economic potential, which also includes scientific and technical, production, technological, labor, investment, information, and transport capabilities. Certainly, the key link in the functioning of the transport system of countries in the tasks of developing foreign trade turnover are seaports, since sea transport mainly carries out external, export-import transportation. A sufficiently large volume of cargo to seaports is delivered by rail. In this regard, the well-or-

ganized work of port and railway workers, as well as the capabilities of the infrastructure are fundamental factors in the integration of these types of transport. Improving interaction in port transport and technological systems (PTTS) occurs in several forms: technical, technological, economic, informational, as well as organizational and legal [1-4] (Table 1). Within the framework of the strategies for the development of information technologies in rail and sea communication, an important place is occupied by the Digital Railway project, implemented by Russian Railways (RZD) [5]. The formation of this project is based on the revision and adjustment of management approaches, the features of which are shown in Figure 1.

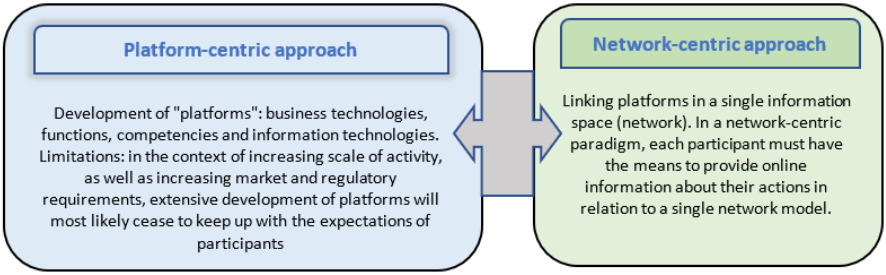

Figure 1. *Types of approaches to the development of information platforms*

Since the holding company JSC Russian Railways has achieved a high level of automation of functions, it is possible to move to “network-centric” management. The network-centric approach to management is based on “augmented analytics” with the addition of operational assessments of the network status and information about current events. In connection with the above, it is necessary to analyze the information tools used in the planning and organization of rail and sea transportation.

Table 1

Forms of interaction between different types of transport

FORMS OF INTERACTION BETWEEN DIFFERENT TYPES OF TRANSPORT	
Technological	**Technical**
– organization of cargo transportation by several modes of transport according to agreed combined contact schedules of rolling stock movement; – operation of rolling stock and loading and unloading mechanisms during cargo handling according to a single technological process to ensure minimum downtime of wagons, cars and vessels during cargo operations; ensuring rhythmic loading, unloading of cargo, shunting work in accordance with the volume of transportation; – application of agreed standards for providing transshipment points with rolling stock and loading and unloading mechanisms; – creation of the necessary conditions for maximum development of the most efficient non-transshipment transportation; – introduction of a direct option for transshipment of cargo from one mode of transport to another, bypassing the stage of their warehouse storage; – operational planning of the work of transport enterprises in hubs; – coordination of loaded wagon flows sent by cargo owners to the address of sea terminal operators	- coordination of the throughput and processing capacity of systems and devices through which cargo flows proceed; - coordination of the parameters of rolling stock and containers in terms of dimensions, load-carrying capacity, and capacity in order to effectively use handling equipment; - creation of interconnected technical communication facilities for employees of various types of transport managing the transportation process and handling of cargo in intra-transport hubs
Economic	**Informational**
– development of a transport development strategy; – development and coordination of plans and forecasts of demand for transport services; – determination of volumes of mixed transport by region; – determination of the size of investments and methods of subsidization; – development of a unified methodological basis for determining operating costs, cost of transport, efficiency of capital investments, labor productivity, indicators of transport provision of enterprises and regions; – justification and coordination of indicators for accounting of transport costs and income in mixed transport; – justification of the effectiveness of joint projects for transport services to clients; – conducting payment transactions between carriers of different types of transport; – unification of planned and reporting indicators of the work of types of transport	– creation of a unified information environment for the transport complex and analytical information systems to support the management of development and regulation of the functioning processes of the transport complex, – development of automated control systems for interacting modes of transport, – development of intelligent and digital technologies, – development of digital platforms

Information technologies for managing freight and wagon flows in the transportation process, taking into account the principle of concentration of dispatch control, involve the use of a complex of interconnected information and control automated systems and technologies. Important areas of research into the interaction of the station and the port are information transfer and cargo flow support. It should be noted that this process was previously considered in sufficient detail in [6], descriptive models of documentary support of imported cargo from the moment of the vessel's arrival to the moment of transfer of documents to the agency of the branded transport service and from the moment of acceptance of documents to the moment of departure of the train were developed. All these systems allow the management and dispatch personnel to generate data for operational control of the transportation process and automated analysis. Thus, automated control systems (ACS) of sea ports have a large volume of information about wagons, ships, cargo, and the state of warehouses. The port information system with "network-centric" control also receives a set of messages about operations with wagons addressed to it and builds its reference system on their basis. The most complete exchange of information between rail transport and sea ports was carried out on the basis of the Road Information and Logistics System (corporate ACS).

Practical significance, proposals and results of implementation.

Let us highlight the stages of creation and functionality of this program, as well as changes in the operation of the port railway (Table 2).

Table 4.6

Evolution of the development of rail and sea transportation management based on information and logistics principles

Period	Changes in the system and management tools	Changes in technology, results of decisions	Changes in information logistics
1	2	3	4
1999–2005	2003 – the first Logistics Center appeared on the Russian railway network	Recognition of the need for a market approach in planning and regulating the transportation process	Development of corporate information management systems of JSC Russian Railways
2011–2012	Development of a comprehensive integrated technology for managing the movement of freight trains according to schedule	Development of logistics principles for transportation management	Expansion of services (train movement according to schedule, etc.)

Continuation of table 2

1	2	3	4
2013–2016	Development of technology for a Unified Integrated Technological Process for Transport Hubs	Development of technological forms of interaction between modes of transport and participants of the PTTS	Creation of a unified interface for planning train supply, implementation of unified criteria for assessing the quality of planning
2017–2018	Development of a set of tasks for managing the supply of trains heading to port stations, connecting new port operators at stations	Expansion of the number of users, improvement of the quality of information received from sea ports. Diversification of services for port railways («ship lots», «freight express»)	Implementation of an algorithm for automated calculation of the supply plan based on a multi-criteria assessment of the demand for cargo, development of a set of tasks for working with ship lots.
2019–2025	Assessment of infrastructure loading in intelligent control systems (including for port railways)	Formation of a client loading plan. Development of structured supply of trains along junctions to the port railway, taking into account operational modes	Accounting for the capabilities of port roads and port stations for processing wagon flows

For effective interaction with ports and port terminals, the formation of a supply plan can be carried out manually or automatically (based on an algorithm). Taking into account the fact that over the past ten years the nomenclature of cargo arriving at ports has doubled, and within the nomenclature there has been a division into assortment, the task of automatically drawing up a plan for supplying to ports in terms of not only the nomenclature, but also, to a large extent, the assortment comes to the fore. The assortment of cargo nomenclature is dynamically expanding, and the system “does not have time” to update to new data. It was found that not all shippers working in corporate ACS indicated contract numbers, cargo brands in the railway bill of lading. As a result, the automatic calculation of the supply plan had inaccuracies in the distribution of cargo by port areas. As a result of the study and analysis of the ACS operation, non-automated stages were identified (the station manager enters cargo data into the system (order), the Logistics Center dispatcher analyzes the preliminary supply plan and makes adjustments), while the lack of dynamic updating of information on the status of warehouses, weather, etc. was noted, which affected the quality of the plan.

Further development of logistics management tools for PTTS in interaction with rail transport can occur both within the framework of platform-centric and network-centric management (Figure 1).

Modern innovative concepts for organizing the interaction of participants in PTTS, the development of technologies aimed at maximum use of the throughput and carrying capacities of the national transport complex, are in the field of optimization of transport processes based on various modeling methods, as well as digital technologies for improving control systems using artificial intelligence (AI) technologies (Figure 2).

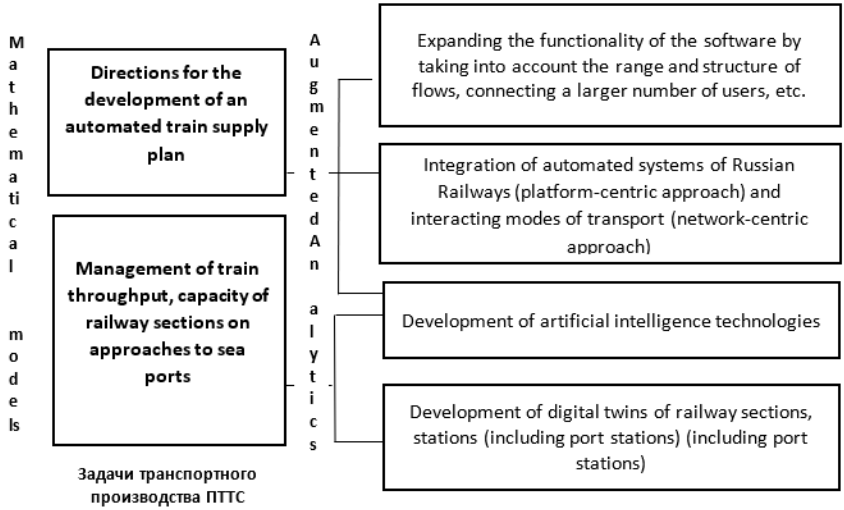

Figure 2. *Directions for the development of information support in the tasks of managing rail freight transportation to sea ports*

Informatization, intellectualization and digitalization of transportation process management are the most important areas of qualitative transformation of PTTS transport production. In the future, it is necessary to focus on the development of digital platforms that ensure increased competitiveness of the holding company JSC Russian Railways by building effective processes that can be flexibly adapted to changes in market conditions; development of digital technologies for solving transportation process management problems based on predictive analytics using modeling, self-training, accumulated knowledge and experience of specialists, with the creation of digital twins of PTTS objects. The core of such systems can include models and methods of artificial intelligence.

The publication was carried out as part of the implementation of a grant from JSC Russian Railways for the development of scientific and pedagogical schools in the field of railway transport.

References

1. *Telegina, V. A. Interaction of modes of transport in freight transportation / V. A. Telegina. – Khabarovsk : DVGUPS, 2013. – 90 p.*
2. *Features of the technology of operation of junction stations and non-public tracks in a single technological process / S. P. Vakulenko, N. P. Zhuravlev, A. A. Sidrakov, M. Yu. Savelyev // Problems of prospective development of railway stations and junctions. – 2022. – No. 1 (4). – P. 52–55.*
3. *Vakulenko, S. P. Improving the interaction between the shipper and the carrier in seaports / S. P. Vakulenko, N. P. Zhuravlev, A. A. Sidrakov // Problems of prospective development of railway stations and junctions. 2020. No. 1 (2). P. 20–29.*
4. *Kurenkov, P.V. Prospects for the Development of Railway Transport in the Context of the Problems of Globalization and Regionalization of the World Economy / P. V. Kurenkov, I. A. Solop, E. A. Chebotareva // Trends and Prospects for the Development of Finance in the Context of Digitalization: Collection of Works of the 1st International Scientific and Practical Internet Conference. – Donetsk, 2024. – P. 219-223.*
5. *The Scientific and Technical Council of JSC Russian Railways approved the concept of the "Digital Railway" // JSC Russian Railways [website]. – 11/30/2017. - URL: https://www.rzd.ru/ru/9284/page/3102?id=56885 (date of access: 06/05/2025).*
6. *Nikiforova, G. I. Study of information interaction of rail and sea transport in logistics chains of cargo delivery / G. I. Nikiforova // Bulletin of the St. Petersburg University of Railway Engineering. – 2022. – Vol. 19, No. 1. – P. 82–89. – DOI 10.20295/1815-588X-2022-19-1-82-89.*

DOI 10.34660/INF.2025.99.38.059
UOT 621.311.22

高参数能量块燃料减排方法研究
RESEARCH OF FUEL REDUCTION METHODS IN HIGH PARAMETER ENERGY BLOCKS

Mammadova Jamila Pasha
PhD, Associate Professor
Babayeva Sevinj Shulan
PhD, Associate Professor
Allahverdiyeva Aytaj Yusif
PhD, Associate Professor
Azerbaijan State Oil and Industry University

摘要：为确保符合新一代超临界、超临界和超超临界参数运行的有前景的发电机组的技术和经济目标，已研究了一系列科学技术方案。研究了初始参数的提高、采用双中间加热、提高回热系统给水温度对电站工作系数和燃料节省的影响，并比较了电站的热效率。

关键词：临界、压力、超临界、温度、超超临界、燃料经济性、工作系数、生态学。

Abstract. *A number of scientific and technical solutions have been investigated to ensure compliance with the technical and economic goals of the creation of promising new generation power units operating with higher than critical, supercritical and ultrasupercritical parameters. Increase of the initial parameters, using double intermediate heating, raise in the temperature of the feed water in the regenerative system, effect on the coefficient of the work of the station and fuel saving were studied and the thermal efficiency of the stations was compared.*

Keywords: *critical, pressure, supercritical, temperature, ultrasupercritical, fuel economy, work coefficient, ecology.*

The socio-economic development of the country is directly related to the production of required electricity. The traditional development of energy around the world and in our country is related to the extraction and use of natural fuels (oil, gas and coal). It should be noted that the growth and demand of hydrocarbon-containing fuels prevails over other energy sources. Despite the increase in directions related to the development of the use of non-traditional technologies in the

production of electric energy, natural fuels are mainly used in the field of world energy and their number is increasing.

According to the information provided by the International Energy Agency [1], in 2018, 26,615 TWh of electricity was produced in the world, the main part (~65%) of which was the share of thermal power plants. 92% of the electricity produced in the Republic of Azerbaijan is generated in thermal power plants. In the next decade, HES are predicted to be at the forefront of the world energy system.

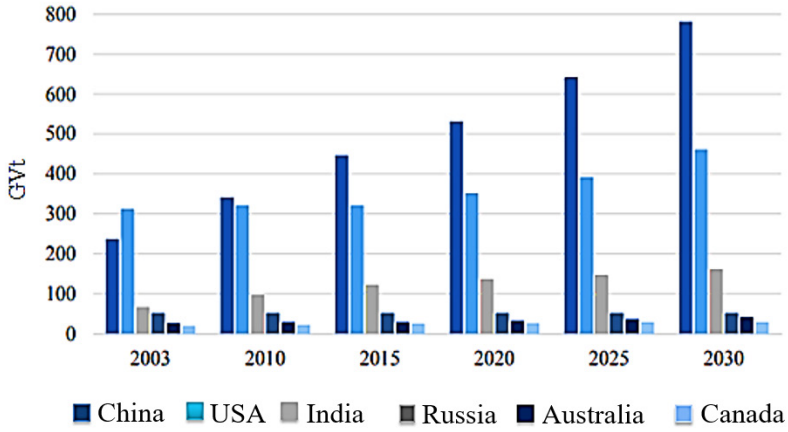

Figure 1. *Growth dynamics of the installed capacity of HES operating on organic fuels over the years*

Therefore, increasing the energy efficiency of steam-turbine installations is one of the urgent issues. The equipment used in steam turbine power plants is almost highly advanced.

Increasing the technical and economic indicators of such devices can be achieved by raising the initial parameters of steam in the thermodynamic cycle.

Currently, in the field of heat energy, researches and studies are being carried out in the field of transition to supercritical and ultrasupercritical parameters of steam [2,3]. With the raise of the initial parameters of the steam, the heat drop in the turbine raises, the power of the unit increases, the turbine efficiency increases, which leads to an increase in the overall efficiency of the unit and the thermal power plant, and as a result, the specific fuel consumption decreases. This means saving tons of fuel per year. When fuel is saved, the amount of smoke gases emitted into the atmosphere decreases, which leads to the improvement of environmental indicators.

At pressures of steam higher than critical (P_{cr}=22.1 MPa for water), the latent heat of vaporization is zero. Therefore, the heat required for vaporization at a pressure above the critical is much less than at a pressure below the critical. Accordingly, fuel consumption is much lower in steam generators operating at supercritical pressure. Thus, the main way to save fuel in thermal power plants is to increase the initial parameters of steam (pressure P_0, temperature t_0), as a result, the power of the units increases, and the fuel is saved and the environmental load is reduced.

Turbines with a power of 300, 500, 800, 1200 MW operate with parameters higher than critical (P_0=24 MPa, t_0=565^{0}C). One of the main directions is the creation of blocks working with stronger supercritical parameters (P_0=31 MPa, t_0=630^{0}C), ultrasupercritical parameters (P_0=38 MPa, t_0=650-700^{0}C). In such blocks, it is possible to get more than 50% efficiency of electricity production [4,5].

The use of hydrocarbons in the production of electricity, the presence of harmful gases in the gases released into the atmosphere with flue gases, and their impact on the environment cause climate change. The high concentration of carbon dioxide (CO_2) in the atmosphere, mainly contained in smoke gases, seriously affects people. Due to the increase in the starting parameters of the steam, the amount of smoke gases emitted into the atmosphere and the amount of sulfur gases decreases as the fuel consumption decreases.

Calculations show that when comparing a block with a power of 300 MW and operating at highcritical parameters (P_0=24 MPa, t_0=540^{0}C) with a block of the same power but operating at supercritical parameters (P_0=31 MPa, t_0=630^{0}C), the specific fuel The reduction in consumption is shown in the table below.

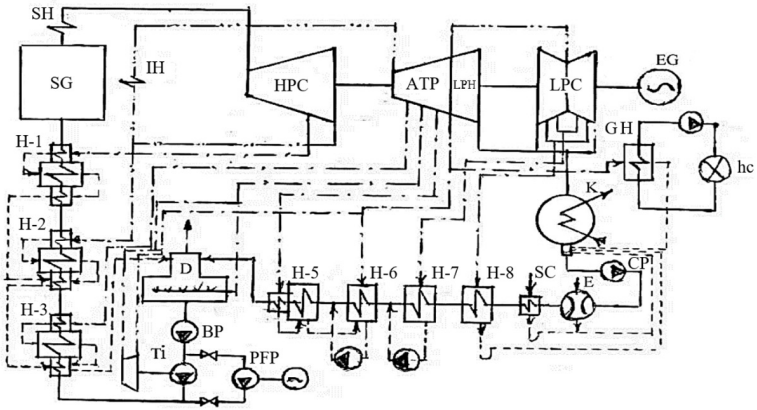

Figure 2. *The principle heating scheme of the K-300-240 type power unit operating with parameters higher than critical*

Table 1

Comparison of the block operating at high-critical and supercritical parameters

Factors that reduce specific fuel consumption	Reduction of specific fuel consumption,%
Fresh steam pressure increase from P_0=24 MPa to P_0=31 MPa	2,1
Fresh steam temperature increase from t_0=540^{0}C to 630^{0}C	2,4
Increasing the temperature of the steam in the intermediate heating of the first stage	0,8
Increasing the temperature of the steam in the second stage intermediate heating	1,8
Increasing the temperature of the feeding water from 270^{0}C to 310^{0}C	0,8

It can be seen from the table that the reduction of specific fuel consumption is 7%. The accuracy of these values coincides with the values indicated in external sources for the considered block [6]. Thus, when comparing the block with the feed water temperature $t_{f.w}$=273^{0}C at the pressure P_0=31 MPa, temperature t_0=600 (560) 565^{0}C, with the base standard block, conventional fuel saving is 14.8 g/kWh.

However, according to calculations carried out within the framework of EPPJ programs, capital costs increase by 30-40% when comparing a unit with high-critical power with a supercritical unit. The reason for this is that heat-resistant, higher quality steels are used in such a station. However, despite this, the blocks working with high parameters are considered more economical.

When considering the characteristics of steam-power plants, the thermodynamic characteristics of using elevated parameters should be taken into account. Thus, the increase in temperature has a positive effect on the increase in efficiency. When the pressure raises, moisture increases in the final stages of the turbine. Increasing both parameters (P_0, t_0) together gives a higher result. Single and double intermediate heating is used to overcome the disadvantage of pressure increase and to increase the efficiency. Below is the principle heating scheme of a 1000 MW unit operating at ultra-supercritical parameters with one-time intermediate heating. It can be seen from the table that the reduction of specific fuel consumption is 7%. The accuracy of these values coincides with the values indicated in external sources for the considered block [6]. Thus, when comparing the block with the feed water temperature $t_{f.w}$=273^{0}C at the pressure P_0=31 MPa, temperature t_0=600 (560) 565^{0}C, with the base standard block, conventional fuel saving is 14.8 g/kWh.

However, according to calculations carried out within the framework of EPPJ programs, capital costs increase by 30-40% when comparing a high-critical power unit with a supercritical unit. The reason for this is that heat-resistant, higher qual-

ity steels are used in such a station. However, despite this, the blocks working with high parameters are considered more economical.

When considering the characteristics of steam-power plants, the thermodynamic characteristics of using elevated parameters should be taken into account. Thus, the increase in temperature has a positive effect on the increase in efficiency. When the pressure increases, moisture increases in the final stages of the turbine. Increasing both parameters (P_0, t_0) together gives a higher result. Single and double intermediate heating is used to overcome the disadvantage of pressure increase and to increase the efficiency. Below is the principle heating scheme of a 1000 MW unit operating at ultra-supercritical parameters with one-time intermediate heating.

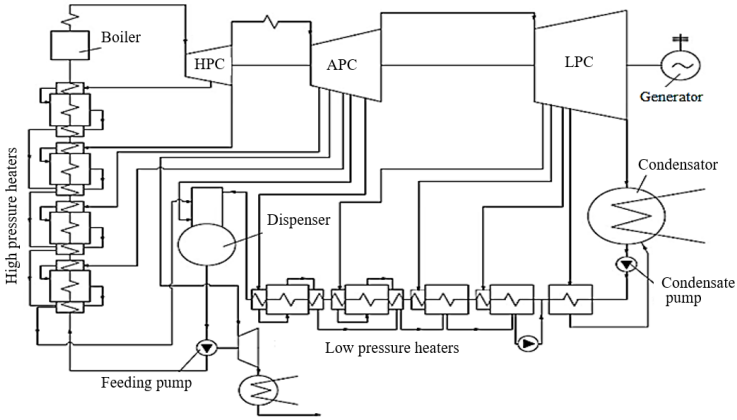

Figure 3. *The principle heating scheme of a block with a power of 1000 MW single intermediate heating operating at ultrasupercritical parameters*

When this block works with the initial parameters P_0=35 MPa, t_0=700^{0}C, the moisture content in the final stages is 19% higher than the norm, and when using one-time intermediate heating, the moisture content in the final stages is 7.42%.

In units operating with ultrasupercritical parameters, since the initial pressure exceeds 30 MPa, double intermediate heating is used. Then the pressure of the first intermediate heating is taken as 15-25% of the initial pressure, and the pressure of the second intermediate heating as 6-9% of the initial pressure.

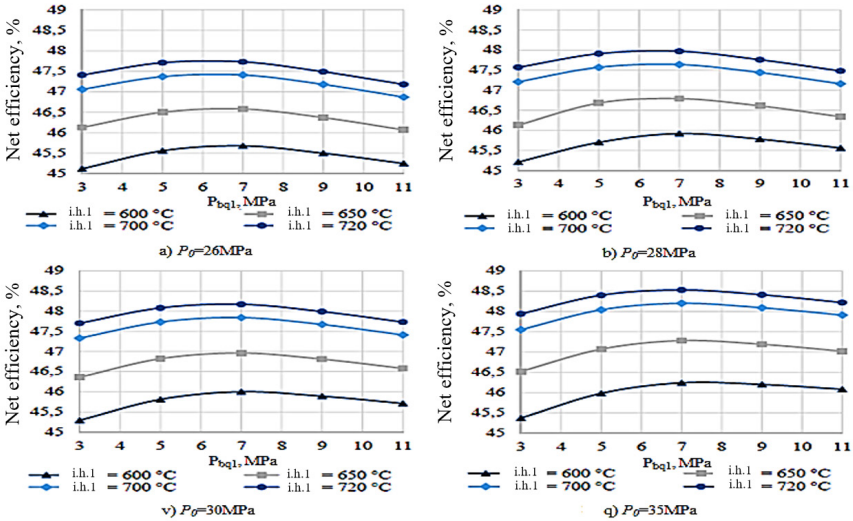

Figure 4. *Dependence of the net efficiency on the pressure of intermediate steam heating at a constant initial pressure*

Figure 4 shows the dependence of net fuel efficiency on pressure ($P_{i.h}$) of intermediate heating at different pressures of fresh steam (P_0=26 MPa, P_0=35 MPa). In the increase of pressure from 26 MPa to 35 MPa, the favorable price of efficiency increases by 1.6%.

One of the factors influencing the increase of the utility of the station and the reduction of fuel is the regenerative heating of the feed water. Choosing the appropriate temperature of the feed water is a technical and economic issue, because many factors affect this factor - fuel price, electrical load schedule, turbine separations, circuit design, etc.

The temperature of the feed water depends on the parameters of the high-pressure heaters located in front of the boiler. It is the initial parameters of the steam that affect the favorable temperature of the feed water.

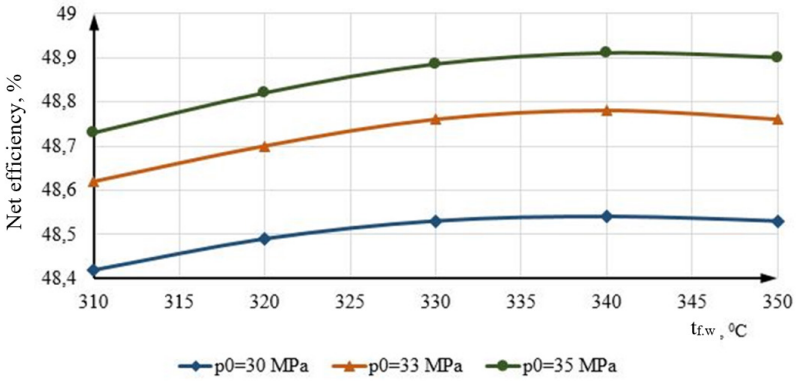

Figure 5. *Dependence of Net efficiency on the temperature of the feed water: $t_{f.w}$; MPa*

At different values of initial steam pressure, different favorable value of feed water temperature is obtained. As the pressure increases, so does the temperature of the feed water. At pressures of 30-35 MPa, the favorable temperature of the feed water is 330-340^{0}C. As the feed water temperature increases, the net efficiency of the unit increases and fuel is saved. The calculation of the principle heating scheme of 1000 MW power block operating with ultra-supercritical parameters was carried out and the following results were obtained: gross efficiency 50.96%; net efficiency 48.5%. Specific consumption of fuel for electricity production is 240 g/kWh. The specific consumption of fuel according to the released energy is 254 g/kWh.

If to compare the obtained results with the indicators of the 300 MW block operating with parameters higher than critical (η^{gr}=43%; η^{net}=41%; b^{gr}=286 g/kWh; b^{net}=300.2 g/kWh), in the ultrasupercritical block efficiency increased from 41% to 48.5%, specific fuel consumption decreased from 300.2 g/kWh to 254 g/kWh.

The obtained characteristics show that it is possible to create power units with an efficiency of 50-51%, and currently, units having an efficiency of 48-51% operating with an ultrasupercritical parameter have been created. As fuel consumption is reduced, the amount of smoke and harmful gases emitted into the atmosphere is reduced and the environmental burden is reduced. Both steam turbine and combined steam-gas turbine HESs are widely used in the field of energy, and natural gas fuels are used in these plants. When the starting temperature of the working body is 1500^{0}C, the efficiency is reached up to 60% [7]. Improving the technology of steam-gas plants and using solid fuel in them is one of the main issues. One of

the priority issues is to improve the efficiency of steam turbine plants to the efficiency of steam-gas turbine plants.

Conclusion

1. To increase the efficiency of steam power plants, it is more convenient to operate them in high-critical, supercritical and ultrasupercritical parameters of steam.

2. When comparing the block operating with high-critical parameters to the block operating with supercritical parameters, the specific fuel consumption is reduced by 7%, that is, the amount of conventional fuel is saved by 14.8 g/kWh.

3. Comparing the high-critical unit with the ultrasupercritical unit, the net efficiency increased from 41% to 48% and the specific fuel consumption decreased from 300.2 gr/kWh to 254 gr/kWh.

4. Due to the reduced fuel consumption in high-parameter stations, the amount of smoke gases released and the environmental burden decrease.

References

1. Electricity information 2017 Edition – Paris: İnternational Energy Agency 2017-p.71.

2. Olkhovsky G.G. Thermal power technologies until 2030 // News of the Russian Academy of Sciences. Energy – 2008, No. 6 – pp.79-94.

3. Fedorov M.P. Energy technologies of the 21st century: development trends. Part 1 // Academy of Energy 2009, No. 3, pp. 12-25.

4. Stepczynska K. Calculation of a 900 MW conceptual 700/720^{0}C coalfired power unit with a nauxili aryex traction-back pressure turbine // journal of power technologies – 2012 - № 92(4) – pp. 266-273.

5. Storm C. Advanced manufacturing and assembly strategies for nickel-based super alloys applied at ultra – super critical power plants/C storm // Proceeding of Workshop on Advanced Ultrasupercritical Cool Fried Power Plants – Vienna, Austria, 2012.

6. Kjaer S. Experience in the design and operation of power units for supercritical steam parameters in Denmark // Electric Stations. 2002, No. 3, pp. 63-68.

7. Tsanev S.V. Gas turbine combined-cycle plants of thermal power plants: a textbook for universities - M. Publishing house MPEI, 2002 - p. 584.

DOI 10.34660/INF.2025.10.55.060
UDC 504.06

废墟下的最新探测设备
THE LATEST DETECTION DEVICES UNDER THE RUBBLE

Tomshin Evgeny Alexandrovich
PhD student
Kosygin State University of Russia

Akatiev Vladimir Andreevich
Doctor of Technical Sciences, Professor
Kosygin State University of Russia

Shuvarikov Denis Vladimirovich
Senior Engineer
Scientific and Technological Centre of Unique Instrumentation of the Russian Academy of Sciences

摘要。本文致力于探讨使用非接触式探测方法（光谱分析结合高温测量法）对废墟下人员进行搜救的有效性。研究的目的是记录使用俄罗斯科学院特种仪器工程科学技术中心（以下简称 STC UP RAS）研制的对比度计进行的现场试验结果。顾名思义，该设备的主要工作原理是确定背景环境温度与搜救对象（尤其是人员）之间的对比度。现场试验于 2025 年在卡卢加州进行。实验方法包括组织 11 个不同的场地，模拟堵塞情况并在场地上放置物体（金属、非金属和温暖的模拟生物体）。研究人员采用了最新的对比度计曝光方法，改进了其技术特性（曝光深度增加至1.0米），并证明了其作为救生员个人装备中有效工具的优势。研究人员采用了实证方法评估结果。在测试过程中，证实了该设备能够照射所有类型的公共物体，模拟各种堵塞情况。此外，还发现了其在紧急救援行动中的应用前景，包括在难以到达的地点搜救人员。

关键词：高温计、对比度计、搜救行动、废墟下人员搜救、实验。

Abstract. *The article is devoted to the effectiveness of the search and rescue of people under the rubble using contactless methods of disclosure (spectral analysis in combination with the pyrometric measurement method). The purpose of the study is to record the results of field experiments on the use of a contrast meter developed by the Scientific and Technical Center for Unique Instrument Engineering of the Russian Academy of Sciences (hereinafter STC UP RAS). As the name of the device implies, the main principle of its operation is to determine the contrast between the ambient temperature of the background environment and the search object, in particular, a person. Field experiments were conducted*

in 2025 in the Kaluga Region. The experimental methodology consisted in the organization of eleven different sites that simulate the conditions of blockages and the placement of objects (metallic, non–metallic, and warm - simulating living biological organisms) on the sites. The latest methods of exposure using a contrast meter have been used, its technical characteristics have been improved (the depth of exposure has been increased to 1.0 m), and the advantages of using it as an effective tool in a lifeguard's individual set of equipment have been proven. Empirical methods were used to evaluate the results. During the tests of the device, its capabilities of making public objects of all types, on all types of sites simulating a blockage, were confirmed. Promising directions for its use in emergency rescue operations, including for the search and rescue of people in hard-to-reach places, have also been identified.

Keywords: *pyrometer, contrast meter, search and rescue operations, search for people under rubble, experiment.*

Search and rescue of people under rubble often face one of the most difficult problems: the need to reduce the impact on the rubble. Here, the structure of the rubble and the presence of victims in it are of great importance. If large equipment is used in a rescue operation, this, as a rule, is fraught with the collapse of individual structures, which significantly worsens the overall situation for people under the rubble. As part of the systematization of approaches that would solve this problem and reduce the risk of additional victims [1], the issue of using the latest methods and means of searching for people under rubble, including the existing instrumentation and hardware base for searching for victims under rubble, is relevant. In this case, preference should be given to remote and contactless detection. Such means include Doppler radars [2] and pyrometric devices [3]. These means are capable of detecting temperature anomalies in the rubble layers, which allows detecting people in voids. In addition to these devices, it is advisable to use acoustic sensors [4], which can additionally confirm the presence of people under the rubble. In the specialized literature it is noted that the combined use of various search methods and the complexity of the search approach allow not only to increase the effectiveness of the rescue operation, but also to increase the accuracy of determining the location of people, reducing the risk of their subsequent injury as a result of the collapse of the rubble [5, 6].

Research methods. The physical phenomena described in the Wien displacement laws, the Kirchhoff and Planck thermal radiation, the Stefan-Boltzmann blackbody radiation, the patterns of the average spectral-energy contrast [7-10], including determining the difference in radiation of the body and the background surrounding it, were taken as a basis.

The purpose of the article is to consider the efficiency of using one of the newest non-contact devices for detecting various objects under rubble. Also, the

task is to show the features of the practical use of the tool when working to detect various objects under rubble. Such a tool is a compact portable contrast meter of the 2025 model. The device combines the technology of non-contact temperature measurement and spectrum determination. This hand-held measuring device was not originally intended for searching for people under rubble (Fig. 1).

Figure 1. *Appearance of the device*

The device weighs 700 g and has an autonomous power supply, has a minimum of parts and does not require special adjustment, which makes it ideal for use in the field of emergency rescue operations. During testing, the prototype demonstrated the following technical characteristics: operating temperature range from minus 20 to +50 °C, sensitivity up to ±0.2 °C, wavelength from 1.0 to 15.0 μm, sighting index of 24. The working hypothesis for using it to search for victims was that the contrast meter is capable of accurately determining the location of various objects under rubble. For the experiment, metal, glass, plastic, biological objects were used, placed under the ground and simulated rubble at a depth of up to 0.5 m.

For full-scale testing, a rubble was simulated in which wood waste, soil turf and soil layers, various fractions of construction rubble, and household waste were artificially placed. Metal scraps (weighing up to 2 kg), plastic dummy explosive devices, biological waste, and a rubber hot-water bottle with warm water (30-40 C) were also used as detection objects.

Results and discussion. Field tests of the device were conducted in April 2025 in the Kaluga Region. The tests were attended by researchers and engineers of the Scientific and Technical Center of the Ukrainian Institute of Machine Building, students and postgraduates of the A.N. Kosygin Russian State University, employees of the Center for Conducting Special Risk Rescue Operations “Leader” of the Russian Emergencies Ministry, as well as representatives of a wide range of search and rescue and public organizations.

As an experimental testing ground [11], the participants created several model sites, each of which imitated a rubble and one or another object for detection, located at different depths. The contrast meter was used by the operator (rescuer) when examining each site with a blockage, the examination was carried out in manual mode, the angle of inclination to the surface was arbitrary, the distance to the surface was about 1.2 m.

Table 1.

Test procedure

№	Experimental site	Method of implementation
1	Control	A contrast meter examines an «empty» area to assess the average spectral-energy contrast (AEC) of the soil.
2	Earth surface (clean experiment)	A pile of dead wood, garbage, 0.5 m soil layer, no objects to search for.
3	Pit 1 (dry area)	Sequential placement of a metal object/organic matter/thermal object (heater) on the surface of the earth outside the rubble.
4	Pit 2 (swampy area)	Determination of the AEC of the object and soil.
5	Imitation of a blockage (an embankment above the soil surface, consisting of rotted leaves, fresh turf, dry grass, concrete chips, garbage, wood waste, stones, soil)	Sequential placement of a metal object/organic matter/thermal object (heater) under the surface (depth of 0.3 m, 0.5 m, and also additionally to a depth exceeding the detection characteristics of 1.0 m for this device). Determination of the AEC of the object and soil.

The evaluation results demonstrated that the device under study is capable of detecting all types of objects under rubble, including in conditions with high humidity. It was found that when used to detect warm objects (imitation of victims), the contrast meter is operational both at the calculated depth level and at a depth of up to 1.0 m (which is 2 times greater than the calculated depth). It is important that the autonomy of the contrast meter allowed it to remain operational throughout the entire experiment without recharging, reconfiguration or calibration. This feature makes it indispensable in the individual rescuer's equipment kit. Conclusions. The search for people and objects trapped under rubble is one of the most pressing modern tasks due to the growth of man-made accidents, the presence of seismically active zones, as well as destruction caused by military conflicts in various regions. As practice shows, more than a third of victims may die during the first day after the start of rescue operations. Especially if the rubble clearance is carried out chaotically and is accompanied by significant soil movements, and there is no information about the location of people under the rubble, which can lead to serious injuries during the rescue operation. Modern devices of the Russian Academy

of Sciences, including the contrast meter described in this article, effectively solve two key problems: non-invasive detection of people under rubble (without violating the integrity of the rubble layers); accelerated detection of victims (increasing their likelihood of survival). It should also be noted that in a number of the equipment and instrumentation base used today for rescue operations [12], this contrast meter has a number of advantages. First of all, the detection itself is carried out in a simple and accessible way, does not require additional technical means or resources, takes several minutes, and its results are displayed on the screen and are understandable even intuitively. Despite the fact that the device will need to be modified for more effective use in conditions of high humidity (floods, waterlogging), today the technical characteristics of the contrast meter have already been fully confirmed by tests, and the device itself can be used in search and rescue operations of any complexity and location.

References

1. Kozulov K. V., Aksenov S. G. On the Features of Conducting Emergency Rescue Operations // Stolypin Bulletin. 2022. No. 8. URL: https://cyberleninka.ru/article/n/k-voprosu-ob-osobennostyah-provedeniya-avariyno-spasatelnyh-rabot (date of access: 24.04.2025).

2. Yurochkin A. G., Panarin D. G. Problems of Modeling the Processes of Detecting People Under Construction Rubble in Emergency Situations. Modeling, Optimization and Information Technology. 2016; 4 (3). URL: https://moit.vivt.ru/wp-content/uploads/2016/10/PanarinYurochkin_3_16_3.pdf DOI:

3. Pozhar V.E., Balashov A.A., Bulatov M.F. Modern spectral optical devices of the Scientific and Technical Center of the Ukrainian Academy of Sciences // NP. 2018. No. 4. URL: https://cyberleninka.ru/article/n/sovremennye-spektralnye-opticheskie-pribory-ntts-up-ran (date of access: 07.04.2025).

4. Turov A.T., Konstantinov Yu.A., Barkov F.L., Claude D. Study of the parameters of a simple distributed acoustic sensor // Photon-express. 2023. No. 6 (190). URL: https://cyberleninka.ru/article/n/issledovanie-parametrov-prostogo-raspredelennogo-akusticheskogo-datchika (date of access: 24.04.2025).

5. Malfi H. A., Masaed N., Mokshantsev A. V. On the use of a radar signal system module during search and rescue operations // Fires and Emergencies. 2022. No. 4. URL: https://cyberleninka.ru/article/n/o-primenenii-modulya-sistemy-radiolokatsionnyh-signalov-pri-provedenii-poiskovo-spasatelnyh-rabot (date of access: 24.04.2025).

6. Zakharchenko V. A., Lobov D. G., Shkaev A. G., Valke A. A. Pyrometer with video monitoring of the measurement area // ONV. 2022. No. 1 (181). URL: https://cyberleninka.ru/article/n/pirometr-s-videokontrolem-oblasti-izmereniy (date of access: 04/24/2025).

7. Belousov Yu. I., Postnikov E. S. Infrared photonics. Part I. Features of the formation and propagation of IR radiation. Textbook. - St. Petersburg: ITMO University, 2019. - 82 p.

8. Koshman V. S. On the issue of searching for the longevity equation of the Planck epoch // Sciences of Europe. 2020. No. 61-1. URL: https://cyberleninka.ru/article/n/k-voprosu-poiska-uravneniya-dolgovechnosti-epohi-planka (date of access: 24.04.2025).

9. Bulatov Kamil Maratovich, Zinin Pavel Valentinovich, Khramov Nikita Andreevich Modified method of spectral ratio for remote measurement of temperature distribution by multispectral video cameras // KO. 2025. No. 1. URL: https://cyberleninka.ru/article/n/modifitsirovannyy-metod-spektralnogo-otnosheniya-dlya-distantsionnogo-izmereniya-raspredeleniya-temperatur-multispektralnymi (date of access: 24.04.2025).

10. Zenchenko S. S. Features and results of IR field measurements from a 4-slit target disk and an absolutely black body in the spectral range of 7-14 μm // Proceedings of the Krylov State Research Center. 2022. No. 4 (402). URL: https://cyberleninka.ru/article/n/osobennosti-i-rezultaty-izmereniy-ik-polya-ot-4-schelevoy-disk-misheni-i-absolyutno-chernogo-tela-v-diapazone-spektra-7-14-mkm (date of access: 04.04.2025).

11. Vinokurov M. V., Krasnov I. A., Kichaikin V. V., Nitkin A. N., Chumakov E. S., Belov D. S. Development of a training ground for the development of practical skills and abilities in emergency rescue operations in conditions of limited space and visibility during the elimination of fires and emergency situations accompanied by the collapse of building structures, destruction of engineering and technological communications "STALKER" // Modern problems of civil protection. 2020. No. 4 (37). URL: https://cyberleninka.ru/article/n/razrabotka-uchebno-trenazhernogo-poligona-dlya-formirovaniya-prakticheskih-umeniy-i-navykov-provedeniya-avariyno-spasatelnyh-rabot (date of access: 04/21/2025).

12. Tkhakokhov A. A. Innovative technologies and equipment for emergency response // International Journal of Humanities and Natural Sciences. 2023. No. 5-4 (80). URL: https://cyberleninka.ru/article/n/innovatsionnye-tehnologii-i-tehnika-dlya-likvidatsii-chrezvychaynyh-situatsiy (date of access: 04/24/2025).

DOI 10.34660/INF.2025.49.77.061

用于改善消费设备供电质量的现代设备
MODERN DEVICES FOR IMPROVING THE QUALITY OF POWER SUPPLY TO CONSUMER EQUIPMENT

Mikhailov Yuri Stepanovich
General Director
Limited Liability Company "Innovative Technologies Plant"
Romanov Roman Artemyevich
Candidate of Technical Sciences, Associate Professor
Chuvash State University named after I.N. Ulyanov

摘要：本文探讨了在俄罗斯联邦经济发展典型条件下如何提高用户供电质量的问题。对现有的高速设备进行了分析，并提出了一种利用直流母线控制和稳定装置提高用户供电质量的方法。经过研究和测试的直流稳压器的特点是采用了超级电容器储能和独特的IGBT功率晶体管工作算法，从而确保了高速度、长使用寿命和高质量的电能指标。

关键词：供电质量、电压暂降、短时电压中断、高速设备、直流稳压器。

Abstract. *The article is devoted to the issues of improving the quality of electricity supply to consumers in the conditions typical for the economic development of the Russian Federation. An analysis of existing high-speed devices is conducted and a method for improving the quality of electricity supply to consumers using a DC link control and stabilization device is proposed. The peculiarity of the considered and tested DC voltage stabilizer is the use of a supercapacitor storage and unique algorithms for the operation of power IGBT keys, which ensure high speed, long service life and high quality indicators of electrical energy.*

Keywords: *quality of electricity supply, voltage dips, short-term voltage interruptions, high-speed equipment, DC voltage stabilizer.*

In recent years, the relevance of issues related to improving the quality of electricity supply to consumers has increased in Russia, which is determined by a combination of a number of factors:

- high wear and tear of electric grid facilities of energy sales and grid companies [1];
- the emergence of new types and an increase in the number of equipment sensitive to the quality of electricity supply (electric transport, data processing centers, operational dispatch control systems, etc.) [2; 3];

- integration of active industrial energy complexes [4 - 6] and microgeneration facilities [1] into the energy system;

- development of the fuel and energy and transport infrastructure of Russia in the direction of the Asia-Pacific region [3];

- the need to increase the pace of automation of the Russian economy [7];

- solving the socio-economic problems of the state related to improving the quality of power supply to housing and communal services facilities [2].

The most significant contribution to financial losses is made by voltage dips and short-term interruptions (up to 60%). According to the studies cited in [8], the consumer experiences on average up to 50 technological violations per year caused by voltage dips, and up to 36 cases - critical interruptions (data for 2019). Despite the serious impact of power quality violations on consumers' electrical equipment, the number of dips and short-term interruptions is not standardized in state regulatory documents (GOST 32144-2013). Consequently, ensuring the reliability of electrical equipment falls entirely on the energy services of consumers.

The problem of power quality violations is most pressing in the oil and gas sector, where electrical equipment of various reliability categories for power supply that is sensitive to voltage drops and interruptions is widely used:

- electric motors of various pumps (supplying oil to the compressor lubrication system, raw materials to tubular furnaces of pyrolysis and thermal cracking processes, etc.);

- electric valves installed on compressed air receivers and at the inlet of high-pressure steam;

- electric drives (on the lines supplying fuel to the furnace and water vapor to the steam curtain, on the suction and discharge of gas compressors, compressor equipment interlock systems, etc.);

- compressors (for circulating the gas mixture in reforming units, hydrotreating, etc.);

A fairly extensive list of equipment is also used in the mining industry:

- fire-fighting pumping units;

- mine and quarry drainage systems;

- main ventilation fans for gas-hazardous mines and coal mines;

- underground installations servicing the descent and ascent of people;

- central underground substations, etc.

With the development of digital control systems in the energy sector and the introduction of distributed generation complexes (including those based on renewable energy sources - RES) [6], the range of equipment that ensures the stable operation of operational dispatch control systems for energy facilities is expanding. A similar situation is developing in digital control systems of government agencies (FSB, Ministry of Internal Affairs, etc.), healthcare, railway transport,

data processing centers, etc. It is noted that limiting the mode of electricity consumption of these facilities can lead to serious economic, social and environmental consequences.

Among the proposed measures to reduce voltage dips and short-term interruptions (rational selection of equipment and technical systems, correct choice of connection points), the need to use modern high-speed equipment is noted:

- high-speed automatic input reserve devices (AIRD);
- uninterruptible power supplies (UPS);
- dynamic voltage distortion compensators (DVDC).

At the state level, questions are being raised about the need to develop domestic equipment to ensure technological safety and the introduction of technological innovations at enterprises in the fuel and energy complex [4]. The choice of methods and types of applicable equipment depends on the technical characteristics and operating conditions of the consumer's electrical equipment. Automatic transfer switch (ATS) devices have become widely used in electrical networks to combat long voltage interruptions. The use of BATS in 6-10 kV networks instead of ATS theoretically allows reducing the duration of voltage interruption to 40-70 ms. However, such durations of voltage dips are ensured only under ideal conditions. In reality, the short circuit duration is determined by the short circuit disconnection time of distance protection (DZ 2 and 3 stages) and can range from 140 to 1500 ms, taking into account the duration of circuit breaker operation. At least 2-5 seconds pass before the time of successful operation of the automatic reclosing device or detection of a damaged input. Such duration leads to failures in the operation of electrical equipment, "dropping out" of magnetic starters, unacceptable reductions in torque on the shaft of electric motors and other equipment. The situation is especially critical in external power supply networks with network substations using sectional switches, where determining the location of the fault can be significantly complicated. Thus, the use of BAVR and AVR in medium-voltage electrical networks in real conditions does not allow completely eliminating the negative impact of voltage dips and short-term interruptions. In systems where it is necessary to ensure higher speed (operational dispatch control systems, data processing centers (DPC), drawing mills, etc.), it is preferable to use devices such as UPS or DCS. UPS are optionally suitable for compensating interruptions (long and short) and voltage dips in both DC and AC networks. The key disadvantage of the UPS is the excessively laid power for the starting currents of the load, which is used in rare cases, which negatively affects the efficiency of the device, increases the dimensions and weight of the products. At the same time, UPS often use rechargeable batteries (AKB) with a short service life and number of charge/discharge cycles. Consequently, in networks with low power supply quality indicators, the cost of operation and maintenance of systems with UPS increases significantly.

Compared to battery UPS, DC UPS have better characteristics in both speed and weight and size indicators, due to the use of DC link capacitor energy. At the same time, they are designed to solve a wider range of problems in AC networks (filtering harmonic components, power factor correction, etc.), which may be excessive for the consumer and, as a result, a more expensive solution.

The key role in the selection of electrical equipment can be played by the features of the consumer's power supply circuit and equipment connection points. Power supply of a fairly wide class of devices of a special group is associated with the conversion of electric current frequency (data centers, renewable energy sources, frequency-controlled converters, etc.), including a complete transition from alternating to direct and back. If there are direct current circuits in the power supply circuit, the solution of a wide range of problems to ensure the quality of power supply can be reduced to the solution of one problem: voltage stabilization in the direct current link. The power circuit of a constant voltage stabilizer (DVS) can be built on the principle of a bidirectional DC-DC converter (Fig. 1).

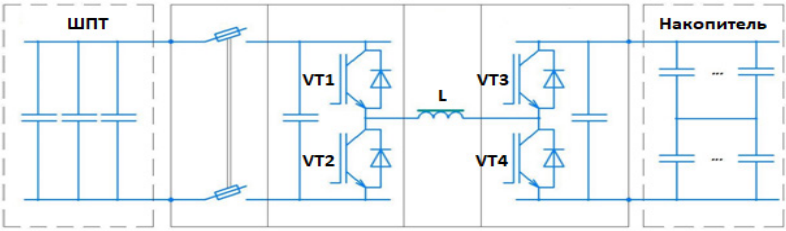

DCB– DC bus of the frequency converter; L – choke; VT1, VT2 – IGBT transistors of the first half-bridge; VT3, VT4 – IGBT transistors of the first half-bridge.
Figure 1. *Functional diagram of SCV720-250*

The main elements of the power circuit are two IGBT half-bridges (switches VT1/VT2 and VT3/VT4) and choke L. The SCV control system monitors the voltage level on the DC bus (DCB) and, when the nominal voltage value appears, switches switch VT1 to the dynamic operating mode (Atop function in Figure 2). SCV switches to the storage battery charging mode. The power unit operates in the step-down DC-DC converter mode and increases the voltage in the storage battery to the voltage level in the DCB.

When the voltage level in the storage device reaches the value of the DCB voltage, the VT1 switch is switched to a static open state, and VT4 switches to the dynamic mode (Bbot function). The DCB switches to the step-up DC-DC converter mode and operates until the nominal voltage value is established on the storage device. The parameters of the pulse-width modulation (PWM) of the dynamic

operating mode of the VT1 switch are determined by the permissible charging duration, the current value, and the storage device capacity. After the specified voltage value is established on the storage device, the control system switches the DCB to the standby mode, monitoring the voltage levels in the DCB and the storage device with a specified discreteness.

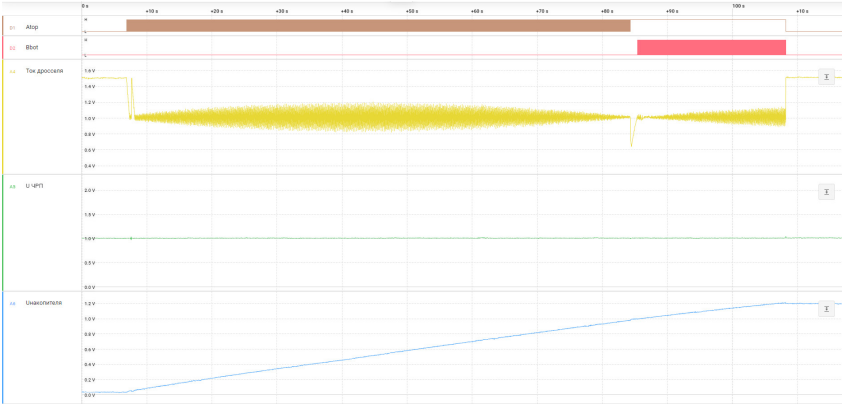

D1 – voltage on VT1; D2 – voltage on VT4; A4 – current in the choke; $U_{чрп}$ – voltage on the DBS;
$U_{storage\ device}$ – voltage on the supercapacitor storage unit
Figure 2. *Storage unit charge graphs*

In case of technological failures, the SCV control system registers a voltage drop in the DCB and switches the VT3 switch to the dynamic mode (Btop function in Figure 3). The SCV switches to the step-down DC-DC converter mode with the transfer of electrical energy from the storage unit to the DCB. At this point, a decrease in the voltage level is observed on the storage unit (Udc4 in Figure 3).

When the voltage in the storage unit drops below the voltage level on the DCB, the control system switches the SCV to the step-up DC-DC converter mode, while the VT3 switch opens completely, and the VT2 switch (Abot function in Figure 3) switches to the dynamic mode. Maintaining the power balance can be ensured by using adaptive control algorithms that change the PWM parameters in such a way as to ensure a proportional increase in current to the voltage drop.

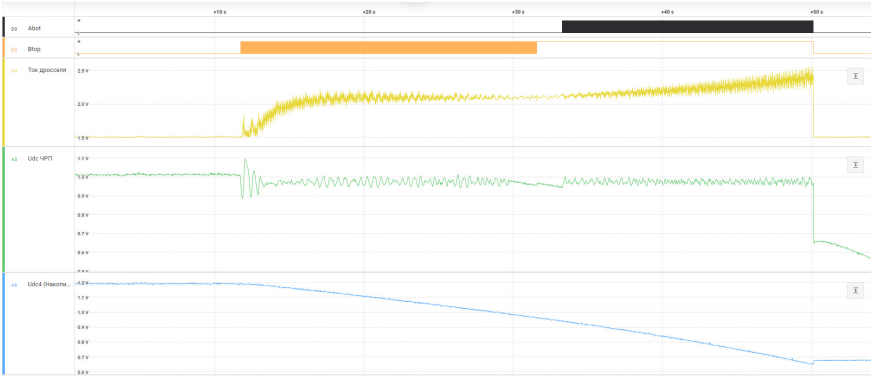

D0 – voltage on VT2; D3 – voltage on VT3; A4 – Current in the choke (inverted graph); $U_{dcЧРП}$ – voltage on the DCB; U_{dc4} – voltage on supercapacitor storage
Figure 3. *Graphs of the storage device discharge process*

In the discharge mode, the SCV can operate until one of two events occurs: the restoration of the network voltage on the SCV or reaching the lower threshold of the permissible voltage level on the storage device. When the lower voltage threshold is reached, the control system switches off the power circuit and switches the SCV to the standby mode for the appearance of voltage on the SCV.

In order to confirm the operability of the proposed technical solution, a cabinet-type SCV unit (Fig. 4) with a supercapacitor storage device was developed and tested.

The proposed algorithms of adapted control with automatic regulation of the PWM parameters of IGBT keys (graphs in Figures 2 and 3) were tested and developed on the pilot unit. To compensate for the self-discharge phenomenon in the absence of technological disruptions in the power supply, algorithms and software for the control system were developed. When the voltage drops below the set value, the control system switches the SCV to the step-up DC-DC converter mode and maintains the voltage on the storage device within the specified range. The cyclicity and duration of operation in the recharge mode depend on the selected voltage interval, the capacity of the storage device and the characteristics of the capacitors used. For example, when using a supercapacitor buffer storage device with a capacity of 6.3 F, the voltage drop due to the self-discharge phenomenon is about 100 V per day (from 720 to 620 V).

Left – design of the power unit of the prototype; Right – pre-production sample
Figure 4. *DC voltage stabilizer SCV720-250 of cabinet design*

The key disadvantage of the SCV is the need to connect to a DC link, the elements of which in many cases are internal elements of the design of frequency converters and may be physically inaccessible.

Conclusions:

Today, in the electric power industry and electrical engineering, there are various methods and means for improving the quality of power supply to consumers. The most common technical solutions in electrical networks do not allow eliminating voltage dips and short-term interruptions.

The choice of a specific type of equipment and the necessary measures to reduce dips and short-term interruptions in voltage, including to ensure the required quality of electricity, depend on the consumer's power supply scheme and the statistics of technological failures at the facility.

For power supply schemes with a DC link, a DC voltage stabilization unit with a supercapacitor storage has been developed and tested. The pilot plant was used to test unique control algorithms for a bidirectional DC-DC converter, which make it possible to maintain the required voltage level in the DC-DC converter when the voltage in the storage device drops, which is confirmed by the results of experimental studies.

References

1. Federal Law "On Electric Power Industry" dated March 26, 2003 No. 35-FZ (as amended on May 1, 2022).

2. "Energy Strategy of the Russian Federation for the Period up to 2050". Approved by the Order of the Government of the Russian Federation dated April 12, 2025 No. 908-r.

3. State Program of the Russian Federation "Development of Energy". Approved by the Resolution of the Government of the Russian Federation dated April 15, 2014 No. 321 (as amended by the Resolution of the Government of the Russian Federation dated March 28, 2019 No. 335).

4. RF Government Resolution No. 442 of 04.05.2012 (as amended on 27.12.2024) "On the functioning of retail electricity markets, full and (or) partial restriction of the electricity consumption regime" (together with the "Basic Provisions for the Functioning of Retail Electricity Markets", "Rules for Full and (or) Partial Restriction of the Electricity Consumption Regime") (as amended and supplemented, entered into force on 17.04.2025).

5. Dzyuba A.P., Semikolenov A.S. Management of flexible AEC systems in the industrial sector based on indicators of complex demand for electricity and gas consumption // Bulletin of Udmurt University. Series Economics and Law. 2025. Vol. 35. No. 1. - pp. 33-42.

6. Kravchenko G.A. Prospects for the Application of Hybrid Power Supply Systems / G.A. Kravchenko, A.N. Matyunin, T.V. Myasnikova, R.A. Romanov // Alley of Science. – 2018. – Vol. 3, No. 7 (23). – P. 847-854.

7. Order of the Government of the Russian Federation of August 19, 2020 No. 2129-r "On approval of the Concept for the development of regulation of relations in the field of artificial intelligence and robotics technologies until 2024".

8. Sodovnikov V.E. Methodology for processing statistical information on voltage dips and short-term interruptions in electrical networks / E.V. Solodovnikov, V.N. Tulsky, R.G. Shamonov // Electricity. 2019. – No. 1. – P. 4-16.

DOI 10.34660/INF.2025.25.67.062
UDC 539.32:536.2

利用刘维尔方法得到的积分方程求解热场中旋转异形极正交各向异性圆盘的非轴对称平面热弹性问题

SOLVING A NON-AXISYMMETRIC PLANAR THERMOELASTICITY PROBLEM FOR PROFILED POLAR-ORTHOTROPIC ANNULAR DISKS ROTATING IN A THERMAL FIELD USING INTEGRAL EQUATIONS OBTAINED BY THE LIOUVILLE METHOD

Karalevich Uladzimir Vasil'evich
Professor
International Center for Modern Education (ICME),
Prague, Czech Republic

Medvedev Dmitri Georgievich
Doctor of Pedagogical Sciences, Candidate of Physical and Mathematical Sciences, Professor
Belarusian State University,
Minsk, Belarus

摘要：本文讨论了计算热场中旋转的异型极正交各向异性涡轮盘应力-应变状态的理论基础。假设各向异性盘的热弹性状态为平面非轴对称。平面热弹性问题简化为两个二阶偏微分方程组，分别表示位移矢量分量和温度函数。将径向、切向位移和温度函数分解为关于角坐标θ的余弦和正弦的傅里叶级数，得到展开式分量的二阶常微分方程组。作者建议使用由刘维尔方法得到的第二类沃尔泰拉积分方程来求解所得到的常微分方程组。后者通过逐次逼近求解。给出了盘中应力、变形和位移分量的表达式。常数积分由边界条件确定。

关键词：傅里叶级数、刘维尔方法、极正交各向异性圆盘、径向、切向和剪应力、径向位移、预解式、常微分方程组、温度函数、第二类沃尔泰拉积分方程。

Abstract. *The article discusses the theoretical foundations of calculating the stress-strain state of a profiled polar-orthotropic turbine disk rotating in a thermal field. It is assumed that the thermoelastic state of the anisotropic disk is flat and non-axisymmetric. The planar thermoelasticity problem reduces to a system of two 2nd-order partial differential equations for the components of the displacement vector and a 2nd-order partial differential equation for the temperature function. Decomposing the radial, tangential displacement, and temperature function into Fourier series with respect to the cosines and sines of the angular coordinate*

θ, we obtain systems of ordinary differential equations of the 2nd order for the components of the expansion. The authors propose to solve the obtained systems of ordinary differential equations using Volterra integral equations of the 2nd kind obtained by the Liouville method. The latter are solved by successive approximations. Expressions for the components of stresses, deformations, and displacements in the disk are given. The constant integrations are found from the boundary conditions.

Keywords: *Fourier series, Liouville method, polar-orthotropic disk, radial, tangential and shear stresses, radial displacement, resolvents, system of ordinary differential equations, temperature function, Volterra integral equation of the 2nd kind.*

Introduction

The main working body of gas turbine engines of modern aircraft, steam turbines of thermal power plants and nuclear power plants are profiled anisotropic disks bearing blades on the outer contour [1]. Made of heavy-duty composite materials, they rotate at high angular velocity ω_0 around a normal axis. As a rule, the disk with the turbine blades is located in intense thermal fields. Consequently, the bladed turbine disk will simultaneously experience mechanical deformation from the action of centrifugal forces and thermal deformation from the thermal field.

In this paper, we consider a turbine rotor in the form of a profiled polar-orthotropic annular disk, which is connected to a rim on the outer contour of radius *R*, bearing an even number of *N* equidistant identical blades. The disc is tensioned onto the shaft, so that a contact pressure p_0 acts on its inner contour of the radius r_0. Or the disk is rigidly connected to the shaft, so that there are no displacements of the points of the inner contour of the disk.

The action of the blades on the disc is modeled by the application of *N* concentrated forces on the outer surface of the rim. Here, *the concentrated force* is the inertia force of the i–th blade, which occurs when the disk rotates with an angular velocity ω_0 equal to: $F_i^b = m_b\omega_0^2 R_{c.g.}^b$, where *m* is the mass of the blade, $R_{c.g.}^b$ is the distance from the axis of rotation to the center of gravity of the blade. These forces are applied to small areas of the outer surface of the rim and are directed along the radius *r*. The centrifugal forces acting in a rotating profiled disk lie in the plane of the disk and are also directed along the radius *r*. The thickness of the disk is much smaller than the size of the disk. It is assumed that the temperature field in the disk depends on the radius *r* and the angular coordinate *θ*. Consequently, the thermoelastic state in such a flattened profiled polar-orthotropic annular turbine disk rotating in a thermal field will be *flat* and *non-axisymmetric*.

Many works have been devoted to calculations on the strength and dynamics of turbine blades [1] and we will not consider this problem here.

In [2, 3], we investigated the temperature $T(r,\theta)$ distribution in profiled anisotropic annular disks with thermally insulated bases and in the case of heat exchange with the external environment through both bases.

In this paper, we consider the mode of *stationary rotation* of a turbine disk at a certain operating frequency rotating, which does not coincide with any of the proper oscillation frequencies of the disk or the oscillation frequencies of other structural elements of a turbo machine.

Problem statement and basic equations

Let the disk material have cylindrical anisotropy, and the axis of anisotropy coincides with the geometric axis of the disk, and at each point of the disk there are three mutually orthogonal planes of elastic symmetry. The bladed disk rotates uniformly in an intense thermal field with an angular velocity ω_0 around the axis of rotation coinciding with the axis of anisotropy and perpendicular to the median plane of the disk. On the outer contour of radius *R*, the disk is connected to a rim carrying a system of *N* identical concentrated forces $F_i^b \left(i=\overline{1,N}\right)$. The contact pressure p_0 acts on the inner contour of the disc from its tensioning on the shaft, or the disc is rigidly connected to the shaft, which means that there are no displacements on the inner contour of the disc.

It is required to find the distribution of stresses, deformations, and displacements in a given anisotropic annular disk of variable thickness rotating in an intense thermal field, as well as in the rim. We introduce a cylindrical coordinate system, placing the origin at the intersection of the anisotropy axis with the median plane of the disk. Let's point the z-axis vertically upwards.

Let us isolate from the disk by two meridional planes forming angles θ and $\theta+d\theta$ with the coordinate plane *rz*, and by two cylindrical surfaces with radii *r* and *r+dr* normal to the median plane, an infinitesimal element of the disk. Projecting all applied internal and external forces in radial and tangential directions, we obtain a system of equilibrium equations for an infinitesimal element of a rotating disk of variable thickness [4, p. 21]:

$$\begin{cases} \frac{1}{r}\left(\frac{\partial N_r r}{\partial r}+\frac{\partial N_{r\theta}}{\partial \theta}-N_\theta\right)+q_r=0, \\ \frac{1}{r}\left(\frac{\partial N_{r\theta} r}{\partial r}+\frac{\partial N_\theta}{\partial \theta}+N_{r\theta}\right)+q_\theta=0, \end{cases} \quad (1)$$

where $N_r(r,\theta)=h(r)\sigma_r(r,\theta)$ is the radial effort in the disk, $N_\theta(r,\theta)=h(r)\sigma_\theta(r,\theta)$ is the tangential effort in the disk, $N_{r\theta}(r,\theta)=N_{\theta r}(r,\theta)=h(r)\tau_{r\theta}(r,\theta)$ is the shear effort in the disk, $\sigma_r(r,\theta)$ is the radial component of the stresses in the disk, $\sigma_\theta(r,\theta)$ is the tangential component of the stresses in the disk, $\tau_{r\theta}(r,\theta)=\tau_{\theta r}(r,\theta)$ is the shear components of the stresses in the disk, $q_r=h(r)\rho\omega_0^2 r$ is the intensity of the radial component of the centrifugal force, $q_\theta=0$ is the intensity of the tangential component of the centrifugal force equal to zero, ρ is the density of the material the disk.

The equations of equilibrium (1) in stresses will be written as:

$$\begin{cases} \dfrac{\partial \sigma_r}{\partial r}+\dfrac{1}{r}\dfrac{\partial \tau_{r\theta}}{\partial \theta}+\left(\dfrac{h'(r)}{h(r)}+\dfrac{1}{r}\right)\sigma_r(r,\theta)-\dfrac{1}{r}\sigma_\theta(r,\theta)=-\rho\omega_0^2 r, \\ \dfrac{1}{r}\dfrac{\partial \sigma_\theta}{\partial \theta}+\dfrac{\partial \tau_{r\theta}}{\partial r}+\left(\dfrac{h'(r)}{h(r)}+\dfrac{2}{r}\right)\tau_{r\theta}(r,\theta)=0. \end{cases} \quad (2)$$

The relations of thermoelasticity in polar coordinates for a polar-orthotropic body in the case of a flat stressed state are [5, p. 12]:

$$\begin{cases} \varepsilon_r(r,\theta)=\dfrac{1}{E_r}\sigma_r(r,\theta)-\dfrac{\nu_{\theta r}}{E_\theta}\sigma_\theta(r,\theta)+\Theta_r(r,\theta)=\dfrac{1}{E_\theta}\left(k^2\sigma_r(r,\theta)-\nu_{\theta r}\sigma_\theta(r,\theta)\right)+\Theta_r(r,\theta), \\ \varepsilon_\theta(r,\theta)=-\dfrac{\nu_{r\theta}}{E_r}\sigma_r(r,\theta)+\dfrac{1}{E_\theta}\sigma_\theta(r,\theta)+\Theta_\theta(r,\theta)=\dfrac{1}{E_\theta}\left(-\nu_{\theta r}\sigma_r(r,\theta)+\sigma_\theta(r,\theta)\right)+\Theta_\theta(r,\theta), \\ \gamma_{r\theta}(r,\theta)=\dfrac{1}{G_{r\theta}}\tau_{r\theta}(r,\theta), \end{cases} \quad (3)$$

where $\varepsilon_r(r,\theta),\varepsilon_\theta(r,\theta)$ are the radial and tangential components of the disk deformations, respectively, and $\gamma_{r\theta}(r,\theta)$ are the shear deformation in the disk; $\Theta_r(r,\theta)=\alpha_r\cdot\left(T(r,\theta)-\tilde{T}_0\right)$ - radial thermal deformation of the disk, $\Theta_\theta(r,\theta)=\alpha_\theta\cdot\left(T(r,\theta)-\tilde{T}_0\right)$ - tangential thermal deformation of the disk, α_r,α_θ - radial and tangential coefficients of linear thermal expansion of the disk material, respectively, $\tilde{T}_0$ - initial temperature in the disk (usually $\tilde{T}_0=273K\left(0^\circ C\right)$ or $\tilde{T}_0=293K\left(20^\circ C\right)$); E_r,E_θ - elastic modulus under tension (compression) of a cylindrical anisotropic body in radial and tangential directions, respectively, $k^2=E_\theta/E_r$, $\nu_{r\theta},\nu_{\theta r}$ - Poisson coefficients, $G_{r\theta}$ - the shear modulus. It is assumed that elastic constants and coefficients of linear thermal expansion of a material α_r,α_θ are constant values independent of temperature $T(r,\theta)$.

For a cylindrical anisotropic body, the following equality holds:

$$\frac{\nu_{r\theta}}{E_r}=\frac{\nu_{\theta r}}{E_\theta}.$$

From equations (3), we express the stress components $\sigma_r(r.\theta),\sigma_\theta(r,\theta),\tau_{r\theta}(r,\theta)$ in terms of the deformation components $\varepsilon_r(r,\theta),\varepsilon_\theta(r,\theta),\gamma(r,\theta)$:

$$\begin{cases} \sigma_r(r,\theta)=\dfrac{E_\theta}{\left(k^2-\nu_{\theta r}^2\right)}\left[\left(\varepsilon_r(r,\theta)+\nu_{\theta r}\cdot\varepsilon_\theta(r,\theta)\right)-\left(\alpha_r+\nu_{\theta r}\alpha_\theta\right)\cdot\Theta(r,\theta)\right], \\ \sigma_\theta(r,\theta)=\dfrac{E_\theta}{\left(k^2-\nu_{\theta r}^2\right)}\left[\left(\nu_{\theta r}\cdot\varepsilon_r(r,\theta)+k^2\cdot\varepsilon_\theta(r,\theta)\right)-\left(\nu_{\theta r}\alpha_r+k^2\alpha_\theta\right)\cdot\Theta(r,\theta)\right], \\ \tau_{r\theta}(r,\theta)=G_{r\theta}\cdot\gamma_{r\theta}(r,\theta). \end{cases} \quad (4)$$

Let ‘s denote the components of the displacement vector $\vec{U}$ in the disk in the radial direction by $u(r,\theta)$, and in the tangential direction by $v(r,\theta)$.

The relationship of the deformation components $\varepsilon_r(r,\theta),\varepsilon_\theta(r,\theta),\gamma_{r\theta}(r,\theta)$ in the disk with the components $u(r,\theta),v(r,\theta)$ of the displacement vector $\vec{U}$ is given by the Cauchy differential relations [5, p. 21]:

$$\varepsilon_r(r,\theta)=\frac{\partial u(r,\theta)}{\partial r},\quad \varepsilon_\theta(r,\theta)=\frac{u(r,\theta)}{r}+\frac{1}{r}\frac{\partial v(r,\theta)}{\partial \theta},\tag{5}$$

$$\gamma_{r\theta}(r,\theta)=\frac{1}{r}\frac{\partial u(r,\theta)}{\partial \theta}+\frac{\partial v(r,\theta)}{\partial r}-\frac{v(r,\theta)}{r}.$$

We express the components of deformations $\varepsilon_r(r,\theta),\varepsilon_\theta(r,\theta),\gamma_{r\theta}(r,\theta)$ in formulas (4) in terms of radial displacement $u(r,\theta)$, tangential displacement $v(r,\theta)$, and temperature function $\Theta(r,\theta)$:

$$\begin{cases}\sigma_r(r,\theta)=\dfrac{E_\theta}{\left(k^2-\nu_{\theta r}^2\right)}\left[\left(\dfrac{\partial u}{\partial r}+\dfrac{\nu_{\theta r}}{r}u+\dfrac{\nu_{\theta r}}{r}\dfrac{\partial v}{\partial \theta}\right)-\left(\alpha_r+\nu_{\theta r}\alpha_\theta\right)\cdot\Theta(r,\theta)\right],\\ \sigma_\theta(r,\theta)=\dfrac{E_\theta}{\left(k^2-\nu_{\theta r}^2\right)}\left[\left(\nu_{\theta r}\dfrac{\partial u}{\partial r}+\dfrac{k^2}{r}u+\dfrac{k^2}{r}\dfrac{\partial v}{\partial \theta}\right)-\left(\nu_{\theta r}\alpha_r+k^2\alpha_\theta\right)\cdot\Theta(r,\theta)\right],\\ \tau_{r\theta}(r,\theta)=G_{r\theta}\left(\dfrac{1}{r}\dfrac{\partial u}{\partial \theta}+\dfrac{\partial v}{\partial r}-\dfrac{v}{r}\right).\end{cases}\tag{6}$$

Substituting the expressions for the stress components $\sigma_r(r.\theta),\sigma_\theta(r,\theta),\tau_{r\theta}(r,\theta)$ from formulas (6) into the equilibrium equations (2), we obtain a system of two 2nd-order partial differential equations for the displacement components $u(r,\theta),v(r,\theta)$:

$$\begin{cases}\dfrac{\partial^2 u}{\partial r^2}+\left(\dfrac{h'(r)}{h(r)}+\dfrac{1}{r}\right)\dfrac{\partial u}{\partial r}+\left[\nu_{\theta r}\left(\dfrac{h'(r)}{h(r)}\right)-\dfrac{k^2}{r}\right]\dfrac{1}{r}u+\dfrac{a}{r^2}\dfrac{\partial^2 u}{\partial \theta^2}+\dfrac{\left(a+\nu_{\theta r}\right)}{r}\dfrac{\partial^2 v}{\partial r\partial \theta}+\left[\nu_{\theta r}\left(\dfrac{h'(r)}{h(r)}\right)-\dfrac{\left(a+k^2\right)}{r}\right]\times\\ \times\dfrac{1}{r}\dfrac{\partial v}{\partial \theta}=-\dfrac{\left(k^2-\nu_{\theta r}^2\right)}{E_\theta}\rho\omega_0^2 r+\left(\alpha_r+\nu_{\theta r}\alpha_\theta\right)\dfrac{\partial\Theta}{\partial r}+\left\{\left(\alpha_r+\nu_{\theta r}\alpha_\theta\right)\left(\dfrac{h'(r)}{h(r)}\right)+\dfrac{1}{r}\left[\left(1-\nu_{\theta r}\right)\alpha_r-\right.\right.\\ \left.\left.-\left(k^2-\nu_{\theta r}\right)\alpha_\theta\right]\right\}\Theta(r,\theta),\\ \dfrac{\left(a+\nu_{\theta r}\right)}{r}\dfrac{\partial^2 u}{\partial r\partial \theta}+\left[a\left(\dfrac{h'(r)}{h(r)}\right)+\dfrac{\left(a+k^2\right)}{r}\right]\dfrac{1}{r}\dfrac{\partial u}{\partial \theta}+a\left[\dfrac{\partial^2 v}{\partial r^2}+\left(\dfrac{h'(r)}{h(r)}+\dfrac{1}{r}\right)\dfrac{\partial v}{\partial r}-\left(\dfrac{h'(r)}{h(r)}+\dfrac{1}{r}\right)\dfrac{v}{r}\right]+\\ +\dfrac{k^2}{r^2}\dfrac{\partial^2 v}{\partial \theta^2}=\dfrac{\left(\nu_{\theta r}\alpha_r+k^2\alpha_\theta\right)}{r}\dfrac{\partial\Theta}{\partial \theta},\end{cases}\tag{7}$$

where $a=\dfrac{\left(k^2-\nu_{\theta r}^2\right)G_{r\theta}}{E_\theta}$.

Let us supplement the system of differential equations (7) with the equation of thermal conductivity of a polar-orthotropic annular plate of variable thickness, taking into account heat exchange with the external environment through both bases of the plate:

$$\frac{\partial^2\Theta}{\partial r^2}+\left[\left(\frac{h'(r)}{h(r)}\right)+\frac{1}{r}\right]\frac{\partial\Theta}{\partial r}+\frac{\lambda_\varphi}{\lambda_r}\frac{1}{r^2}\frac{\partial^2\Theta}{\partial\theta^2}-\frac{2H}{\lambda_r h(r)}\left[1+\frac{1}{4}\left(\frac{dh}{dr}\right)^2\right]^{1/2}\Theta(r,\theta)=0, \tag{8}$$

where H is the heat transfer coefficient of the plate surface.

It is assumed that the heat transfer through the side surface of the plate is negligible. There are no internal heat sources in the anisotropic annular plate.

Let us write down the boundary conditions for the force problem of elasticity theory

: – for the mixed problem:

$$\begin{cases}\sigma_r(r_0,\theta)=-p_0, \quad \tau_{r\theta}(r_0,\theta)=0,\\ u(R,\theta)=u^{(r.)}(\theta), \quad v(R,\theta)=0,\end{cases} \tag{9}$$

where $u^{(r.)}(\theta)$ is the radial displacement of the inner points of the rim with the blades:

- for the 2nd main problem of elasticity theory:

$$\begin{cases}u(r_0,\theta)=0, \quad v(r_0,\theta)=0,\\ u(R,\theta)=u^{(r.)}(\theta), \quad v(R,\theta)=0.\end{cases} \tag{10}$$

Boundary conditions for the temperature problem:

$$\Theta(r_0,\theta)=T_1^*+\tilde{T}_0, \quad \Theta(R,\theta)=T_2^*(\theta)+\tilde{T}_0. \tag{11}$$

The calculation of stresses and displacements in the turbine rim was considered by us in [6].

Since an even number N equally spaced, identical and symmetrical concentrated forces $F_i^b\left(i=\overline{1,N}\right)$ are applied to the outer contour of the disk with a rim, simulating heated blades, we decompose the displacement components $u(r,\theta),v(r,\theta)$ and the temperature function $\Theta(r,\theta)$ into Fourier series along the cosines and sines of the angular coordinate θ with even numbers:

$$\begin{gathered}u(r,\theta)=u_0(r)+\sum_{n=1}^{\infty}u_{Nn}(r)\cos Nn\theta, \quad v(r,\theta)=\sum_{n=1}^{\infty}v_{Nn}(r)\sin Nn\theta,\\ \Theta(r,\theta)=\Theta_0(r)+\sum_{n=1}^{\infty}\Theta_{Nn}(r)\cos Nn\theta.\end{gathered} \tag{12}$$

Substituting expansions (12) into the system of equations (7) and the equation of thermal conductivity (8), we obtain an infinite system of inhomogeneous ordinary differential equations for the coefficients $u_0(r),u_{Nn}(r),v_{Nn}(r)$ of expansion of the displacement components and the coefficients $\Theta_0(r),\Theta_{Nn}(r)$ of expansion of the temperature function in the Fourier series:

$(n=0)$

(13)

$$\begin{cases} \dfrac{d^2u_0}{dr^2}+\left[\left(\dfrac{h'(r)}{h(r)}\right)+\dfrac{1}{r}\right]\dfrac{du_0}{dr}+\left[\nu_{\theta r}\left(\dfrac{h'(r)}{h(r)}\right)-\dfrac{k^2}{r}\right]\dfrac{1}{r}u_0(r)=-\dfrac{\left(k^2-\nu_{\theta r}^2\right)}{E_\theta}\rho\omega_0^2 r+\left(\alpha_r+\nu_{\theta r}\alpha_\theta\right)\dfrac{d\Theta_0}{dr}+ \\ =\left\{\left(\alpha_r+\nu_{\theta r}\alpha_\theta\right)\left(\dfrac{h'(r)}{h(r)}\right)+\dfrac{1}{r}\left[\left(1-\nu_{\theta r}\right)\alpha_r-\left(k^2-\nu_{\theta r}\right)\alpha_\theta\right]\right\}\Theta(r), \\ \dfrac{d^2\Theta_0}{dr^2}+\left[\left(\dfrac{h'(r)}{h(r)}\right)+\dfrac{1}{r}\right]\dfrac{d\Theta_0}{dr}-\dfrac{2H}{\lambda_r}\sqrt{\dfrac{1}{h^2(r)}+\dfrac{1}{4}\left(\dfrac{h'(r)}{h(r)}\right)^2}\,\Theta_0(r)=0; \end{cases}$$

$(n\geq 1)$

(14)

$$\begin{cases} \dfrac{d^2u_{Nn}}{dr^2}+\left[\left(\dfrac{h'(r)}{h(r)}\right)+\dfrac{1}{r}\right]\dfrac{du_{Nn}}{dr}+\left[\nu_{\theta r}\left(\dfrac{h'(r)}{h(r)}\right)-\dfrac{\left[k^2+(Nn)^2\cdot a\right]}{r}\right]\dfrac{1}{r}u_{Nn}(r)+(Nn)\dfrac{(a+\nu_{\theta r})}{r}\dfrac{dv_{Nn}}{dr}+ \\ +(Nn)\left[\nu_{\theta r}\left(\dfrac{h'(r)}{h(r)}\right)-\dfrac{(a+k^2)}{r}\right]\dfrac{1}{r}v_{Nn}(r)=\left(\alpha_r+\nu_{\theta r}\alpha_\theta\right)\dfrac{d\Theta_{Nn}}{dr}+\left\{\left(\alpha_r+\nu_{\theta r}\alpha_\theta\right)\left(\dfrac{h'(r)}{h(r)}\right)+\right. \\ \left.+\dfrac{1}{r}\left[\left(1-\nu_{\theta r}\right)\alpha_r-\left(k^2-\nu_{\theta r}\right)\alpha_\theta\right]\right\}\Theta_{Nn}(r), \\ \dfrac{d^2v_{Nn}}{dr^2}+\left[\left(\dfrac{h'(r)}{h(r)}\right)+\dfrac{1}{r}\right]\dfrac{dv_{Nn}}{dr}-\left[\left(\dfrac{h'(r)}{h(r)}\right)+\dfrac{1}{r}\left(1+(Nn)^2\dfrac{k^2}{a}\right)\right]\dfrac{1}{r}v_{Nn}(r)-(Nn)\left(1+\dfrac{\nu_{\theta r}}{a}\right)\dfrac{1}{r}\dfrac{du_{Nn}}{dr}- \\ -(Nn)\left[\left(\dfrac{h'(r)}{h(r)}\right)+\dfrac{1}{r}\left(1+\dfrac{k^2}{a}\right)\right]\dfrac{1}{r}u_{Nn}(r)=-(Nn)\dfrac{\left(\nu_{\theta r}\alpha_r+k^2\alpha_\theta\right)}{a}\dfrac{1}{r}\Theta_{Nn}(r), \\ \dfrac{d^2\Theta_{Nn}}{dr^2}+\left[\left(\dfrac{h'(r)}{h(r)}\right)+\dfrac{1}{r}\right]\dfrac{d\Theta_{Nn}}{dr}-\left\{\dfrac{2H}{\lambda_r h(r)}\left[1+\dfrac{1}{4}\left(\dfrac{dh}{dr}\right)^2\right]^{1/2}+\dfrac{(Nn)^2}{r^2}\dfrac{\lambda_\theta}{\lambda_r}\right\}\Theta_{Nn}(r)=0. \end{cases}$$

In the new variable $t=\ln\left(\dfrac{r}{r_0}\right)$, where $t\in\left[0;\ln\left(\dfrac{R}{r_0}\right)\right]$, we write systems of inhomogeneous ordinary differential equations of the 2nd order (13) and (14) in the following form:

$(n=0)$

(15)

$$\begin{cases} \dfrac{d^2u_0}{dt^2}+\left(\dfrac{h'(t)}{h(t)}\right)\dfrac{du_0}{dt}+\left[\nu_{\theta r}\left(\dfrac{h'(t)}{h(t)}\right)-k^2\right]u_0(t)=-\dfrac{\left(k^2-\nu_{\theta r}^2\right)}{E_\theta}\rho\omega_0^2r_0^3e^{3t}+\left(\alpha_r+\nu_{\theta r}\alpha_\theta\right)r_0e^t\dfrac{d\Theta_0}{dt}+ \\ +\left\{\left(\alpha_r+\nu_{\theta r}\alpha_\theta\right)\left(\dfrac{h'(t)}{h(t)}\right)+\left[\left(1-\nu_{\theta r}\right)\alpha_r-\left(k^2-\nu_{\theta r}\right)\alpha_\theta\right]\right\}r_0\cdot e^t\Theta(t); \\ \dfrac{d^2\Theta_0}{dt^2}+\left(\dfrac{h'(t)}{h(t)}\right)\dfrac{d\Theta_0}{dt}-\dfrac{2H}{\lambda_r h_0}\cdot h_0\left[\dfrac{r_0^4e^{4t}}{h^2(t)}+\dfrac{1}{4}\left(\dfrac{h'(t)}{h(t)}\right)^2r_0^2e^{2t}\right]^{1/2}\cdot\Theta_0(t)=0; \end{cases}$$

$(n\geq 1)$

(16)

$$\begin{cases} \dfrac{d^2u_{Nn}}{dt^2}+\left(\dfrac{h'(t)}{h(t)}\right)\dfrac{du_{Nn}}{dt}+\left[\nu_{\theta r}\left(\dfrac{h'(t)}{h(t)}\right)-\left(k^2+(Nn)^2\cdot a\right)\right]u_{Nn}(t)+(Nn)(a+\nu_{\theta r})\dfrac{dv_{Nn}}{dt}+ \\ +(Nn)\left[\nu_{\theta r}\left(\dfrac{h'(t)}{h(t)}\right)-\left(a+k^2\right)\right]v_{Nn}(t)=(\alpha_r+\nu_{\theta r}\alpha_\theta)r_0\cdot e^t\dfrac{d\Theta_{Nn}}{dt}+\left\{(\alpha_r+\nu_{\theta r}\alpha_\theta)\left(\dfrac{h'(t)}{h(t)}\right)+\right. \\ \left.+\left[(1-\nu_{\theta r})\alpha_r-\left(k^2-\nu_{\theta r}\right)\alpha_\theta\right]\right\}r_0\cdot e^t\Theta_{Nn}(t), \\ \dfrac{d^2v_{Nn}}{dt^2}+\left(\dfrac{h'(t)}{h(t)}\right)\dfrac{dv_{Nn}}{dt}-\left[\left(\dfrac{h'(t)}{h(t)}\right)+\left(1+(Nn)^2\dfrac{k^2}{a}\right)\right]v_{Nn}(t)-(Nn)\left(1+\dfrac{\nu_{\theta r}}{a}\right)\dfrac{du_{Nn}}{dt}- \\ -(Nn)\left[\left(\dfrac{h'(t)}{h(t)}\right)+\left(1+\dfrac{k^2}{a}\right)\right]u_{Nn}(t)=-(Nn)\dfrac{\left(\nu_{\theta r}\alpha_r+k^2\alpha_\theta\right)}{a}r_0\cdot e^t\Theta_{Nn}(t), \\ \dfrac{d^2\Theta_{Nn}}{dt^2}+\left(\dfrac{h_0'(t)}{h(t)}\right)\dfrac{d\Theta_{Nn}}{dt}-\left[\dfrac{2H}{\lambda_r h_0}\cdot h_0\sqrt{\dfrac{r_0^4e^{4i}}{h^2(t)}+\dfrac{1}{4}\left(\dfrac{h'(t)}{h(t)}\right)^2r_0^2e^{2t}}+(Nn)^2\dfrac{\lambda_\theta}{\lambda_r}\right]\cdot\Theta_{Nn}(t)=0, \end{cases}$$

where h_0 is the thickness of the disk on the inner contour of the radius r_0.

To solve systems of ordinary differential equations (15) and (16), we use the method of J. Liouville, which reduces the solution of an ordinary differential equation of the 2nd order of the form [7]:

$$y''+\left[\lambda^2-\nu(t)\right]y(t)=0$$

to the Volterra linear integral equation of the 2nd kind for the desired function y(t):

$$y(t)=\frac{1}{\lambda}\int_a^t\nu(s)\sin\lambda(y-s)y(s)ds+C_1\cos\lambda t+C_2\sin\lambda t,$$

where C_1, C_2 are the constants determined from the initial conditions: $y(a)=y_0$ and $y'(a)=y_0'$.

To do this, we transform the systems of inhomogeneous ordinary differential equations of the 2nd order (15) and (16) to the form:

$(n=0)$

(17)

$$\begin{cases} \dfrac{d^2u_0}{dt^2}-k^2\cdot u_0(t)=-\left(\dfrac{h'(t)}{h(t)}\right)\dfrac{du_0}{dt}-\nu_{\theta r}\left(\dfrac{h'(t)}{h(t)}\right)u_0(t)-\dfrac{\left(k^2-\nu_{\theta r}^2\right)}{E_\theta}\rho\omega_0^2r_0^3e^{3t}+\left(\alpha_r+\nu_{\theta r}\alpha_\theta\right)r_0e^t\dfrac{d\Theta_0}{dt}+ \\ +\left\{\left(\alpha_r+\nu_{\theta r}\alpha_\theta\right)\left(\dfrac{h'(t)}{h(t)}\right)+\left[\left(1-\nu_{\theta r}\right)\alpha_r-\left(k^2-\nu_{\theta r}\right)\alpha_\theta\right]\right\}r_0\cdot e^t\Theta(t), \\ \dfrac{d^2\Theta_0}{dt^2}+\dfrac{2H}{\lambda_r h_0}\cdot\Theta_0(t)=-\left(\dfrac{h'(t)}{h(t)}\right)\dfrac{d\Theta_0}{dt}+\dfrac{2H}{\lambda_r h_0}\left[1+h_0\sqrt{\dfrac{r_0^4e^{4t}}{h^2(t)}+\dfrac{1}{4}\left(\dfrac{h'(t)}{h(t)}\right)^2r_0^2e^{2t}}\right]\cdot\Theta_0(t); \end{cases}$$

$(n\geq 1)$

(18)

$$\begin{cases} \dfrac{d^2u_{Nn}}{dt^2}-\left(k^2+(Nn)^2\cdot a\right)\cdot u_{Nn}(t)=-\left(\dfrac{h'(t)}{h(t)}\right)\dfrac{du_{Nn}}{dt}-\nu_{\theta r}\left(\dfrac{h'(t)}{h(t)}\right)u_{Nn}(t)-(Nn)(a+\nu_{\theta r})\dfrac{dv_{Nn}}{dt}- \\ -(Nn)\left[\nu_{\theta r}\left(\dfrac{h'(t)}{h(t)}\right)-\left(a+k^2\right)\right]v_{Nn}(t)+\left(\alpha_r+\nu_{\theta r}\alpha_\theta\right)r_0\cdot e^t\dfrac{d\Theta_{Nn}}{dt}+\left\{\left(\alpha_r+\nu_{\theta r}\alpha_\theta\right)\left(\dfrac{h'(t)}{h(t)}\right)+\right. \\ \left.+\left[\left(1-\nu_{\theta r}\right)\alpha_r-\left(k^2-\nu_{\theta r}\right)\alpha_\theta\right]\right\}r_0\cdot e^t\Theta_{Nn}(t), \\ \dfrac{d^2v_{Nn}}{dt^2}-\left(1+(Nn)^2\dfrac{k^2}{a}\right)\cdot v_{Nn}(t)=-\left(\dfrac{h'(t)}{h(t)}\right)\dfrac{dv_{Nn}}{dt}+\left(\dfrac{h'(t)}{h(t)}\right)v_{Nn}(t)+(Nn)\left(1+\dfrac{\nu_{\theta r}}{a}\right)\dfrac{du_{Nn}}{dt}+ \\ +(Nn)\left[\left(\dfrac{h'(t)}{h(t)}\right)+\left(1+\dfrac{k^2}{a}\right)\right]u_{Nn}(t)-(Nn)\dfrac{\left(\nu_{\theta r}\alpha_r+k^2\alpha_\theta\right)}{a}r_0\cdot e^t\Theta_{Nn}(t). \\ \dfrac{d^2\Theta_{Nn}}{dt^2}+\left[\dfrac{2H}{\lambda_r h_0}-(Nn)^2\dfrac{\lambda_\theta}{\lambda_r}\right]\Theta_{Nn}(t)=-\left(\dfrac{h_0'(t)}{h(t)}\right)\dfrac{d\Theta_{Nn}}{dt}+\dfrac{2H}{\lambda_r h_0}\left[1+h_0\sqrt{\dfrac{r_0^4e^{4i}}{h^2(t)}+\dfrac{1}{4}\left(\dfrac{h'(t)}{h(t)}\right)^2r_0^2e^{2t}}\right]\times \\ \times\Theta_{Nn}(t). \end{cases}$$

Using the Liouville method, we reduce the systems of ordinary differential equations of the 2nd order (17) and (18) to systems of Volterra integral equations of the 2nd kind [8].

$(n=0)$

(19)

$$\begin{cases} u_0(t)=\dfrac{1}{k}\int_0^t K_u^{(0)}(t,\tau)u_0(\tau)\,d\tau+\dfrac{1}{k}\int_0^t M_\Theta^{(0)}(t,\tau)\Theta(\tau)\,d\tau+\dfrac{\left(k^2-\nu_{\theta r}^2\right)}{\left(k^2-9\right)}\dfrac{\rho\omega_0^2r_0^3}{E_\theta}e^{3t}+ \\ +\tilde{C}_1^{(0)}ch(kt)+\tilde{C}_2^{(0)}sh(kt), \\ \Theta_0(t)=\dfrac{1}{\Omega}\int_0^t K_\Theta^{(0)}(t,\tau)\Theta_0(\tau)\,d\tau+D_1^{(0)}\cos\Omega t+D_2^{(0)}\sin\Omega t, \end{cases}$$

where $\Omega_0=\sqrt{\dfrac{2H}{\lambda_r h_0}}$ is the numeric parameter;

$$K_u^{(0)}(t,\tau)=\left\{\left[\left(\frac{h'(\tau)}{h(\tau)}\right)'-\nu_{\theta r}\left(\frac{h'(\tau)}{h(\tau)}\right)\right]sh\left(k(t-\tau)\right)-k\left(\frac{h'(\tau)}{h(\tau)}\right)ch\left(k(t-\tau)\right)\right\},$$

$$K_\Theta^{(0)}(t,\tau)=\left\{\left[\left(\frac{h'(\tau)}{h(\tau)}\right)'+\Omega^2\left(1+h_0\sqrt{\frac{r_0^4e^{4t}}{h^2(\tau)}+\frac{1}{4}\left(\frac{h'(\tau)}{h(\tau)}\right)^2r_0^2e^{2t}}\right)\right]\sin\Omega(t-\tau)-\right.$$

$$\left.-\Omega\left(\frac{h'(t)}{h(t)}\right)\cos\Omega(t-\tau)\right\}$$

– kernels of integral equations of the system (19);

$$M_\Theta^{(0)}(t,\tau)=e^\tau\left\{\left[\left(\alpha_r+\nu_{\theta r}\cdot\alpha_\theta\right)\left(\frac{h'(r)}{h(r)}\right)-\left(\nu_{\theta r}\cdot\alpha_r+k^2\cdot\alpha_\theta\right)\right]sh\left(k(t-\tau)\right)+\right.$$

$$\left.+k\left(\alpha_r+\nu_{\theta r}\cdot\alpha_\theta\right)ch\left(k(t-\tau)\right)\right\}r_0;$$

$C_1^{(0)},C_2^{(0)},D_1^{(0)},D_2^{(0)}$ – arbitrary constants determined from boundary conditions.

$(n\geq 1)$

$$\begin{cases}u_{Nn}(t)=\dfrac{1}{\lambda_{Nn}}\int\limits_0^t K_u^{(Nn)}(t,\tau)u_{Nn}(\tau)\,d\tau-\dfrac{1}{\lambda_{Nn}}\left[\int\limits_0^t M_v^{(Nn)}(t,\tau)v_{Nn}(\tau)\,d\tau-\int\limits_0^t M_\Theta^{(Nn)}(t,\tau)\Theta_{Nn}(\tau)\,d\tau\right]+\\ +C_1^{(Nn)}ch\left(\lambda_{Nn}t\right)+\tilde{C}_2^{(Nn)}sh\left(\lambda_{Nn}t\right),\\ v_{Nn}(t)=\dfrac{1}{\mu_{Nn}}\int\limits_0^t K_v^{(Nn)}(t,\tau)v_{Nn}(\tau)\,d\tau+\dfrac{1}{\mu_{Nn}}\left[\int\limits_0^t N_u^{(Nn)}(t,\tau)u_{Nn}(\tau)\,d\tau-\int\limits_0^t N_\Theta^{(Nn)}(t,\tau)\Theta_{Nn}(\tau)\,d\tau\right]+\\ +C_3^{(Nn)}ch\left(\mu_{Nn}t\right)+\tilde{C}_4^{(Nn)}sh\left(\mu_{Nn}t\right),\\ \Theta_{Nn}(t)=\dfrac{1}{\Omega_{Nn}}\int\limits_0^t K_\Theta^{(Nn)}(t,\tau)\Theta_{Nn}(\tau)\,d\tau+D_1^{(Nn)}\cos\left(\Omega_{Nn}t\right)+D_2^{(Nn)}\sin\left(\Omega_{Nn}t\right),\end{cases}\qquad(20)$$

where $\lambda_{Nn}=\sqrt{k^2+(Nn)^2a}$, $\mu_{Nn}=\sqrt{1+(Nn)^2\dfrac{k^2}{a}}$, $\Omega_{Nn}=\sqrt{\dfrac{2H}{\lambda_r h_0}-(Nn)^2\dfrac{\lambda_\varphi}{\lambda_r}}$ – numeric parameters,

$$K_u^{(Nn)}(t,\tau)=\left\{\left[\left(\frac{h'(\tau)}{h(\tau)}\right)'-\nu_{\theta r}\left(\frac{h'(\tau)}{h(\tau)}\right)\right]sh\left(\lambda_{Nn}(t-\tau)\right)-\lambda_{Nn}\left(\frac{h'(\tau)}{h(\tau)}\right)ch\left(\lambda_{Nn}(t-\tau)\right)\right\},$$

$$K_v^{(Nn)}(t,\tau)=\left\{\left[\left(\frac{h'(\tau)}{h(\tau)}\right)'+\left(\frac{h'(\tau)}{h(\tau)}\right)\right]sh\left(\mu_{Nn}(t-\tau)\right)-\mu_{Nn}\left(\frac{h'(\tau)}{h(\tau)}\right)ch\left(\mu_{Nn}(t-\tau)\right)\right\},$$

$$K_{\Theta}^{(Nn)}(t,\tau)=\left\{\left(\left(\frac{h'(\tau)}{h(\tau)}\right)'+\frac{2H}{\lambda_r h_0}\left[1+h_0\sqrt{\frac{r_0^4 e^{4t}}{h^2(t)}+\frac{1}{4}\left(\frac{h'(\tau)}{h(\tau)}\right)^2 r_0^2 e^{2t}}\right]\right)\sin\Omega_{Nn}(t-\tau)-\right.$$

$$\left.-\Omega_{Nn}\left(\frac{h'(\tau)}{h(\tau)}\right)\cos\Omega_{Nn}(t-\tau)\right\}$$

– kernels of integral equations of the system (20),

$$M_{v}^{(Nn)}(t,\tau)=(Nn)\left\{\left[\nu_{\theta r}\left(\frac{h'(\tau)}{h(\tau)}\right)-\left(a+k^2\right)\right]sh\left(\lambda_{Nn}(t-\tau)\right)+\lambda_{Nn}\left(a+\nu_{\theta r}\right)ch\left(\lambda_{Nn}(t-\tau)\right)\right\},$$

$$M_{\Theta}^{(Nn)}(t,\tau)=\left\{\left(\left[\left(1-\nu_{\theta r}\right)\alpha_r-\left(k^2-\nu_{\theta r}\right)\alpha_\theta\right]r_0-\left(\alpha_r+\nu_{\theta r}\cdot\alpha_\theta\right)\right)\cdot sh\left(\lambda_{Nn}(t-\tau)\right)+\right.$$

$$\left.+\lambda_{Nn}\left(a+\nu_{\theta r}\right)\cdot ch\left(\lambda_{Nn}(t-\tau)\right)\right\},$$

$$N_{u}^{(Nn)}(t,\tau)=(Nn)\left\{\left[\left(\frac{h'(\tau)}{h(\tau)}\right)+\left(1+\frac{k^2}{a}\right)\right]\cdot sh\left(\mu_{Nn}(t-\tau)\right)-\mu_{Nn}\left(1+\frac{\nu_{\theta r}}{a}\right)\cdot ch\left(\mu_{Nn}(t-\tau)\right)\right\},$$

$$N_{\Theta}^{(Nn)}(t,\tau)=(Nn)\left(\nu_{\theta r}\cdot\alpha_r+k^2\cdot\alpha_\theta\right)r_0\cdot e^{\tau}sh\left(\mu_{Nn}(t-\tau)\right),$$

$C_i^{(Nn)}$, $D_j^{(Nn)}$ $\left(i=\overline{1;4},\ j=\overline{1;2}\right)$ – arbitrary constants determined from boundary conditions.

To solve the systems of integral equations (19), (20), we apply the *method of successive approximations*:

$(n=0)$

$$\begin{cases} u_0^{(m)}(t)=\dfrac{1}{k}\int\limits_0^t K_u^{(0)}(t,\tau)u_0^{(m-1)}(\tau)d\tau+\dfrac{1}{k}\int\limits_0^t M_{\Theta}^{(0)}(t,\tau)\Theta_0^{(m-1)}(\tau)d\tau+\dfrac{\left(k^2-\nu_{\theta r}^2\right)}{\left(k^2-9\right)}\dfrac{\rho\omega_0^2 r_0^3}{E_\theta}e^{3t}+ \\ +\tilde{C}_1^{(0)}ch(kt)+\tilde{C}_2^{(0)}sh(kt), \\ \Theta_0^{(m)}(t)=\dfrac{1}{\Omega_0}\int\limits_0^t K_{\Theta}^{(0)}(t,\tau)\Theta_0^{(m-1)}(\tau)d\tau+D_1^{(0)}\cos\Omega_0 t+D_2^{(0)}\sin\Omega_0 t, \end{cases} \qquad (21)$$

where m is the iteration number.

$(n \geq 1)$

(22)

$$\begin{cases} u_{Nn}^{(m)}(t) = \dfrac{1}{\lambda_{Nn}} \int\limits_0^t K_u^{(Nn)}(t,\tau) u_{Nn}^{(m-1)}(\tau) d\tau - \dfrac{1}{\lambda_{Nn}} \left[\int\limits_0^t M_v^{(Nn)}(t,\tau) v_{Nn}^{(m-1)}(\tau) d\tau - \int\limits_0^t M_\Theta^{(Nn)}(t,\tau) \Theta_{Nn}^{(m-1)}(\tau) d\tau \right] + \\ + C_1^{(Nn)} ch(\lambda_{Nn} t) + \tilde{C}_2^{(Nn)} sh(\lambda_{Nn} t), \\ v_{Nn}^{(m)}(t) = \dfrac{1}{\mu_{Nn}} \int\limits_0^t K_v^{(Nn)}(t,\tau) v_{Nn}^{(m-1)}(\tau) d\tau + \dfrac{1}{\mu_{Nn}} \left[\int\limits_0^t N_u^{(Nn)}(t,\tau) u_{Nn}^{(m-1)}(\tau) d\tau - \int\limits_0^t N_\Theta^{(Nn)}(t,\tau) \Theta_{Nn}^{(m-1)}(\tau) d\tau \right] + \\ + C_3^{(Nn)} ch(\mu_{Nn} t) + \tilde{C}_4^{(Nn)} sh(\mu_{Nn} t), \\ \Theta_{Nn}^{(m)}(t) = \dfrac{1}{\Omega_{Nn}} \int\limits_0^t K_\Theta^{(Nn)}(t,\tau) \Theta_{Nn}^{(m-1)}(\tau) d\tau + D_1^{(Nn)} \cos(\Omega_{Nn} t) + D_2^{(Nn)} \sin(\Omega_{Nn} t). \end{cases}$$

As a zero approximation, we assume: $u_0^{(0)}(t) = 0$, $\Theta_0^{(0)}(t) = 0$, $u_{Nn}^{(0)}(t) = 0$, $v_{Nn}^{(0)}(t) = 0$,

$\Theta_{Nn}^{(0)}(t) = 0$.

Let us represent each integral equation of systems (21), (22) as:

$$y_{Nn}^{(m)}(t) = \frac{1}{\beta_{Nn}} \int\limits_0^t K_y^{(Nn)}(t,\tau) y_{Nn}^{(m-1)}(\tau) d\tau + f_{Nn}(t), \tag{23}$$

where β_{Nn} is a numeric parameter that takes the values λ_{Nn}, either μ_{Nn}, or Ω_{Nn}.

If $f_{Nn}(t)$ is continuous on the segment $\left[0; \ln\left(\frac{R}{r_0}\right)\right]$ and the kernel $K_y^{(Nn)}(t,\tau)$ is continuous at $0 \leq t \leq \ln\left(R/r_0\right)$, $0 \leq \tau \leq t$, then the sequence converges $\{y_{Nn}(t)\}$ at $m \to \infty$ to the solution $y_{Nn}(t)$ of the Volterra integral equation of the 2nd kind (23):

$$y_{Nn}(t) = \lim_{m \to \infty} y_{Nn}^{(m)}(t).$$

The constant integrations $C_1^{(0)}, C_2^{(0)}, D_1^{(0)}, D_2^{(0)}; C_i^{(Nn)}, D_j^{(Nn)}$ $\left(i = \overline{1;4},\ j = \overline{1;2}\right)$ are determined from the boundary conditions (9) – (11) at each iteration step.

Bibliographic references

1. Malinin N.N. The strength of turbomachines. 2nd ed. Academic year. handbook for undergraduate and graduate studies. Moscow: YURAYT. 2018 (in Russian).

2. Karalevich U.V., Medvedev D.G. Solving a non-axisymmetric stationary problem thermal conductivity for a polar-orthotropic annular plate of variable thickness with thermally insulated bases// Journal of BSU. Mathematics. Computer science. 2018. No. 1. pp. 77-87 (in Russian).

3. Karalevich U.V.. The solution of a non-axisymmetric stationary thermal conductivity problem for a polar-orthotropic annular plate of variable thickness, taking into account heat exchange with the external environment. Mathematics. Computer science. 2020. No. 1. pp. 47-58 (in Russian).

4. Kovalenko A.D. Plates and shells in turbomachinery rotors. Kiev: Publishing House of the Academy of Sciences of the Ukrainian SSR, 1955 (in Russian).

5. Uzdalev A.I. Some problems of thermoelasticity of an anisotropic body. Saratov. Publishing house of Saratov State University. University, 1967 (in Russian).

6. Karalevich U.V., Medvedev D.G. Solution of a non-axisymmetric planar thermoelectric problem- problems for profiled polar-orthotropic annular disks rotating in a thermal field using the Volterra integral equation of the second kind. Proceedings of the international scientific conference "Russia–UAE Conference on Applied and Interdisciplinary Research" Dubai. UAE. June 18. 2025. Part 2. P. 138 – 151.

7. Krasnov M.L., Kiselev A.I., Makarenko G.I. Integral equations: problems and examples with detailed solutions. Moscow: KomKniga. 2007 (in Russian).

8. Karalevich U.V., Medvedev D.G. Integral equations of a plane problem of elasticity theory for rotating polar-orthotropic annular disks of variable thickness obtained by the Liouville method. Proceedings of the 10th International Seminar AMADE – 2021, September 13-17, 2021, Minsk, Belarus, BSU. – Minsk: IVC of the Ministry of Finance, 2022. pp. 29-34 (in Russian).

DOI 10.34660/INF.2025.26.17.063
UDC 631.8:631.839

天然注射器作为农业钾肥的有效性
THE EFFECTIVENESS OF NATURAL SYRINGES AS POTASH FERTILIZERS IN AGRICULTURE

Akanova Natalia Ivanovna
Doctor of Biological Sciences, Full Professor
All-Russian Research Institute of Agrochemistry named after D. N. Pryanishnikov,
Moscow, Russia

Kamenev Roman Alexandrovich
Doctor of Agricultural Sciences, Full Professor
Don State Agrarian University,
Persianovsky settlement, Rostov Oblast, Russia

Sidorov Jan Andreevich
Postgraduate
Don State Agrarian University,
Persianovsky settlement, Rostov Oblast, Russia

摘要：本文对非黑钙土地区马铃薯种植技术中增加天然复合肥钾肥施用剂量的有效性进行了农业生态学评估。结果表明，复合肥对马铃薯块茎产量和品质的形成具有积极作用。施用复合肥时，当钾肥施用量为90-120 kg/公顷时，马铃薯产量可靠地提高了18-36%。马铃薯块茎商品部分的产量为84-88%（对照组为68%）。复合肥的使用有助于改善pHKCL指标，即增加0-20 cm土壤中游离钾的含量。

关键词：复合肥、钾肥、作物产量、土壤肥力、改良剂、土壤酸度、马铃薯。

Abstract. *The article considers the results of agroecological assessment of the effectiveness of natural synnyrites used in increasing doses as potassium fertilizers in potato cultivation technology in the Non-Chernozem zone. A positive effect of synnyrites on the formation of potato tuber yield and their quality was established. A reliable increase in potato yield of 18-36% was obtained when synnyrites were applied at a dose of 90-120 kg K2O/ha, respectively. The yield of the commercial fraction of potato tubers was 84-88% (68% in the control). The use of synnyrites contributed to the improvement of the pHKCL indicator, an increase in the content of mobile potassium in the 0-20 cm layer of the soil.*

Keywords: *synnyrites, potash fertilizers, crop yield, soil fertility, ameliorant, soil acidity, potato.*

Potassium is an important nutrient that plays a key role in various physiological and biochemical functions of plants. The application of potash fertilizers promotes better growth and development of plants. Even with significant gross reserves of potassium in the soil, potassium nutrition can be limited by sorption-desorption processes. Probable reasons for the emerging contradictions in the use of potash fertilizers are the incomparability of the objects of study (different granulometric composition, mineralogical composition, soil regimes), the use of different methodological approaches, and the mechanism of transformation of potassium compounds in the soil that has not been fully clarified [2-5].

Studies show that long-term use of physiologically acidic nitrogen fertilizers leads to the destruction of potassium-containing minerals, transformation and transfer of potassium compounds. As a result, an increase in the gross content of potassium and its non-exchangeable form by 20-25% is observed in the subarable soil layer. The application of only nitrogen and phosphorus fertilizers without compensation for the removal of potassium leads to a decrease in the content of exchangeable and non-exchangeable potassium compounds in the upper soil layer 0-20 cm [6-8].

Potatoes are one of the most important food, forage and industrial crops in Russia and the world. Among the main food crops, it ranks 4th after wheat, rice and corn. The most important biological features of potatoes include a high need for potassium. Most scientific papers note the positive effect of potassium fertilizers on increasing potato yields.

One of the promising representatives of potassium fertilizers may be chlorine-free potassium fertilizer produced on the basis of natural synnyrites. To solve the problem, comprehensive studies were conducted on the effectiveness of using natural synnyrites in increasing doses as potash fertilizers.

According to the information available in the literature, synnyrites are rare ores, which are a bare leucocratic dense rock consisting of (vol.%): potassium feldspar - 55-85, kalsilite - up to 35, nepheline - up to 10 and biotite - 1-2 [1]. The Synnyr massif contains ultra-potassium syenites, synnyrites, which can be a potential raw material for the production of chlorine-free potash fertilizers. The predicted resources of raw materials available for open-pit mining are estimated at 2.6 billion tons.

Many studies have been devoted to the issue of potassium interaction in soil. However, it should be noted that synnyrites are characterized by a high content of silicon, which is one of the necessary biophilic macroelements for the formation of plant productivity, their skeletal part, helps to strengthen the stems and optimize their morphometric parameters, actively participates in metabolic processes, including energy exchange, increases the resistance of plants to biotic, abiotic stress, pathogenic phytopathogens.

However, the problem of using potassium-containing fertilizers with a high silicon content in agricultural production has not been sufficiently studied. The main factor that prevents the widespread use of natural agro-ores, such as potassium fertilizers in agricultural practice, produced on the basis of synnyrites, is the low awareness of agricultural producers.

The above determines the relevance of the studies aimed at identifying positive trends in changing the fertility of sod-podzolic soils, increasing the supply of potassium in soils and potato yields, using non-traditional natural sources of mineral nutrition - ground synnyrites. Such studies are especially important in today's difficult economic conditions, import substitution and extreme situations with environmental stress.

Research methodology: The purpose of our research is to give a comparative assessment of the effectiveness of various types of potassium fertilizers in potato cultivation technology depending on the doses of fertilizers applied. The objectives of the research included studying the effect of ground synnyrites on the agrochemical properties of sod-podzolic soils, the yield and quality of potato tubers;

The scientific novelty of the research consists in the scientific substantiation of the feasibility of using ground synnyrites to increase the potassium level of soils. The provision of sod-podzolic soil with available forms of silicon was assessed and the influence of this factor in the formation of the quality of potato tubers was revealed. The use of potassium-silicon-containing fertilizers from natural synnyrite ore will allow a new solution to the problem of improving both the potassium state of sod-podzolic soils and providing available silicon to increase the yield and quality of potato tubers.

Experimental design:

1. Control (without fertilizers)
2. N60P60- background
3. N60P60+ K90 (KCl)
4. N60P60+ K90 (synnyrites)
5. N60P60+ K120 (KCl)
6. N60P60+ K120 (synnyrites)

The doses of synnyrites were calculated based on their potassium content. Synnyrites and potassium chloride were applied in the fall under plowing (to a depth of 22 cm). The plots were placed sequentially. The object of the study was Gala potato. Planting pattern – 30×70. Soil cultivation was generally accepted for the Moscow region. The total plot area was 50 m2.

The soil of the site is sod-podzolic medium loamy medium humus (2.2%), the reaction of the environment is slightly acidic (pHKCl 5.2), the content of mobile phosphorus is average (152 mg/kg) and mobile potassium is low (85 mg/kg).

Discussion of the results: Sampling and determination of the mineral composition of natural synnyrite by the method of X-ray quantitative phase analysis

(XQPA) showed that the main rock-forming minerals are microcline and calisilite, while the secondary ones include nepheline, biotite, pyroxene and garnet (Table 1).

Table 1

Mineral (phase) composition of the original ore according to X-ray quantitative phase analysis (XQPA)

Mineral	**Theoretical formula**	**Mass fraction, %**
Kalsilite	$KAlSiO_4$	25
Nepheline	$(Na,K)AlSiO_4$	4
Potassium feldspar	$KAl[Si_3O_8]$	64
Pyroxene	$Ca(Mg,Fe)[Si_2O_6]$	2
Garnet	$Ca_3Fe_2[SiO_4]_3$	1
Biotite	$K(Mg,Fe)_3[AlSi_3O_{10}](OH)_2$	3
Sum of crystalline phases		99

Potassium feldspar is represented by two varieties - orthoclase and microcline. Kalsilite (nepheline) forms myrmekite-like intergrowths, in the center of such intergrowths “pure” feldspar is noted.

According to the quantitative chemical analysis, the mass content of total potassium oxide K_2O was 17.82% (Table 2). The main elements of the ore are silicon Si, aluminum Al, potassium K, calcium Ca and iron Fe, associated with the main rock-forming minerals: microcline, kalsilite and biotite.

Table 2

Quantitative chemical composition of the original ore

K_2O	**Al_2O_3**	**CaO**	**MgO**	**P_2O_5**	**Fe_2O_3**	**SiO_2**	**ZnO**	**TiO_2**	**$S_{общ}$**	**MnO**
17,82	21,3	1,05	0,23	0,026	1,97	56,9	0,005	0,13	0,015	0,047

It was determined that the average content of phosphorus pentoxide is up to 0.04-0.24 wt.%, sulfur 0.005-0.046%. Potassium in synnyrite is in a water-insoluble form, which prevents it from being washed out of the arable layer. The content of available potassium is 16.5-20%.

When using synnyrites at a dose of 90 and 120 kg K_2O/ha (options 4 and 6), a reliable increase in the yield of potato tubers was obtained (Table 3).

Table 3

The effect of synnyrites on potato yield (2023)

Option	Yield, t/ha	Increase in yield	
		total, t/ha	%, to the background
Control (without fertilizers)	14,5	-	-
N60P60- background	18,7	4,2	-
N60P60+ K90 (KCl)	21,7	7,2	15,8
N60P60+ K90 (synnyrites)	22,1	7,6	18,2
N60P60+ K120 (KCl)	24,8	10,3	32,6
N60P60+ K120 (synnyrites)	25,6	11,1	36,9
HCP_{05}	2,1		

The yield of potato tubers in the variant with the use of 90 kg K_2O/ha in the form of synnyrites was 22.1 t/ha, the total increase was 7.6 t/ha, which is 52.4% of the control, or 18.2% of the background. The yield in the variant with the same dose of potassium, applied in the form of potassium chloride, was 21.7 t/ha, the increase was 7.2 t/ha, which is 49.6% of the control, or 15.8% of the background. With an increase in the dose of potassium fertilizers, the potato yield increased, however, the advantage of synnyrites remained. In the variant with the use of 120 kg K_2O/ha in the form of synnyrites, the tuber yield was 25.6 t/ha, the total increase was 11.1 t/ha, which is 76.6% of the control and 36.9% of the background. The yield in the variant with the same dose of potassium when applying potassium chloride was 24.8 t/ha, the increase was 10.3 t/ha, which is 71.0% of the control and 32.6% of the background. The use of synnyrites was highly effective, their effect on the formation of potato yield exceeded the effect of potassium chloride. The increase in potato yield in variants 4 and 6 was obtained due to the increase in the weight of tubers per bush, the weight of 1 tuber and the number of tubers in a bush (Table 4). The yield of the commercial fraction of potato tubers was 78% in variant 3, and 84% in variant 4 with the introduction of synnyrites. The maximum yield of the commercial fraction of 88% was obtained in variant 6 “background + synnyrites 120 kg K_2O/ha”.

Table 4

Effect of various forms of potash fertilizers on the structure of potato yield

Option	Weight		tuber, g	Commodity fraction, %
	tubers, g/bush	tuber, g		
Контроль (without fertilizers))	437	42	9,2	68
$N_{90}P_{90}$	597	51	10,6	81
$N_{90}P_{90}+K_{90}$ (KCl)	639	56	12,0	78
$N_{90}P_{90}+K_{90}$ (synnyrites)	672	59	12,2	84

$N_{90}P_{90}+K_{120}$ (KCl)	783	66	11,5	84
$N_{90}P_{90}+K_{120}$ (synnyrites)	790	70	12,6	88
$НСР_{05}$	147	11	2,6	7

The maximum content of dry matter and starch in potato tubers was observed in the control variant (without fertilizers) – 20.8 and 15.4%, respectively (Table 5). In the tubers of the variants where synnyrites were used, a decrease in the nitrate content was noted, in comparison with similar variants with the introduction of potassium chloride. However, in none of the variants was the MAC exceeded.

Table 5

Effect of potassium fertilizers on the quality of potato tubers

Option	Dry matter, %	Starch, %	Nitrates, mg/kg
Контроль ((without fertilizers))	20,8	15,4	179
$N_{90}P_{90}$	20,6	14,6	212
$N_{90}P_{90}+K_{90}$ (KCl)	21,0	14,3	225
$N_{90}P_{90}+K_{90}$ (synnyrites)	21,3	14,8	196
$N_{90}P_{90}+K_{120}$ (KCl)	21,6	13,7	245
$N_{90}P_{90}+K_{120}$ (synnyrites)	22,0	14,7	213
$НСР_{05}$	2,1	1,3	62
MAC	-	-	250

The use of synnyrites contributed to the improvement of the acid-base properties of the soil, the pHKCL index increased reliably from 5.2 units (1st var. control) to 5.8 units (maximum dose of synnyrites). The increase in the pHKCL index changed towards a close to neutral environment with an increase in the dose of synnyrites.

Table 6

Effect of potassium fertilizers on the agrochemical properties of sod-podzolic soil (0-20 cm)

Option	pH_{KCL}	$N\text{-}NH_4$	$N\text{-}NO_3$	$N_{мин}$	P_2O_5	K_2O
		мг/кг				
1	5,2	8,5	15,0	23,5	152	89
2	5,2	9,6	23,3	32,9	186	91
3	5,2	9,8	23,3	33,2	193	129
4	5,5	9,7	25,8	35,5	204	131
5	5,3	10,7	23,6	34,3	198	148
6	5,8	11,3	25,1	36,4	212	143
$НСР_{05}$	0,1	23,2	18,9	34,5	25	31

The application of mineral fertilizers resulted in an increase in mineral nitrogen in the soil (by 1.5 times), both due to the ammonium and nitrate parts. When applying synnyrites, an increase in the accumulation of mineral nitrogen was noted. The content of mobile phosphorus in the soil increased reliably when using nitrogen and phosphorus fertilizers, however, against the background of the application of synnyrites, a tendency for the indicator to increase was noted in comparison with the background and options with the application of potassium chloride. The content of mobile potassium in the soil increased significantly with the application of potassium fertilizers. However, when using synnyrites both at a dose of 90 kg K_2O/ha and 120 kg K_2O/ha, the value of the indicator did not exceed the options with the application of potassium chloride in the same doses (Table 6). However, in contrast to the options with the application of potassium chloride, further improvement of the potassium regime of the soil is predicted based on the prolonged property of natural synnyrites.

Conclusion

The results of the studies showed that under the conditions of using potassium-silicon mineral fertilizer produced on the basis of natural synnyrites, a reliable increase in potato yield of 18-36% was obtained. The yield of the commercial fraction of potato tubers in these variants was 84-88% (control variant - 68%). The increase in potato yield occurred due to an increase in the mass of tubers per bush, the mass of 1 tuber and the number of tubers in the bush. The use of synnyrites contributed to an improvement in the pHKCL indicator, an increase in the content of mobile potassium in the soil (0-20 cm) and a tendency to increase the phosphorus content was noted.

References

1. Smyslov S. A., Kayukov A. E., Bystritsky A. O., Sokolova A. N., Sotnikova I. A. New data on the geological structure of the Synnyr ultracalt intrusive massif // Geodynamics and tectonophysics 2022.- No. 13 (4).- P. 1-6.

2. Matsnev I. N., Arzybov V. A. Effect of fertilizers and soil liming on potato productivity // Bulletin of the Michurinsk State Agrarian University. – 2013. – No. 4. – P. 26-29.

3. Mikhailova L. A., Aleshin M. A., Aleshin D. V. Influence of mineral nutrition conditions on the productivity and quality of potatoes grown on sod-podzolic heavy loamy soil//Perm Agrarian Bulletin. 2013. No. 1 (1). P. 9-14.

4. Nosov V.V. The importance of potash fertilizers for maintaining ecological balance // Fertility. 2002. No. 2. P. 28-30.

5. Prokoshev V.V, Deryugin I.P. Potassium and potash fertilizers. Moscow: Ledum, 2000. 185 p.

6. Nosov V.V. The Importance of Potash Fertilizers for Maintaining Ecological Balance // Fertility. 2002. No. 2. P. 28–30.

7. Prokoshev V.V., Deryugin I.P. Potassium and Potassium Fertilizers. Moscow: Ledum, 2000. 185 p.

8. Jakobsen S.T. Interaction between plant nutrients .3. Antagonism between potassium, magnesium and calcium // Acta Agriculturae Scandinavica Sekction B-Soil and plant Science. 1993. T. 43. Вып. 1 С.1-5.

9. Khan S.A., Mulvaney R.L. Ellsworth T.R. The potassium paradox: Implications for soil fertility, crop production and human health // Renewable Agriculture and Food Systems. 2014. 29(1). 3–27.

10. Zhuchenko A.A. Potato growing in Russia. Actual problems of science and practice // Proceedings of the international congress "Potato, Russia – 2007". - M .: Russian Agricultural Academy, 2007. - 360 p.

科学出版物

上合组织国家的科学研究：协同和一体化

国际科学大会的材料

2025年8月27日，中国北京

编辑A.A.Siliverstova
校正A.I.尼古拉耶夫

2025年8月27日，中国北京
USL。沸点：98.7。 订单253.流通500份。

在编辑和出版中心印制
无限出版社